B4

MARTIN MARIETTA ENERGY SYSTEMS LIBRARIES
3 4456 0285439 2

CENTRAL RESEARCH LIBRARY
DOCUMENT COLLECTION

ORNL-3547
UC-80 – Reactor Technology
TID-4500 (26th ed.)

NUCLEAR SAFETY PROGRAM
SEMIANNUAL PROGRESS REPORT
FOR PERIOD ENDING DECEMBER 31, 1963

CENTRAL RESEARCH LIBRARY
DOCUMENT COLLECTION
LIBRARY LOAN COPY
DO NOT TRANSFER TO ANOTHER PERSON
If you wish someone else to see this document, send in name with document and the library will arrange a loan.

OAK RIDGE NATIONAL LABORATORY
operated by
UNION CARBIDE CORPORATION
for the
U.S. ATOMIC ENERGY COMMISSION

Printed in USA. Price: $2.00 Available from the
Office of Technical Services
U. S. Department of Commerce
Washington 25, D. C.

LEGAL NOTICE

This report was prepared as an account of Government sponsored work. Neither the United States, nor the Commission, nor any person acting on behalf of the Commission:

A. Makes any warranty or representation, expressed or implied, with respect to the accuracy, completeness, or usefulness of the information contained in this report, or that the use of any information, apparatus, method, or process disclosed in this report may not infringe privately owned rights; or

B. Assumes any liabilities with respect to the use of, or for damages resulting from the use of any information, apparatus, method, or process disclosed in this report.

As used in the above, "person acting on behalf of the Commission" includes any employee or contractor of the Commission, or employee of such contractor, to the extent that such employee or contractor of the Commission, or employee of such contractor prepares, disseminates, or provides access to, any information pursuant to his employment or contract with the Commission, or his employment with such contractor.

ORNL-3547

Contract No. W-7405-eng-26

NUCLEAR SAFETY PROGRAM SEMIANNUAL PROGRESS REPORT

for Period Ending December 31, 1963

F. R. Bruce, Program Coordinator

W. B. Cottrell, Reactor Division
B. R. Fish, Health Physics Division
C. E. Guthrie, Chemical Technology Division
F. C. Maienschein, Neutron Physics Division
G. M. Watson, Reactor Chemistry Division

MARCH 1964

OAK RIDGE NATIONAL LABORATORY
Oak Ridge, Tennessee
operated by
UNION CARBIDE CORPORATION
for the
U. S. ATOMIC ENERGY COMMISSION

MARTIN MARIETTA ENERGY SYSTEMS LIBRARIES

3 4456 0285439 2

Summary

PART I. FISSION PRODUCT RELEASE AND BEHAVIOR

1. Properties of Fission Product Aerosols Produced by Overheated Reactor Fuels

Fission Product Release from Molten Aluminum-Uranium Alloys. – *Effect of Burnup Level and Sample Geometry.* – Studies of the release of iodine, tellurium, cesium, ruthenium, and the rare gases, from molten aluminum-uranium alloys previously irradiated to nominal burnups of trace level, 3.2%, 9.0%, and 23.6% revealed significant increases in released fractions between trace-level and 3.2% burnup at temperatures from 750°C to 1100°C. Above 3.2% burnup, the fraction released did not appear to increase with increasing burnup. No significant change in fraction released was detected in these experiments (cesium excepted) resulting from a twenty-five-fold increase in sample weight or from the difference in geometries inherent in the change from small-scale laboratory tests to experiments in the Hot-Cell Confinement Facility.

Hot-Cell Tests of ORR Confinement System. – The results of tests in the Hot-Cell Confinement Facility demonstrated that the iodine-retention ability of the proposed ORR confinement system is high (99.97%) and that the aging of the released aerosol from molten aluminum-uranium alloy for more than an hour had little, if any, effect on the retention efficiency.

Distribution of Fission Products Released from Molten Aluminum-Uranium Alloy. – Comparison of the distribution data in dry and moist atmospheres showed that iodine deposited more extensively on dry stainless steel surfaces than on the same surfaces saturated with steam, but the reverse behavior was found true for cesium, indicating that cesium iodide was not an important component of the aerosol formed in these experiments. For the period of aging used in the tests (45 min), deposition was found to be relatively ineffective in reducing the concentration of the total radioactivity in the confinement tank. A reduction factor of 2 to 5 for iodine was observed, but of less than 2 for cesium, tellurium, and ruthenium.

Fission Product Release from Stainless-Steel-Clad UO_2 Melted in Air. – Melting in the Hot-Cell Confinement Facility of UO_2 pellets irradiated at trace level and clad in stainless steel indicated that most of the UO_2 particles were deposited on the furnace tube wall and did not reach the confinement tank or the roughing filter. In addition, the efficiency of bronze screens for removing radioiodine from the gas stream was found to be quite low. The aerosol produced was found to be highly stable and significant fractions remained airborne after several hours of aging. A relatively high percentage (1.4%) of a penetrating form of iodine was found to be present in the aged aerosol.

Multipin UO_2 Melting Experiments. – Design of a 19-pin array of tungsten rods surrounded by cored UO_2 fuel pellets has been completed. This configuration will permit simulation of melting of a fuel rod near the center of a reactor core with cooler fuel around it on which released, low-volatility fission products may deposit. Experiments with this assembly will require a larger power source than is presently available.

Particles Produced by Melting Irradiated Fuel Materials. – Particles remaining airborne after a 45-min or longer aging period in the aerosol tanks were collected on absolute filters, on an electron microscope grid of an electrostatic precipitator, and on walls of diffusion tubes. Particles ranging in size from 10 A to 3 μ were observed, indicating relatively high aerosol stability.

Deposition of Cesium and Distribution of Released Radioiodine Between Molecular and Particulate Forms. – Characterization of particulates associated with radioiodine before and after filtration was carried out by the use of a modified May Pack which incorporated diffusion channel ports. Most of the radioiodine released from aluminum-uranium alloy was found to be in molecular form (95% before filtration, 98% after filtration). The diffusion tube data gave no evidence of the presence of cesium iodide in the aged aerosol. A significantly higher fraction of iodine released from molten UO_2 was found to be associated with particulates (20%).

Iodine Removal from Oxidizing Gases at High Temperatures. – Platinized aluminum was found to be more effective than unplatinized aluminum for the retention of iodine in flowing air at high temperatures. However, both materials release iodine at temperatures above 400°C and would serve only to delay its passage.

Quartz wool was found to be ineffective in iodine retention at temperatures of 200°C or higher.

2. Release of Fission Products on In-Pile Melting of Reactor Fuels Under Transient Reactor Conditions

Two experiments were performed in the TREAT reactor which simulated accidents that could occur during the start-up of a new reactor or during a SPERT-type experiment where the only fission products available for release are those due to fissions that occur during a very short time.

The experiments entailed reactor periods of 108 and 87 msec with integrated power of 320 and 328 Mw-sec respectively. In the first experiment the cladding melted and the UO_2 temperature climbed to an estimated value of 2800°C, but the sample did not melt. The outside diameter of the pellets increased 2%. Approximately 65% of the UO_2 specimen melted in the second experiment, and the outer diameter of the unmelted portion of the specimen increased 18%. Meaningful samples of the released aerosols were collected and particle-size distributions were obtained. Fission product release under the conditions of these experiments was shown to be related to the physical characteristics of precursor species present while the fuel was at or near its maximum temperature. Furthermore, it was determined that the release from the high-temperature zone was less than 2% for isotopes that did not have volatile precursors.

3. Behavior of Fission Products Released During In-Pile Destruction of Reactor Fuels

In-pile experiments are being continued to study the characteristics and behavior of fission products released by melting or vaporizing miniature stainless-steel-clad UO_2 fuel elements in the ORR in a helium atmosphere. Studies have been made of the effects of gas velocity on fission product release and behavior, of the fine-particle and vapor forms of released fission products, of the particulate material collected by filters, of the distribution of released fission products, and of the fractionation of fission products.

Effect of Gas Velocity on Release and Behavior of Fission Products. – In experiments performed to study how the helium sweep gas flow rate affects fission product release, the flow was increased sixfold over previous experiments. Other conditions remained the same as in previous experiments. The increased helium flow rate lowered the maximum temperature of the fuel. At a given temperature, release of fission products generally from the fuel itself, and release of the more volatile isotopes (iodine, tellurium, and cesium) from the high-temperature zone of the furnace do not appear to be affected by an increased flow rate, but the release of the less volatile isotopes from the furnace increased fourfold with a sixfold increase in rate. The diffusion-tube deposit indicated that fission products occurred in the vapor form in the highest flow experiment rather than as 25-A particles.

Released Fission Products Associated with Fine-Particle and Vapor Forms Determined by Diffusion Coefficient Measurement. – The distribution of released fission products and uranium deposited from a gas flowing laminarly through a diffusion tube was analyzed to yield information about vapors, gas-borne particles in the range of 10 to 100 A in diameter, and the amounts of released material associated with these forms. In most of the experiments the data indicate that particles having an average diameter of about 25 A were released. Considerable amounts of released I^{131}, Te^{132}, and Cs^{137} are always carried by these fine particles. Smaller amounts of released Sr^{89} and Ba^{140} always, of uranium frequently, and

of Ru^{106} infrequently are carried by these particles in the UO_2 melting experiments but these substances did not appear to be carried by particles of this size in the uranium carbide–graphite burning experiments. In the case of the UO_2 melting experiments, Zr^{95} and Ce^{144} are very seldom carried by particles of this size, but they are usually carried by these particles in the uranium carbide–graphite burning experiments. Besides being carried by these small particles, the various fission products and uranium are probably also carried by larger particles which pass through the diffusion tube and are retained on the filters.

In the experiment with the highest gas flow rate, considerable amounts of released I^{131}, Sr^{89}, and Ba^{140} and smaller amounts of Te^{132} and Cs^{137} were carried as vapors. However, only small amounts of Zr^{95}, Ce^{144}, Ru^{106}, and uranium are carried as vapors. The appearance of vapor forms of these materials at higher gas velocities could be caused by their more rapid transport from the release site and their greater dilution, both of which would reduce the tendency for particle formation.

Particulate Material Collected by Filters. – The sweep gas from the in-pile fuel melting and burning experiments is passed through a series of filters to obtain information about the particulate material which is formed. Most of the filters, especially those initially encountered by the gas stream, have been too radioactive for electron microscopy, but data on a few filters have been obtained. Particles ranging in size from 0.015 to over 1 μ occurred downstream from the initial filter in the UO_2 melting experiments. Median particle diameters ranged from 0.01 to 5 μ in the corresponding filters in the uranium carbide–graphite burning experiments. In the UO_2 experiments, agglomerates of like-sized particles and particles of various densities were observed. In some cases particles were spheres and in others they appear to be platelets.

Distribution of Released Fission Products Through Off-Gas Systems. – The distribution of the released fission products and uranium among the various parts of the in-pile fuel destruction assemblies is determined by radiochemical and chemical analysis. In a typical experiment, 60 to 90% of the three more volatile fission products (iodine, tellurium, and cesium) escaped from the high-temperature zone of the furnace and were distributed more or less evenly between the cold stainless steel enclosure of the furnace, the diffusion tube, and the roughing filter. The HV-70 filter collected about 3% of the inventory of iodine and cesium. Approximately 3% of the iodine, 4% of the cesium, and less than ½% of the tellurium were found downstream of the HV-70 filter. Four percent of the ruthenium escaped from the hot zone and half of that was stopped by the HV-70 filter. Most of the remainder was found on the membrane filter or its support. The other fission products (strontium, barium, zirconium, and cerium) and uranium were released from the hot zone in amounts of 1% or less. Not more than 0.25% of the inventory of these materials was found downstream from the HV-70 filter. The filters exhibited a rather low percentage of effectiveness against the materials which arrived at their faces, but the materials which penetrated were very small fractions of the total inventory.

Fission Product Fractionation. – In fission product release experiments, fission products appear in varying proportions in various locations, and sample compositions are in general different from those predicted for normal fission yields. This fractionation occurs because differences in the physical and chemical characteristics of individual fission products result in differences in their behavior in release, transport, or deposition processes. Fractionation of fission products is expected to occur similarly in reactor accidents.

A quantitative theoretical analysis of the observed variation in fission product proportions can be used to test the validity of various proposed mechanisms of fractionation. Knowledge of these mechanisms will make available a new tool for the prediction of the hazards of fission product release associated with reactor accidents, and will help to recognize conditions which are important in their effects on fission product release, transport, and deposition so that those conditions might be explored as variables in laboratory experiments.

A study has been made in which the fractionation predicted by several different models was compared with experimental results. The vapor transpiration model, in which fractionation is brought about by evaporation of the fission products from the fuel and by their removal by a carrier gas stream, gives the most satisfactory agreement with the data from the in-pile fission product release experiments. The theory predicts a straight line when certain ratios of fission products are plotted against each other on log-log coordinates.

The theory, with information from the literature on vapor pressures of fission product materials, and experimental data on the amounts vaporized, was used to predict successfully the proportions of the fission products in various experimental samples. This validates the assumptions of the model and identifies the mechanism of fractionation. The heats of vaporization and thus the chemical forms of the fission products during vaporization are also identified in the same operation. In most of the experiments with stainless-steel-clad UO_2, the strontium, barium, and zirconium were vaporized in the metallic form; however, in one they were in the oxide form. This investigation is being continued, specifically being applied to the other fission products for which data are available; iodine, tellurium, cesium, ruthenium, and cerium and under various conditions. The results should provide a better knowledge of fission product release chemistry and make it possible to predict the hazards of various kinds of fission product release accidents.

4. Characterization and Control of Accident-Released Fission Products

Investigation of the Occurrence and Behavior of Different Forms of Radioiodine. – Investigation was continued of the origin and identity of iodine compounds which appear when air and what is presumed to be I_2 vapor are mixed. Information is needed on these points in order to design adequately radioiodine removal systems. Experimentally, deposition of iodine compounds from viscous air flow to diffusion tubes was employed to determine diffusion coefficients of the compounds. The various species were distinguished chemically by the use of diffusion tubes which were composite in that they had successive surfaces of silver, rubber, and activated carbon; the latter was applied as a dust after coating the inside of the tube with an adhesive. Elemental iodine deposited on the silver with its characteristic diffusion coefficient of about 0.08 cm^2/sec; a compound or group of compounds deposited on the rubber to give an indicated diffusion coefficient of about 0.05 cm^2/sec, suggestive of a molecular weight of the order of 300 or higher; another iodine material deposited on the activated carbon to yield a diffusion coefficient of 0.10 cm^2/sec, implying a low-molecular-weight compound such as, for example, HI or CH_3I. This behavior was typical of iodine from two greatly differing sources. The proportion of iodine present as compounds increases as the I_2 in air decreases.

The effectiveness of activated charcoal for removing the volatile compounds of iodine was studied. Moisture in a room-temperature system lowers the effectiveness of charcoal for iodine compounds but this effect diminishes at temperatures around 100°C. Whetlerite charcoal produces efficiencies >99.9% for the removal of iodine compounds in the presence of moisture at a temperature of 100°C.

Measurement of the Characteristics of Radioactive Aerosols by Use of Fibrous Filters. – A method for characterizing radioactive aerosols has been developed, which interprets the distribution of radioactive particles in a series of uniform fiber filters in terms of the three main mechanisms of filtration, that is, diffusion, interception, and inertial impaction. An initial series of experiments was conducted using a radioactive test aerosol containing Zn^{65} particles in the diameter range 20 to 300 A at linear velocities from 0.4 to 88 fpm, and analysis of the data in the diffusion region has been reported previously.

The data obtained in the initial series of experiments, at the higher flow rates of 10 to 88 fpm (interceptional and impaction regions), have been analyzed in terms of theories of fiber filtration. The experiments were conducted with filter mats having volume fraction of fibers well above the region treated theoretically. Extrapolation of the theories has yielded fiber efficiencies not in agreement with those obtained experimentally, making it difficult to estimate particle sizes accurately in the higher flow range. A second series of experiments, in which the volume fraction has been lowered to less than 0.1, has been completed, and analysis of the data is in progress. It is believed that these data can be treated according to a theory of filtration to characterize particle sizes more accurately in this flow region.

5. Measurement and Prediction of Behavior of Released Fission Products in Reactor Systems

Innocuous Simulation of Aerosols Produced by Reactor Accidents. – A program has been started to develop ways of simulating the radioactive materials which would be released during a reactor

accident making use of test materials which are not hazardous themselves. Such innocuous "simulants" will be of great value for investigating the behavior of released fission products in the various stages of reactor containment and in gas cleaning equipment. Since radioiodine is generally considered to be the most significant of the volatile fission products from a hazards standpoint, the behavior of radioiodine and its volatile compounds is being given first consideration. As more understanding of iodine behavior is obtained, the application of normal iodine vapor as a "simulant" for radioiodine vapor will become more reliable. The study of methods or means of simulating other fission products continues.

Decontamination Factors for Particle Deposition in Leaks as Applied to Leak Testing of Containment Vessels. – Study was continued of the process whereby a varying degree of decontamination of radioparticulates results from diffusional deposition of particles in containment vessel leaks. Such particulates would be expected to originate during a nuclear reactor accident and would present a serious hazard. The extent of the calculated decontamination is a strong function of leak size and of particle size and increases as either decreases. The more recent study of this attenuation effect has been concerned with application of the results to containment vessel leak testing, since potentially large credit factors may be claimed by the use of leak testing methods that are highly sensitive and reliable. Calculated decontamination factors of 50 and higher are obtained for particles 2 μ and less in diameter if leaks corresponding to 10^{-6} cm^3/sec in practice, as measured under the accident conditions, are eliminated. Achieving a sensitivity of 10^{-6} cm^3/sec would be very costly, but the hazard reduction could conceivably more than offset the cost. It was shown that conventional leak-testing data could be utilized in estimating decontamination factors for particles even though detailed information on leak size and structure was not available. Diffusional deposition in leaks of fission products in atomic and molecular forms was briefly discussed, and since this process might not be effective for the removal of radioiodine from escaping air, a possible approach to this aspect of the problem was suggested.

In conjunction with the preceding, calculated results pertaining to leak flow rates and the extent of the viscous flow regime were presented for two idealized leak geometries, cylindrical and thin rectangular.

PART II. CONTAINMENT ENGINEERING

6. Nuclear Safety Pilot Plant

The Nuclear Safety Pilot Plant is an experimental facility to study the release, transport, and removal of fission products in a model containment vessel. Installation of the facility at the end of 1963 lacked about one month of completion. The general experimental program during the first six months after completion will be directed toward iodine behavior. Furnace development has, during the period, included improvements in fuel support, temperature distribution tests, incorporation of a two-color pyrometer, and elevated pressure tests.

7. Reactor Containment Handbook

A handbook on reactor containment for the designer, fabricator, and operator is being prepared by ORNL and its subcontractor, Bechtel Corporation. Draft copies now exist on nine of the twelve chapters. The two chapters previously distributed for external review are being revised, and copies of the other seven chapters will be distributed within two months. Drafts of the other three chapters exist in rough form and will be distributed for review in March. It is expected that review of the drafts will be completed this fiscal year and that the handbook will be published this summer.

PART III. NUCLEAR SAFETY INFORMATION CENTER

8. Nuclear Safety Information Center

The Nuclear Safety Information Center was established for the collection, storage, evaluation, and dissemination of pertinent information. Two reports have been issued and more than 750 documents have been incorporated into the information system. In addition to being engaged in several other studies the Center has answered 25 information requests and has had a more extensive correspondence requesting additional information.

Contents

Summary iii

Introduction 1

PART I. FISSION PRODUCT RELEASE AND BEHAVIOR

1. Properties of Fission Product Aerosols Produced by Overheated Reactor Fuels 3
   - Fission Product Release from Aluminum-Uranium Alloys 5
     - Effect of Burnup Level and Sample Geometry 5
     - Hot-Cell Tests of ORR Confinement System 7
     - Distribution of Fission Products Released from Molten Aluminum-Uranium Alloy 9
   - Fission Product Release from Stainless-Steel-Clad UO_2 Melted in Air 10
   - Multipin UO_2 Melting Experiments 15
   - Particles Produced by Melting Irradiated Fuel Materials 15
     - Particles from Melted Aluminum-Uranium Alloy 16
     - Particles from Melted Stainless-Steel-Clad UO_2 16
   - Deposition of Cesium and Distribution of Released Radioiodine Between Molecular and Particulate Forms 16
     - Radioiodine and Cesium Released from Aluminum-Uranium Alloy 16
     - Radioiodine Released from Stainless-Steel-Clad UO_2 22
   - Iodine Removal from Oxidizing Gases at High Temperatures 24

2. Release of Fission Products on In-Pile Melting of Reactor Fuels Under Transient Reactor Conditions 25
   - Experimental Assembly 25
   - Operating Procedure 27
   - Physical Examination of Components of the Experiment 1 Assembly 29
   - Physical Examination of Components of the Experiment 2 Assembly 31
   - Metallographic Examination of Fuel 31
   - Radiochemical Results 36
   - Conclusions 41

3. Behavior of Fission Products Released During In-Pile Destruction of Reactor Fuels 42
   - Effect of Gas Velocity on Release and Behavior of Fission Products 43
   - Released Fission Products Associated with Fine-Particle and Vapor Forms Determined by Diffusion Coefficient Measurement 44
   - Particulate Material Collected by Filters 47
   - Distribution of Released Fission Products Through Off-Gas System 52
   - Fission Product Fractionation 54
     - Vapor Transpiration Model 55
     - Comparison of Theoretical with Experimental Fractionation 58
     - Results of Fractionation Analysis 58

4. Characterization and Control of Accident-Released Fission Products 60
Investigation of the Occurrence and Behavior of Different Forms of Radioiodine 60
Investigation of Iodine Compound Formation at Relatively High Iodine Concentrations 60
Investigation of Iodine Compound Formation at Very Low Concentrations 62
Removal of Iodine and Volatile Iodine Components from Air Systems by Activated Charcoal 63
Measurement of the Characteristics of Radioactive Aerosols by Use of Fibrous Filters 64
5. Measurement and Prediction of Behavior of Released Fission Products in Reactor Systems 66
Innocuous Simulation of Aerosols Produced by Reactor Accidents 66
Decontamination Factors for Particle Deposition in Leaks as Applied to Leak Testing of Containment Vessels 66
Air Flow Rates Through Leaks 67
Particle Decontamination Factors and Leak Testing of Containment Vessels 70
Interpretation and Application of Containment-Vessel Leak-Testing Data 71

PART II. CONTAINMENT ENGINEERING

6. Nuclear Safety Pilot Plant 73
Status of Design and Construction 73
Furnace Development 73
Temperature Distribution Tests 74
Pyrometer Tests 77
Elevated-Pressure Tests 77
Viewing Tools 77
Experimental Program 77
7. Reactor Containment Handbook 78

PART III. NUCLEAR SAFETY INFORMATION CENTER

8. Nuclear Safety Information Center 79
Installations Visited and Meetings Attended 79
Center Studies 80
Nuclear Safety Contract File 80
Behavior of Iodine in Reactor Containment Systems 80
Evaluation of Iodine Effluent Monitoring and Area Monitoring Programs at Savannah River, Hanford, Idaho Falls, and Oak Ridge 80
Reactivity Effects of Fuel Element Bowing 80
Effectiveness of Safety Injection Systems for Emergency Reactivity Control 80
Kinetics of Large Reactor Cores 80
Review of Safety Analysis Procedures and Methods 80
Safety of Fast Gas-Cooled Reactors 80
Other Assignments 80
Other Information Activities 80

Introduction

This is the fourth of a series of semiannual reports describing the Nuclear Safety Research and Development Program which is being carried out at the Oak Ridge National Laboratory.

This program has six objectives: first, establishing critically safe conditions for handling fissionable materials; second, obtaining data which are needed to assess realistically the consequences of accidents in reactors and chemical plants; third, developing and evaluating countermeasures to be employed in the event of accidents entailing radioactive materials; fourth, critically evaluating and compiling, in handbook form, information on reactor containment; fifth, collecting, interpreting, and reporting data in certain key areas of reactor safety; and sixth, studying health problems associated with nuclear rocket debris. To achieve these objectives, the following activities are being pursued.

1. A study has been made of the reactivity effects which may result from fuel-plate displacement which can occur when this type of reactor suffers an accident. Calculational methods have been developed for predicting the magnitude of the reactivity changes and these are being compared with experimental values. This program will be completed by the end of this reporting period, and a final report will be written.
2. Experiments aimed at defining conditions which are safe from a criticality standpoint for the fabrication, storage, and handling of reactor fuels have been carried out. The information which has been developed is incorporated in the *Nuclear Safety Guide*, TID-7016. Further studies will be carried out on important new reactor fuels.
3. Out-of-pile and in-pile measurements are being made to assess the fractional releases of the fission product inventories of important reactor fuels in the event of an accident. Those chemical and physical properties which bear on the removal of the released fission products from containment-vessel atmospheres and on leakage through a containment vessel to the environment are being studied.
4. Promising methods for removing fission product aerosols from a containment-vessel atmosphere in the case of an accident are being investigated.
5. The small-scale investigation of fission product release from fuels and of the behavior of the resulting aerosols will be substantiated on a larger scale in the Nuclear Safety Pilot Plant now being constructed. The pilot plant will be of sufficient size to better assess the time-space behavior of aerosols than is possible in the laboratory studies.
6. Accidents in fuel reprocessing and radioisotope production facilities may have more serious consequences than the accidents which are postulated for reactors. A small program, is being carried out for the purpose of examining the hazards associated with radiochemical plants in the same way that those associated with reactors are being investigated.
7. As an aid to reactor designers, a Reactor Containment Handbook – a critically evaluated compilation of available information on this subject – is in preparation.
8. A Nuclear Safety Information Center has been established and in operation since July 1963.
9. Studies aimed at evaluating the radiobiological hazards resulting from the operation of nuclear-powered spacecraft are under way.

Part I

Fission Product Release and Behavior

Reactor Chemistry Division

W. R. Grimes, Division Director
G. M. Watson, Coordinator

1. Properties of Fission Product Aerosols Produced by Overheated Reactor Fuels

G. W. Parker G. E. Creek
W. J. Martin R. A. Lorenz
C. J. Barton

For a number of years a substantial part of the ORNL Nuclear Safety Program has been devoted to parametric studies of the release of fission products in the out-of-pile melting of reactor fuels. Due in part to these studies, our knowledge of fission product release from fuel elements consisting of aluminum-uranium alloys or of clad uranium dioxide is now sufficiently complete to allow certain useful generalizations[1] to be made concerning the type and fractional release of the various fission products as a function of the experimental conditions. Evaluation and understanding of mechanisms which tend to lessen the severity of reactor accidents represent a logical extension of the out-of-pile fission product release studies. These mechanisms include agglomeration in, and deposition of particles from, aerosols produced by overheated reactor fuels, as well as chemical reactions of the fission products with structural materials. Filtration and sorption characteristics of various fractions of the aerosols also form an important part of the studies. Accordingly, the reactor fuels will continue to be melted as a source of fission products, and the fractional release will continue to be determined, but major emphasis will be placed on the study of the behavior of fission product aerosols. For this purpose the Hot-Cell Confinement Mockup Facility, previously described,[2] is now in full operation. A flow diagram of the facility is shown in Fig. 1.1.

The aerosol confinement tank and the attached filter unit fitted with diffusion tubes provide an opportunity to study the behavior of fission product aerosols as a function of parameters such as:

1. transport of fission products to the confinement tank;
2*a*. plateout in the confinement tank,
b. persistence or stability of the radioaerosol in the confinement tank,
c. deposition velocity to the confinement tank walls;
3*a*. performance characteristics of the simulated filter-charcoal system,

[1] F. R. Bruce, *Status of Nuclear Safety Research and Development at the Oak Ridge National Laboratory*, paper presented at the Atomic Industrial Forum Annual Conference, New York, Nov. 18–21, 1963.

[2] C. J. Barton *et al.*, *Nuclear Safety Program Semiann. Progr. Rept. June 30, 1963*, ORNL-3483, p. 33.

UNCLASSIFIED
ORNL-DWG 63-6052

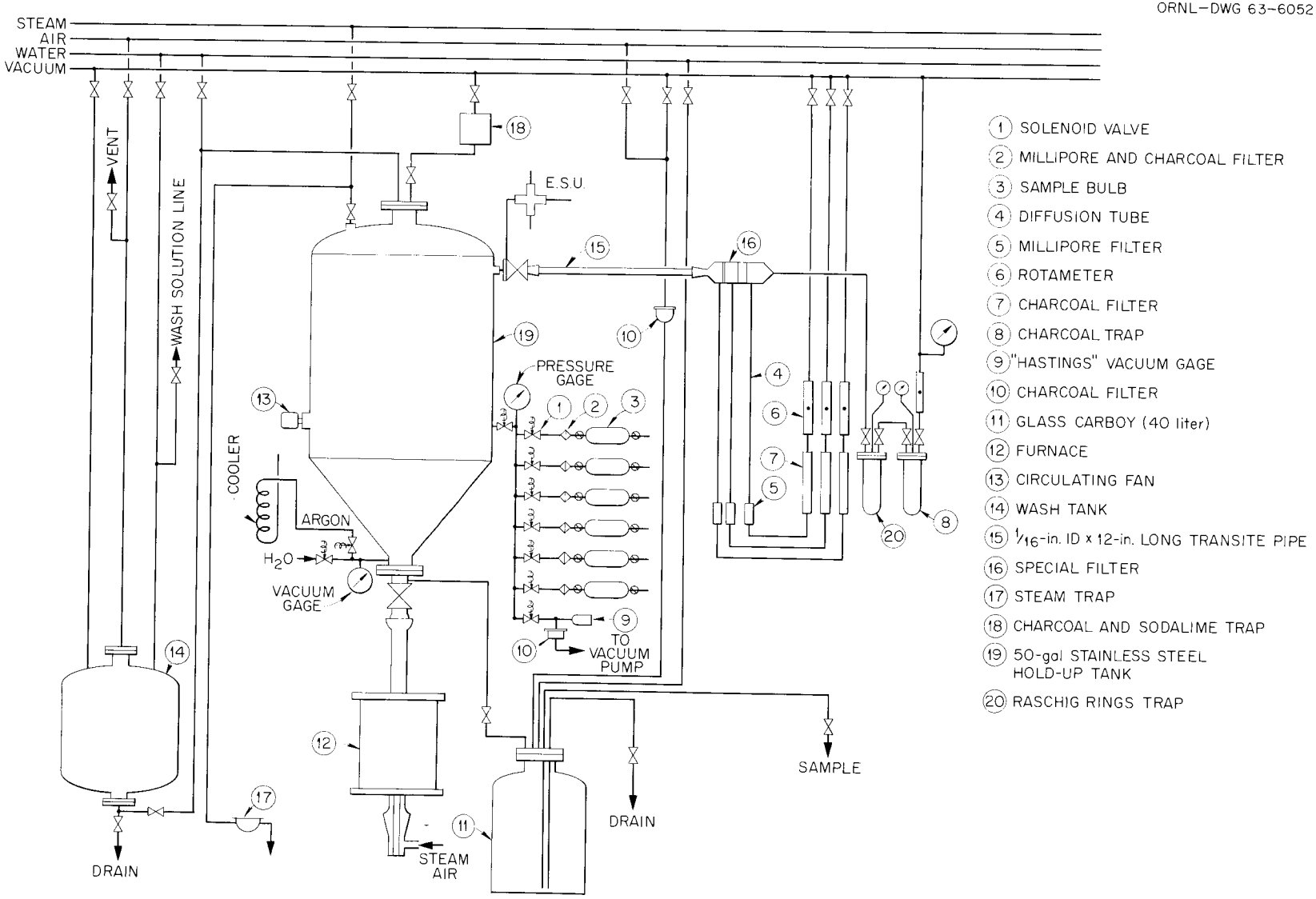

Fig. 1.1. Scaled-up Fission Product Release Experiment.

b. penetration of the charcoal beds by unreactive forms of radioiodine,

c. desorption of iodine from the tank wall;

4. characterization of the smallest particle sizes (molecular to 200 A) of the mixed aerosol by the diffusion-tube method;
5. electron microscopic studies of the particle-size distribution of particles sampled by various means.

This section includes results of studies of the behavior of fission products released from molten aluminum-uranium alloys and from stainless-steel-clad uranium dioxide melted in air. Studies of the properties of the released fission product aerosols including the removal efficiency of radioiodine by a confinement system of the type used in the ORR, the types of particles released, and the distribution of radioiodine between molecular and particulate forms are described. The results of some additional studies on the removal of iodine from oxidizing gases at high temperatures are also included.

FISSION PRODUCT RELEASE FROM ALUMINUM-URANIUM ALLOYS

Effect of Burnup Level and Sample Geometry

The results of experimental work on the effect of several parameters on fission product release from irradiated aluminum-uranium alloy specimens were given in the previous progress report.[3] Data in that report were obtained mainly with 23.6%-burnup fuel specimens and with some specimens irradiated at the tracer level. The present report presents an extension of data on the burnup effect to intermediate levels of irradiation, 3.2 and 9.0% burnup.

A comparison of data in Table 1.1 on fission product release measured in laboratory-scale horizontal furnace equipment with a flowing air stream indicates a relatively small burnup effect except for iodine and the rare gases. While release data at the higher temperatures are somewhat incomplete, the data at the lower temperatures, which are of most importance, generally show an increased release of iodine and the rare gases above that at tracer level by a factor of 3 or 4. In only one other case, that of cesium released from the 23.6%-burnup material, are the release values significantly higher than at tracer level. These are only a factor of about 2 higher than those obtained at the tracer level and at the other burnup levels.

The absence of a clearly definable burnup effect on the release of less-volatile elements suggests that the trace-concentration effect, possibly due to occlusion of atoms or ions in internal crystal structural defects or to a very low solubility limit, is saturated at a relatively low burnup level, below 3.2% (see Fig. 1.2).

A difficulty in interpreting the results of the burnup parameter studies, which was not properly assessed until this investigation was in its final stages, is the relatively wide variation in burnup level of fuel plates as a function of the distance from the point of maximum flux. It is possible, for instance, that some of the "3.2%" burnup samples could have actually had almost as much radiation as some of the "9%" burnup samples. This possibility is being investigated by fission product radiochemical analysis and by mass spectrometer determinations of uranium isotope ratios. The results are not complete, but the data obtained show smaller differences in burnup than the nominal values in Table 1.1 indicate.

In the Hot-Cell Confinement filter tests conducted to measure the transport and retention of fission products released from aluminum-uranium alloy, an opportunity was presented to compare total release values of the major fission products determined previously on a small laboratory scale with those obtained with relatively large samples. In the small-scale work, samples consisting of three punched $^5/_{16}$-in.-diam disks were heated in an open silica boat and thus melted with little, if any, movement.

In contrast to this, in the hot-cell tests, a long strip containing $2\frac{1}{2}$ in.^{2} of fuel plate (a 25-fold increase in sample size) was suspended over an open crucible and was melted beginning from the lower end until the melt dropped into the crucible. There has been speculation that the increase in surface area produced by flowing and dripping would lead to higher releases. The results in Table 1.2 show that the observed release was consistent with the results of small-scale work for iodine at the estimated temperature (750°C), but high values were obtained for cesium. Instead of the expected 3.6% release, values of 8

[3]G. W. Parker *et al.*, *Nuclear Safety Program Semiann. Progr. Rept. June 30, 1963*, ORNL-3483, p. 9.

and 15% were observed. These results were obtained in air and in a steam-air mixture, respectively, with an air flow rate of about 3 liters/min over the sample. The total time molten was less than 10 min. The maximum temperature was more likely to have been higher than the estimated value rather than lower. A higher fuel temperature would have given a corresponding increase in iodine release. It must be concluded, therefore, that the change in geometry in the hot-cell tests, as compared with the laboratory-scale tests, did not produce a significant change in iodine release from high-burnup aluminum-uranium alloy. The release of cesium was found to be higher in the

Table 1.1. Effect of Temperature and Burnup on Fission Product Release from Irradiated Aluminum-Uranium Alloy[a]

Burnup Level (%)	Release (%)				
	Iodine	Tellurium	Cesium	Ruthenium	Rare Gas
			At 750°C		
Trace	3.7	~0.01	~1.2		4.3
3.2	52.8	0.14		0.0005	98.2
9.0	54.2	0.05	1.3	0.004	
23.6	56	~0.3	~3.6	0.07	~98
			At 800°C		
Trace	16.7	0.02	1.6	~0.002	37.2
3.2		~0.3	1.1	0.01	99.4
9.0	71.9	0.04	1.7	~0.01	99.4
23.6	78.6	~0.5	3.8	0.08	99.4
			At 900°C		
Trace	28.8	0.03	2.6	~0.004	54.0
3.2	97.4	6.1	2.7	0.002	>99.5
9.0	95.0	1.9	7.5		>99.5
23.6	92	2.0	6.2	0.1	>99.9
			At 1000°C		
Trace	41.2	0.14			
3.2	98.5	5.3	3.2	0.04	~100
9.0	97.2	6.3	3.5	0.2	~100
23.6	97.3	9.7	8.8	0.25	99.8
			At 1100°C		
Trace	(34.3)	1.3	~6		71.8
3.2	99.5	31.7	9.5	0.03	~100
9.0	93.5	37.1	19.6	0.25	~100
23.6	98.4	~50	12.4	0.6	100

[a]Specimens were heated for 2 min at maximum temperature in air flowing at 250 cc/min.

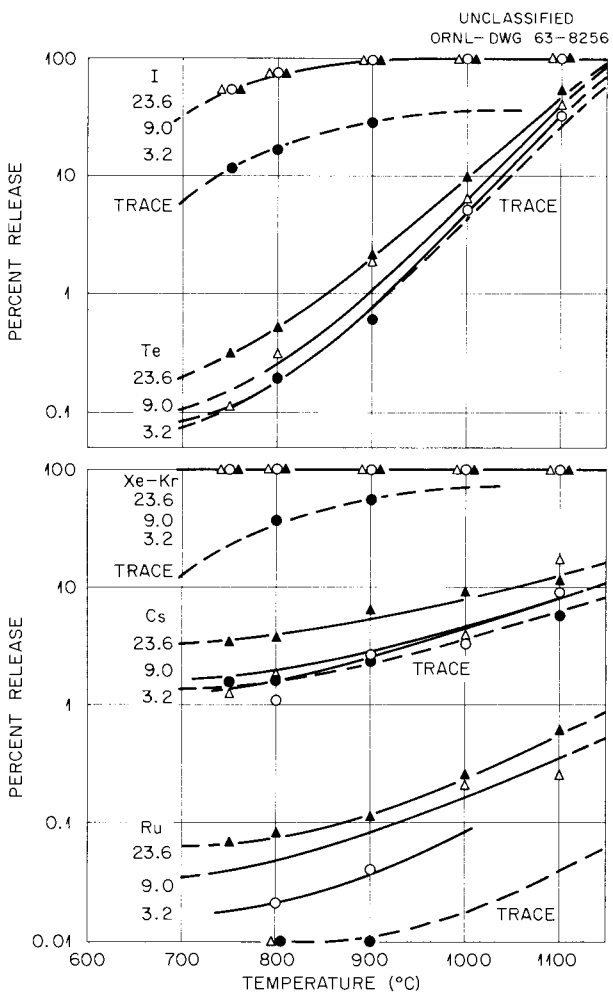

Fig. 1.2. Burnup Effect in Fission Product Release from Aluminum-Uranium Alloy Melted in Air.

Table 1.2. Comparison of Laboratory-Scale and Hot-Cell Releases from 23.6%-burnup Aluminum-Uranium Alloy Specimens

Conditions (at 750°C)	Release (%)	
	Iodine	Cesium
Laboratory, in air	56	3.6
Hot cell, in air	54	8.2
Hot cell, in a steam-air mixture	49	15

hot-cell tests for reasons that are not clear at present.

Hot-Cell Tests of ORR Confinement System

Results of two laboratory tests of the filter and charcoal adsorption traps proposed for use in the containment system of the ORR were presented in the previous progress report.[4] The radioiodine used in these tests was produced by melting irradiated aluminum-uranium alloy specimens, the type of fuel employed in the ORR. However, it was considered desirable to conduct additional tests under more realistic reactor accident conditions, including an appreciable aging period for the released aerosol and meltdown in the presence of steam. Two tests were performed in the Hot-Cell Confinement Mockup Facility mentioned previously. The filter and charcoal holder employed in the previous laboratory tests was modified to permit the addition of two more $\frac{3}{4}$-in.-long charcoal cartridges and one more absolute filter following the charcoal traps. A view of the unassembled filter and charcoal-trap holder is shown in Fig. 1.3.

The hot-cell tests were performed as follows: A strip of irradiated aluminum-uranium alloy plate $\frac{1}{2}$ in. wide by 5 in. long was inserted in the furnace tube of the Hot-Cell Confinement Mockup Facility. A small resistance furnace, preheated to provide a furnace temperature of 750°C, was brought slowly into position to surround the specimen, starting at the bottom. Filtered cell air passed the specimen at a rate of 1 liter/min in the first experiment to carry fission products and particles from the melting fuel specimen into the 180-liter aerosol tank, which was initially at reduced pressure. Soon after the fuel was completely melted, which required a heating period of about 7 min, the furnace was allowed to cool, and the aerosol tank was brought up to atmospheric pressure.

In the second test, a steam-air mixture (0.5 liter/min of air and 8 liters/min of saturated steam) was used instead of filtered air during the melting period (10 min).

After the aerosol had aged for about 45 min with intermittent stirring, the exit valve of the aerosol

[4]C. J. Barton *et al.*, *Nuclear Safety Program Semiann. Progr. Rept. June 30, 1963*, ORNL-3483, p. 34.

Fig. 1.3. Unassembled View of Filter-Charcoal Gas Sampling Unit.

tank was opened, and the contents of the tank was drawn through the filters and charcoal packs at a rate of 3 liters/min by controlled reduced pressure. An amount of argon equivalent to the rate of removal of air was added at the bottom of the aerosol tank to increase the efficiency of displacement of the aerosol. It was observed, by means of an in-line gas activity detector, that the counting rate of xenon activity passing through the filters diminished by a factor of almost 10 during the withdrawal of 1.5 tank volumes from the aerosol tank. Gas velocities corresponding to the 3-liter/min flow rate were 25 fpm through the roughing filter, 5 fpm through the absolute filter, and 50 fpm through the $\frac{3}{4}$-in.-thick charcoal beds.

At the end of the aerosol displacement period, about 90 to 100 min, the filter pack was disassembled, and the filters and charcoal traps were analyzed for I^{131} and Cs^{137}. No other isotopes were released from the aluminum-uranium specimens in significant quantities under the conditions employed. Results of the two hot-cell tests are shown in Table 1.3 in terms of the percentage of released material retained by each part of the filter assembly and by the large backup, refrigerated charcoal trap.

The efficiency of iodine retention (99.97%) found in the present experiments was slightly lower than that found in the previous series of laboratory experiments mentioned above (99.99%). The values found in the hot-cell experiment may be more realistic because of the provision for aerosol aging and because of the additional charcoal traps to permit determination of the amount of iodine that passed through the first two charcoal traps. The level of cesium activity in the charcoal traps was below the limit of detection, and the amount found in the second absolute filter was so low that it was of doubtful significance.

In summary, the results of the hot-cell tests demonstrated that the iodine and cesium retention ability of the proposed ORR confinement system is quite satisfactory and that aging of the released aerosol for more than an hour had little, if any, effect on retention efficiency.

Distribution of Fission Products Released from Molten Aluminum-Uranium Alloy

Observations of fission product transport and of particle behavior were made during the hot-cell tests of the ORR confinement system described in the previous section. Results are presented in Table 1.4. The activity designated in Table 1.4 as retained in the furnace tube includes that recovered from the quartz furnace tube and the quartz "chimney" that extended through the ball valve at the bottom of the aerosol tank. The temperature of these parts of the apparatus during the melting operation varied from the maximum furnace temperature, approximately 800°C, to that of the cell air, about 25°C. This part of the deposited activity, therefore, should not be considered to be plated out solely in a high-temperature zone. The fission products that deposited on the wall of the aerosol tank during the 40- or 45-min aging period and the

Table 1.3. Retention of Iodine and Cesium by ORR Confinement System Components

Component of Filter Pack	Percent of Activity Reaching Filters Retained by Each Component			
	Iodine		Cesium	
	Dry Air	Moist Air	Dry Air	Moist Air
Roughing filter[a]	43.50	11.18	98.56	98.85
1st absolute filter[a]	2.88	12.23	1.44	1.15
1st charcoal trap[a]	53.0	76.2		
2d charcoal trap[a]	0.40	0.39		
3d charcoal trap	0.03	0.026		
4th charcoal trap	0.003	0.008		
2d absolute filter[a]			8×10^{-6}	9×10^{-5}
3d absolute filter			3×10^{-8}	3×10^{-6}
Backup traps	0.007	0.0003	0.0005	$<10^{-5}$
Percent net ORR system efficiency	99.97	99.97	99.99+	99.99+

[a]Units included in the proposed ORR confinement system and included in the calculation of ORR system efficiency.

Table 1.4. Distribution of Iodine and Cesium Released from Molten Aluminum-Uranium Alloy in Hot-Cell Tests

Location of Activity	Percent of Released Material Retained in Each Location			
	Iodine		Cesium	
	Dry Air	Moist Air	Dry Air	Moist Air
Furnace tube	1.8	3.9	45.8	32.5
Aerosol tank	82.0	48.1	17.3	29.4
Steam condensate (30 ml)		6.7		5.9
Transite pipe (12 in. long)	1.2	3.1	0.06	0.2
Filters	6.9	8.9	36.9	32.1
Charcoal beds	8.0	29.2	0	0

1.5-hr displacement period were recovered by washing with dilute nitric and hydrofluoric acids. The amount of steam condensate collected in the moist-air experiment was 30 cm^3, as compared with the calculated value of 100 cm^3 added to the vessel as steam. It is assumed that the remaining 70 cm^3 of water remained as a film on the interior surfaces of the aerosol tank and was consumed in saturating the air of the tank at the ambient temperature.

A Transite pipe was inserted in the exit air stream from the aerosol tank to simulate the air duct in the ORR confinement system that is made of this material. The velocity through the $\frac{1}{8}$-in.-diam hole in the pipe was about 1250 fpm. The filter-charcoal combination is described in the previous section of this report.

Comparison of distribution data in dry and moist atmospheres shows that iodine deposited more rapidly on a dry stainless steel surface than on the same surface saturated with water. This result agrees with data obtained by British investigators.[5] Cesium, on the other hand, deposited more rapidly on the moist surface, which might have been anticipated because of the high water solubility of cesium compounds. The different effect of the wet steel surface on the deposition rates of cesium and iodine indicates that the two elements were not combined as CsI to any large extent in the confinement-tank aerosol. Since the melting of the fuel specimens occurred in the presence of air and moisture, it seems likely that cesium was in the form of Cs_2O or CsOH, neither of which would react readily with molecular iodine. The comparatively small amount of iodine and cesium found in the steam condensate should not discourage interest in steam or water washout methods of removing fission product aerosols from a containment vessel, because the small quantity of water introduced into the confinement vessel in this experiment is not representative of the quantity that could be employed in a reactor accident.

The deposition of such a small amount of iodine and cesium in the Transite pipe probably resulted from the high velocity of the gas. The data thus indicate that only a very small fraction of the fission products would deposit in a duct carrying airborne fission products to a cleanup system unless the duct were quite long or the air velocity were much less than that employed in this test.

The low value for the fraction of iodine collected in the filter-charcoal pack in the dry-air experiment simply indicates that there was not much left in the aerosol tank to be collected because of the rapid deposition of iodine on the dry stainless steel tank surface.

FISSION PRODUCT RELEASE FROM STAINLESS-STEEL-CLAD UO_2 MELTED IN AIR

A slight modification of the hot-cell confinement equipment in the aluminum-alloy melting and filter test experiments described previously was used to melt tracer-level-irradiated, stainless-steel-clad UO_2 by induction heating.

The specimen melted consisted of two 95%-dense pellets (combined weight, 30 g) irradiated at trace level and contained in a welded stainless steel capsule. The arrangement of the furnace tube, zirconia crucible, and induction heating coil is shown in Fig. 1.4. An air flow rate of 3 liters/min was maintained during the melting period, which lasted approximately 2 min. The duration of melting was limited by the time required for the molten UO_2 to form a solid solution with the zirconia crucible and to break through the bottom.

The furnace tube and the melted UO_2 specimen are shown in Fig. 1.5. The segregated stainless steel button surrounded by UO_2-ZrO_2 is also at the bottom of the melt crucible in Fig. 1.6. Melted UO_2 is also seen coating the ZrO_2 crucible walls in the left section of the picture. The most striking difference visually observed between the quiescent melting of aluminum-uranium alloy and of melting UO_2 was in the appearance in the latter case of a brown-to-black smoke trail leading into the confinement vessel and some evidence of boiling in the white-hot mixture in the ZrO_2 crucible.

It was expected that a significant amount of UO_2 would be vaporized and deposited in the confinement system, and it was not surprising to find evidence of this on examination of the sampling filters and the mainstream roughing filter. The total quantity of vaporized UO_2 that penetrated beyond the furnace tubes, however, was found to be

[5] J. F. Croft, R. A. Iles, and R. E. Davis, *Experiments on the Surface Deposition of Air-borne Iodine by High Concentration*, UKAEA Report AEEW-R-265 (June 1963).

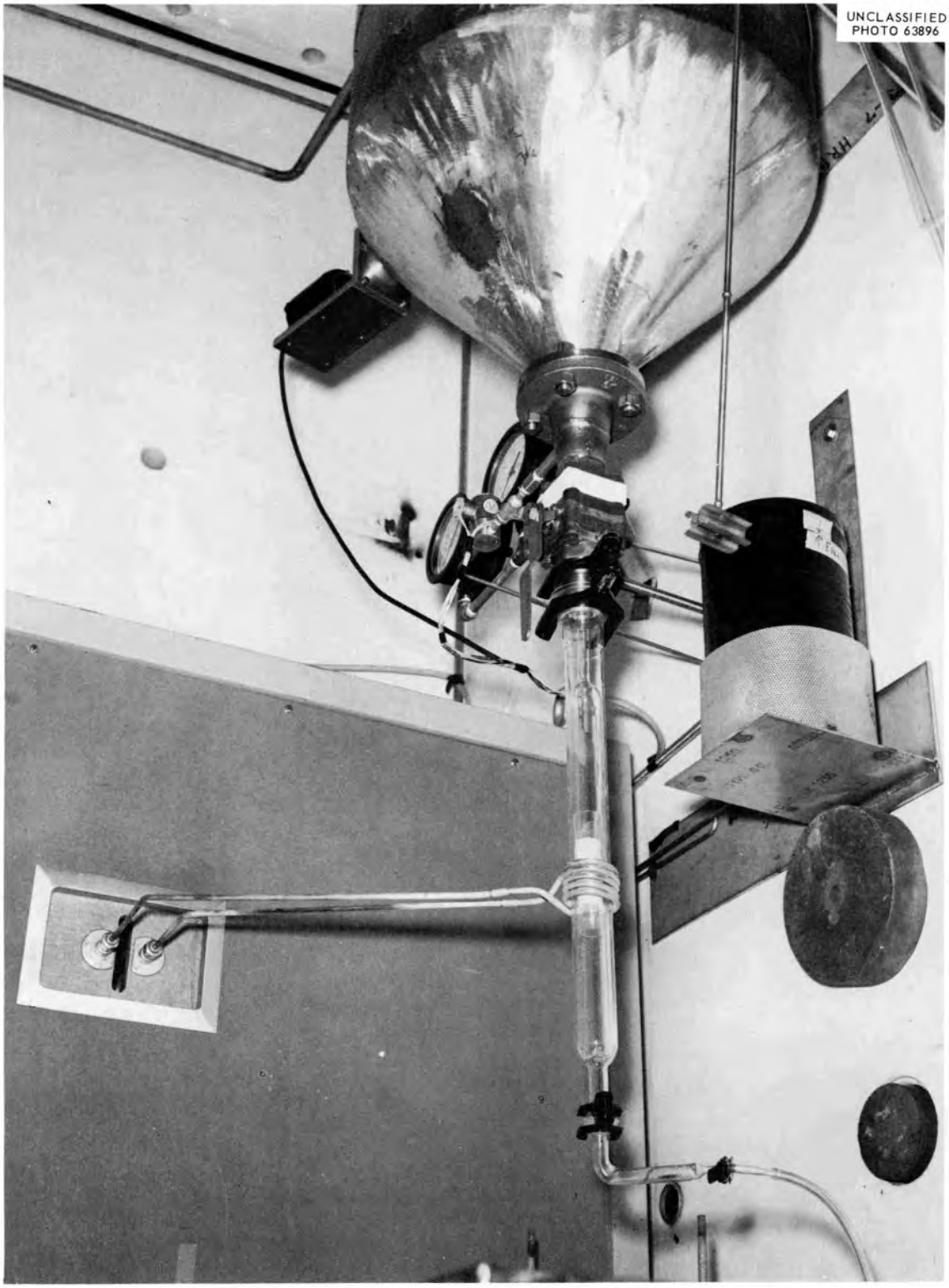

Fig. 1.4. Arrangement of the Furnace Tube, Zirconia Crucible, and Induction Heating Coil.

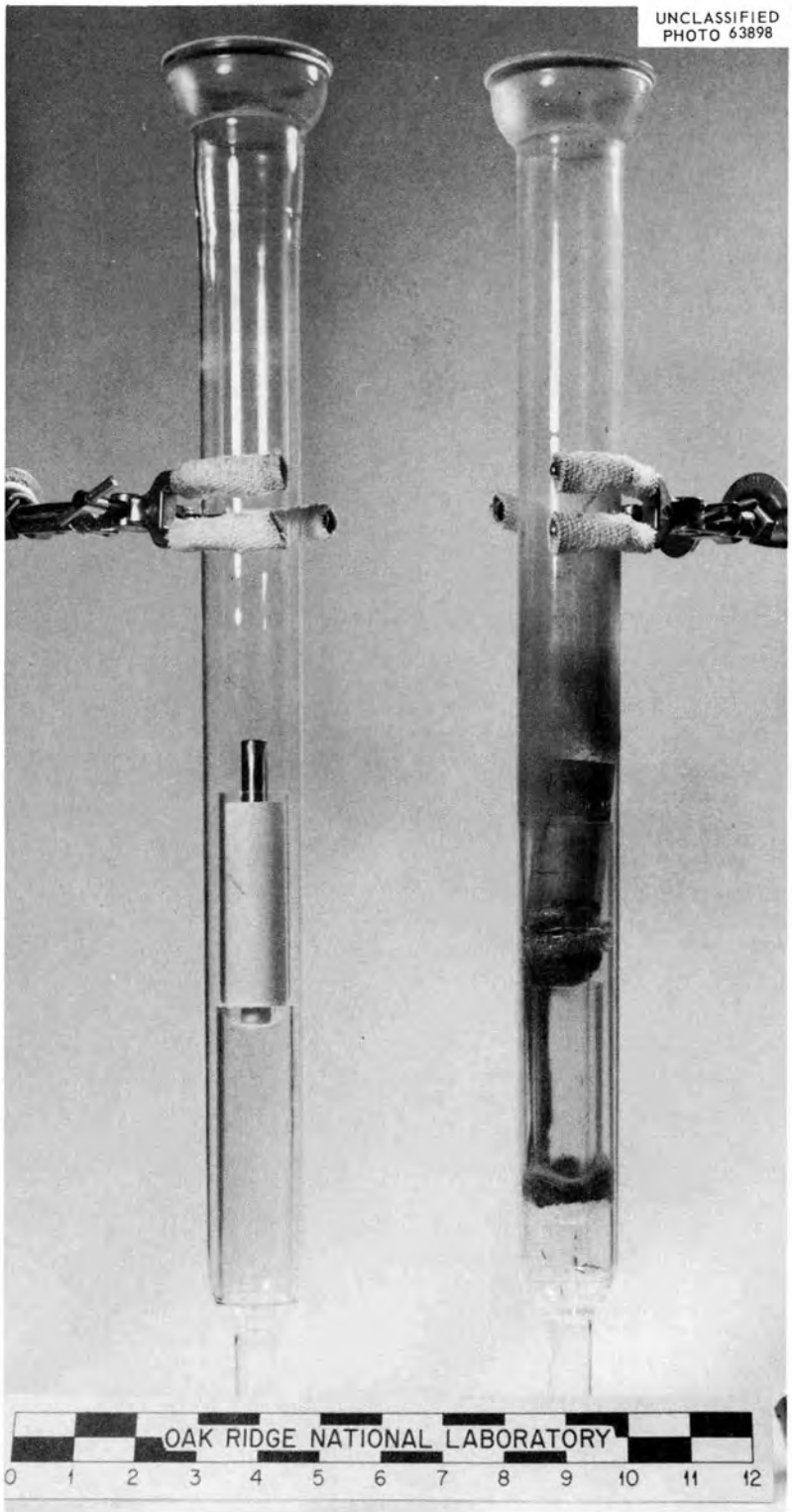

Fig. 1.5. Furnace Tube and UO_2 Specimen Before and After Melting.

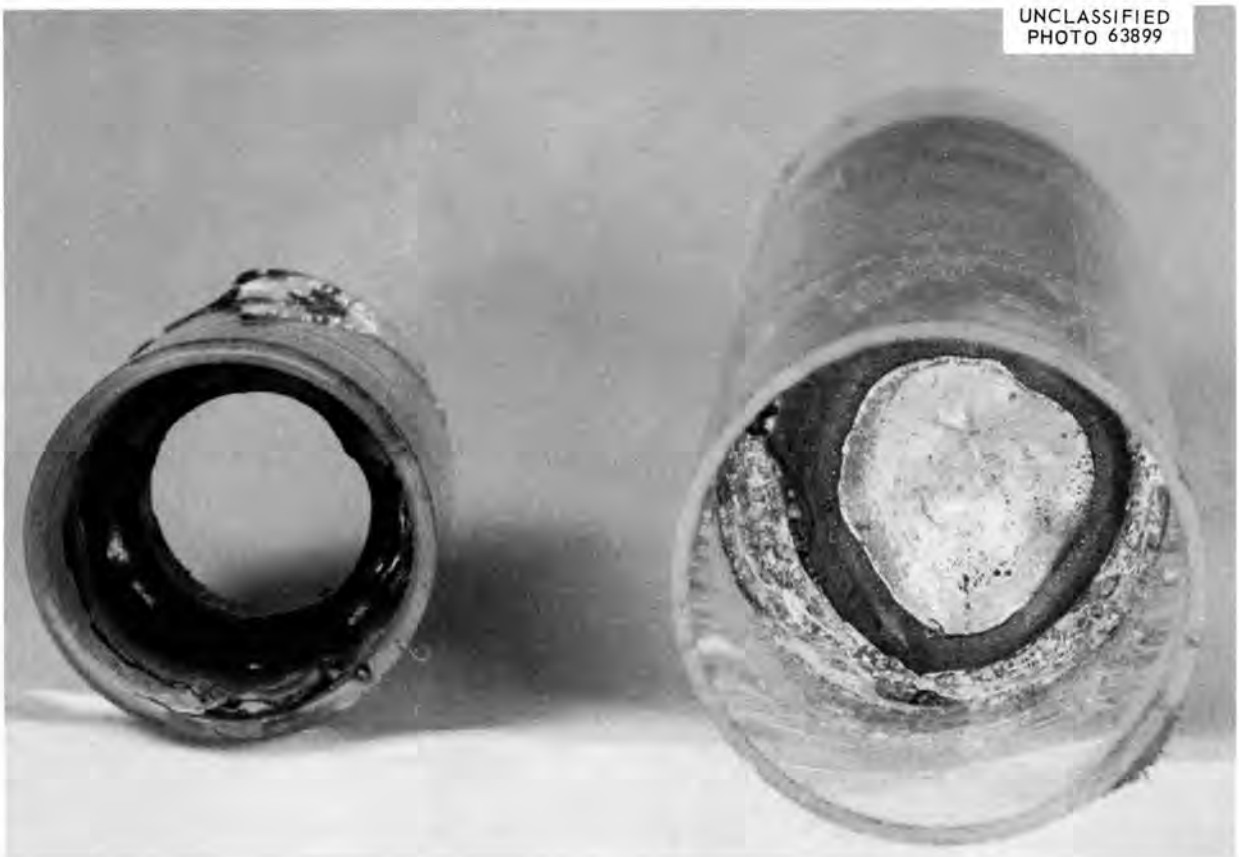

Fig. 1.6. View of Melt Residue Including Fused UO_2 (Left) and Stainless Steel Button (Right).

very small (only 1 mg from 29 g of UO_2), suggesting that most of it was deposited on the furnace tube wall.

In this experiment, bronze screens (alternate for copper) were inserted at two points in the modified filter pack (Fig. 1.7) with the intention of providing additional information on the distribution of the various forms of iodine, as in the Windscale model[6] of the May pack (Fig. 1.8). It was perhaps unfortunate that pure copper screens were not available, since the performance of the bronze screens indicated a fairly low efficiency for the retention of molecular iodine. This was shown by the small difference in uptake between the first and the last screen (only a factor of 2) and by a significant iodine concentration remaining airborne after passage through the screens.

Agglomeration, sedimentation, and deposition of the aerosol occurred in various sections of the equipment, as shown by the distribution of activity given in Table 1.5. The high stability of the aerosol is apparent from the high values (19 to 50%) of the released activity which remained airborne over several hours. The relatively low deposition of iodine (55%) and tellurium (30.5%) on the walls of the confinement vessel may possibly be due to the very low (tracer-level) concentrations of fission products in the aerosol product in this experiment.

A relatively high percentage of a penetrating form of iodine was also indicated by the presence of over 1% of the total iodine in the third and fourth charcoal cartridges and by the apparent loss of 0.3% to the large scavenging traps. Again, as suggested in similar work in the United Kingdom, a low iodine concentration is apparently more likely to give a higher percentage of the penetrating form than may result from the presence of higher, more realistic, concentrations of iodine in the aerosol.

[6] G. W. Parker *et al.*, *Nuclear Safety Program Semiann. Progr. Rept. Dec. 31, 1962*, ORNL-3401, p. 11.

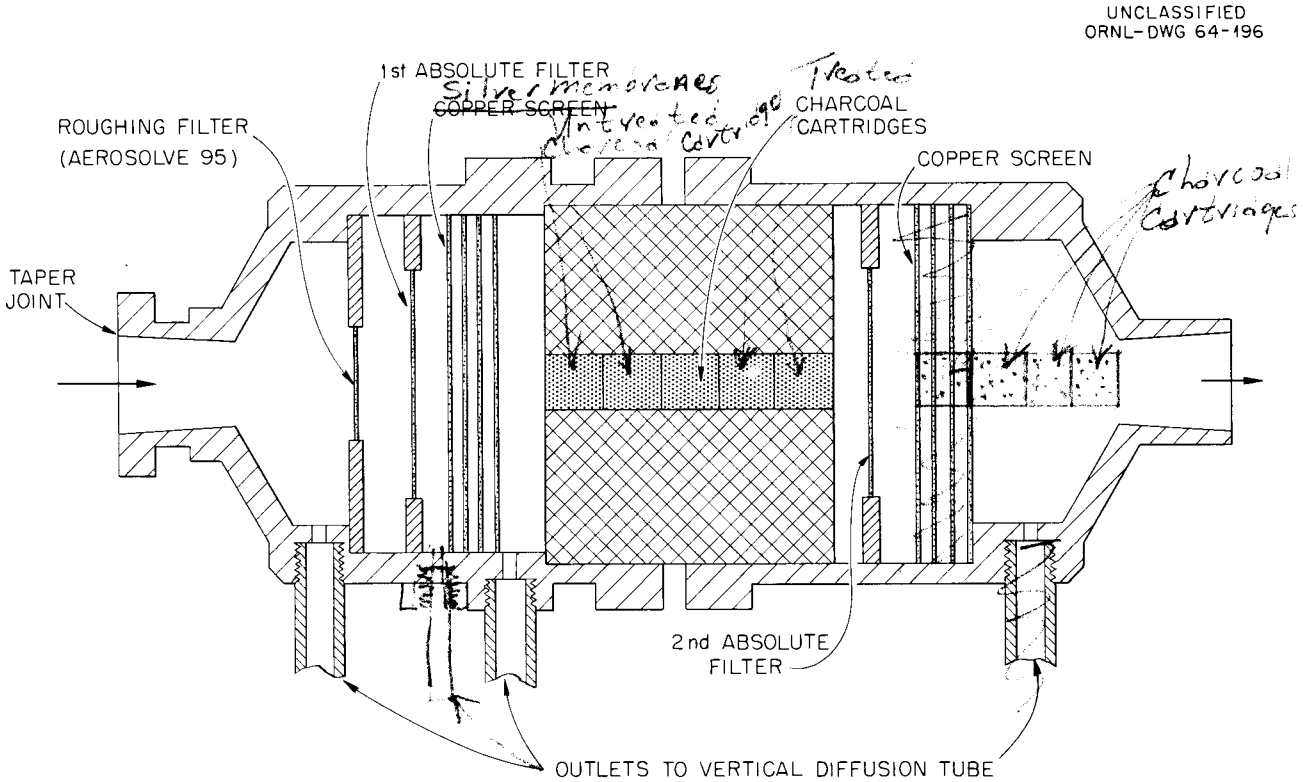

Fig. 1.7. The Radio-Aerosol Test Filter (May Pack). ORNL model with diffusion tube ports.

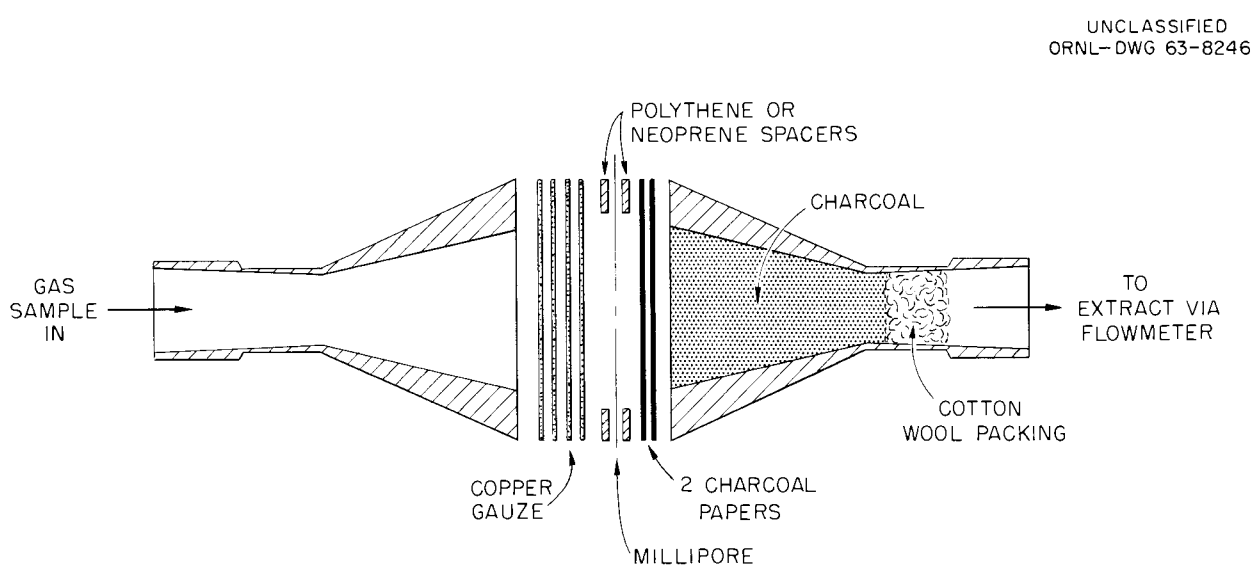

Fig. 1.8. The Radio-Aerosol Test Filter (May Pack). Windscale model.

Table 1.5. Distribution of Activity Released in Hot-Cell UO_2 Meltdown Test and Efficiency of a Confinement Filter System

Location of Activity	Released Material Retained (%)				
	Iodine	Tellurium	Cesium	Ruthenium	Uranium
Furnace tube	7.8	20.1	11	46.9	*a*
Aerosol tank	56.4	30.5	70	32.4	84.4
Filter pack					
Roughing filter	19.0	49.4	16.6	20.6	15.6
1st absolute filter	0.25	0.008	2.4	0.06	
Bronze screens	5.7				
1st charcoal trap	6.6				
2d charcoal trap	2.9				
3d charcoal (added unit)[b]	0.7				
4th charcoal (added unit)[b]	0.4				
2d absolute filter	0.00005				
2d bronze screens (added unit)[b]	0.0002				
Backup traps (added unit)[b]	0.25				
Percent retention	98.6	100	100	100	100

[a]Not included in released fraction.
[b]Not included in retention.

MULTIPIN UO_2 MELTING EXPERIMENTS

G. W. Parker R. A. Lorenz

A considerable amount of information on physical appearance of UO_2 pellets melted by means of centered tungsten resistors, and on the release of fission products from trace-level-irradiated fuel in experiments of this type, was included in previous progress reports.[6,7] This program is still regarded as a potential source of significant information on release of fission products from simulated reactor loss-of-coolant accidents, but no additional information was obtained during this period because of the effort on the TREAT experiments. It was determined that a 110-kw power source would be needed to melt a 19-pin array of UO_2 pellets, a further scaleup of the seven-pin cluster reported earlier.[7] A power source having this capacity is not available at present.

[7]G. W. Parker and R. A. Lorenz, *Nuclear Safety Semiann. Progr. Rept. June 30, 1963*, ORNL-3483, p. 14.

PARTICLES PRODUCED BY MELTING IRRADIATED FUEL MATERIALS

Particles produced by melting high-burnup aluminum-uranium alloy specimens to test the ORR confinement system and during the melting of low-burnup stainless-steel-clad UO_2 (as described in other sections of this report) were collected on three different materials: absolute filters, an electron microscope grid of an electrostatic precipitator, and on walls of diffusion tubes.

Particles from Melted Aluminum-Uranium Alloy

Iodine and cesium were the only fission products released in significant amounts under the conditions of the ORR confinement system tests: irradiated (23.6% burnup) aluminum-uranium alloy heated in flowing air or in a steam-air mixture at 750 to 800°C for 8 to 10 min. The particles included in the present studies were those remaining airborne after at least a $\frac{3}{4}$-hr aging period in the 180-liter aerosol tank and sampled during the 1.5-hr period required to displace the aerosol from the tank.

A photograph of particles resulting from the melting of the aluminum-uranium alloy material in a steam-air atmosphere and collected by an electrostatic precipitator from a side stream immediately after leaving the aerosol tank is shown in Fig. 1.9. The small particles noted in the picture were approximately 150 A in diameter, while the larger ones had an average diameter of about 1500 A. A photograph of particles that were removed by a membrane filter from a side part of the effluent stream from the aerosol tank, sampled just before passing through filters, is shown in Fig. 1.10. This side stream passed through a 10-ft length of silver-coated copper diffusion tube before reaching the filter, thus removing the small particles. The remaining particles ranged in diameter from about 0.05 to 3.0 μ, and the large particles undoubtedly were agglomerates of smaller particles. The identity of the particles and of the activity associated with them cannot be established from the pictures, but cesium was the only radioisotope found on the filters.

Particles from Melted Stainless-Steel-Clad UO_2

Particles produced during the melting of a stainless-steel-clad, trace-irradiated UO_2 specimen in the Hot-Cell Confinement Facility were collected in the same manner used in the aluminum-uranium alloy studies described above. A sample of the aerosol withdrawn about 1 hr after the meltdown and filtered through a membrane showed a unique "rosette" type particle suggestive of the vapor of stainless steel cladding. These particles are reproduced in Fig. 1.11. Sizes range from 0.1 to 1.0 μ. After 2 hr of aging, the aerosol when sampled electrostatically showed a large abundance of particles in the 100- to 200-A size and a few in the 1- to 2-μ size, as shown in Fig. 1.12.

Data obtained with diffusion tubes that sampled side streams of the effluent air from the aerosol tank before and after passing through an "absolute" filter were used to study the distribution of activity as a function of particle size. The analyses of the data are given in the following section.

DEPOSITION OF CESIUM AND DISTRIBUTION OF RELEASED RADIOIODINE BETWEEN MOLECULAR AND PARTICULATE FORMS

The evolution of the filter pack or the "May pack" (Fig. 1.8), a combination of a high-efficiency filter and charcoal beds, has led to the addition of several devices to aid in analyzing the mixed aerosol for its radioiodine content in various chemical and physical states. The first refinement was the addition of copper gauze by May and Megaw,[8] which was found to retain molecular iodine only with a high efficiency. A later addition of charcoal-impregnated filter papers was intended to aid in the distinction between several forms of nonparticulate unreactive iodine which were not retained by the high-efficiency membrane filter. This has been useful in characterizing the fraction of iodine in the form of organic compounds.

In the ORNL test program, a further adaptation of the May pack (Fig. 1.8) has been made by incorporating diffusion-channel ports between stages of the filter unit, providing a means of studying the distribution of aerosol radioactivity (as a function of particle size), including iodine in the molecular form. The ORNL modification of the May pack is shown in Fig. 1.7.

Radioiodine and Cesium Released from Aluminum-Uranium Alloy

Data obtained by use of diffusion tubes that sampled side streams of the effluent air from the aerosol tank before and after passing through an "absolute" filter are shown in Figs. 1.13 and 1.14. Deposition gradients, from which particle sizes were calculated by use of the Browning and Ackley

[8] W. J. Megaw and F. G. May, *Reactor Sci. Technol.* 16, 427–36 (1962).

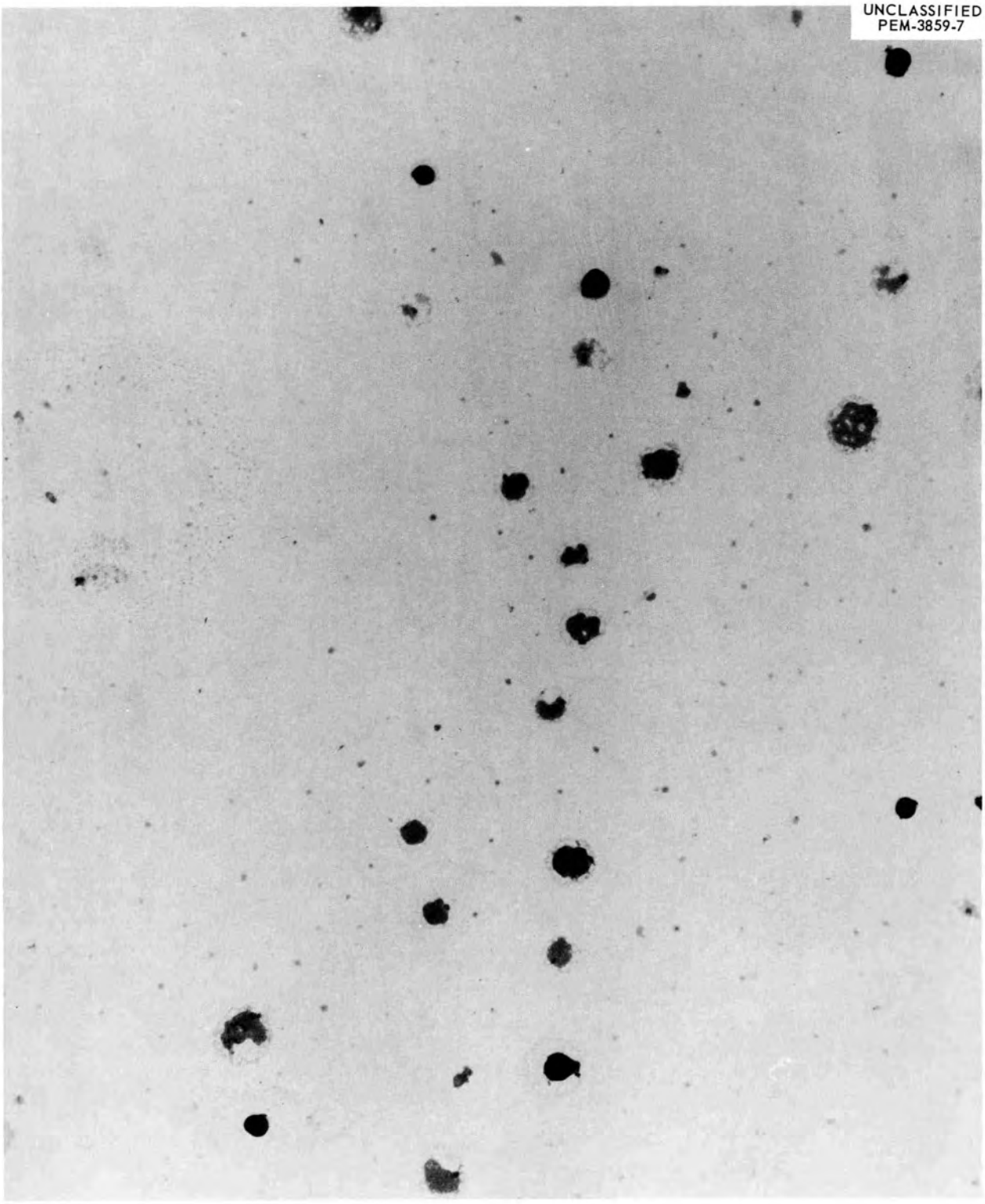

Fig. 1.9. Particles Collected from Aluminum-Uranium Alloy Melting by Electrostatic Precipitator in Moist-Air Experiment. 20,000X.

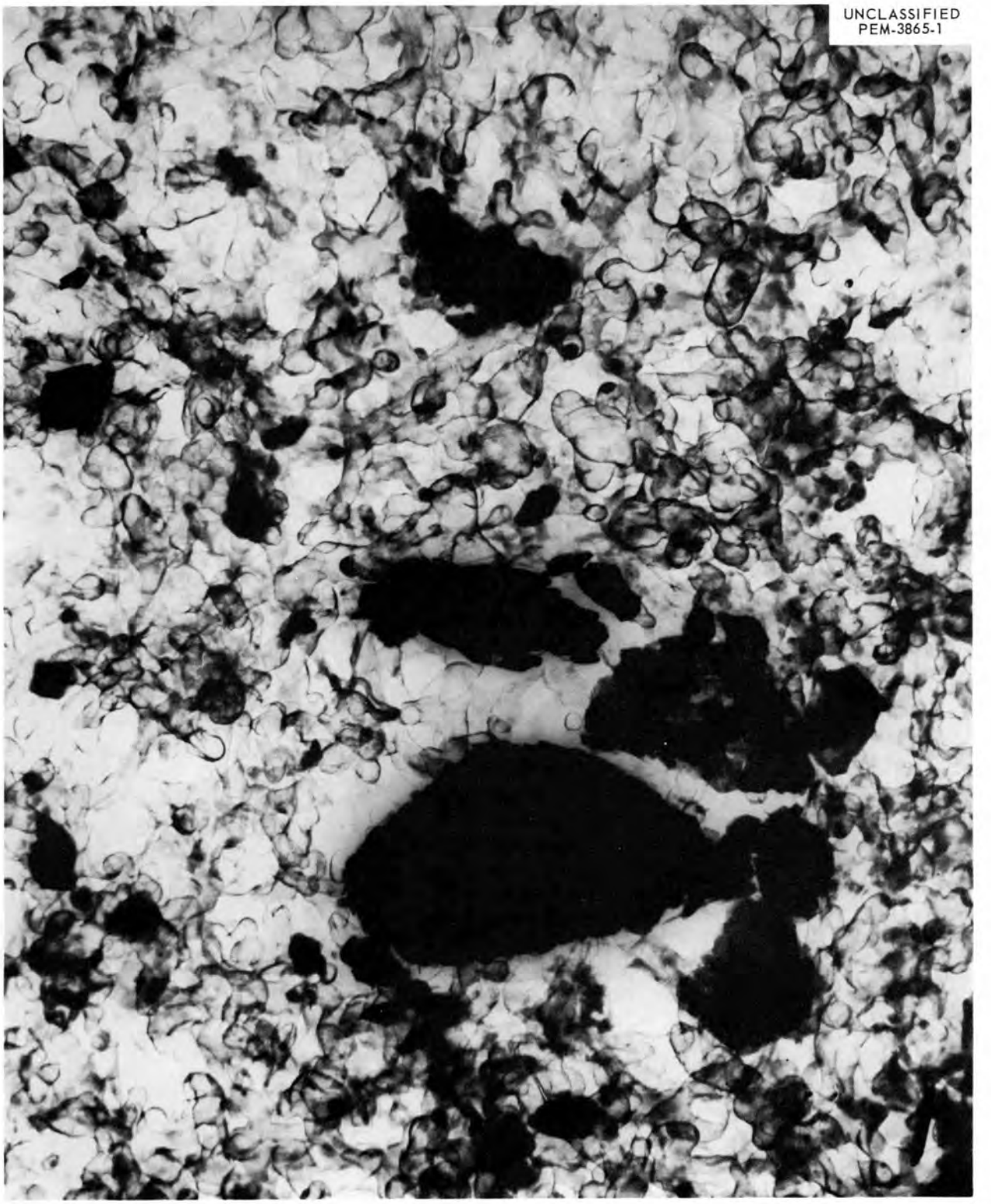

Fig. 1.10. Particles Collected from Aluminum-Uranium Alloy Melting on First Diffusion-Tube Millipore Filter in Moist-Air Experiment. 20,000X.

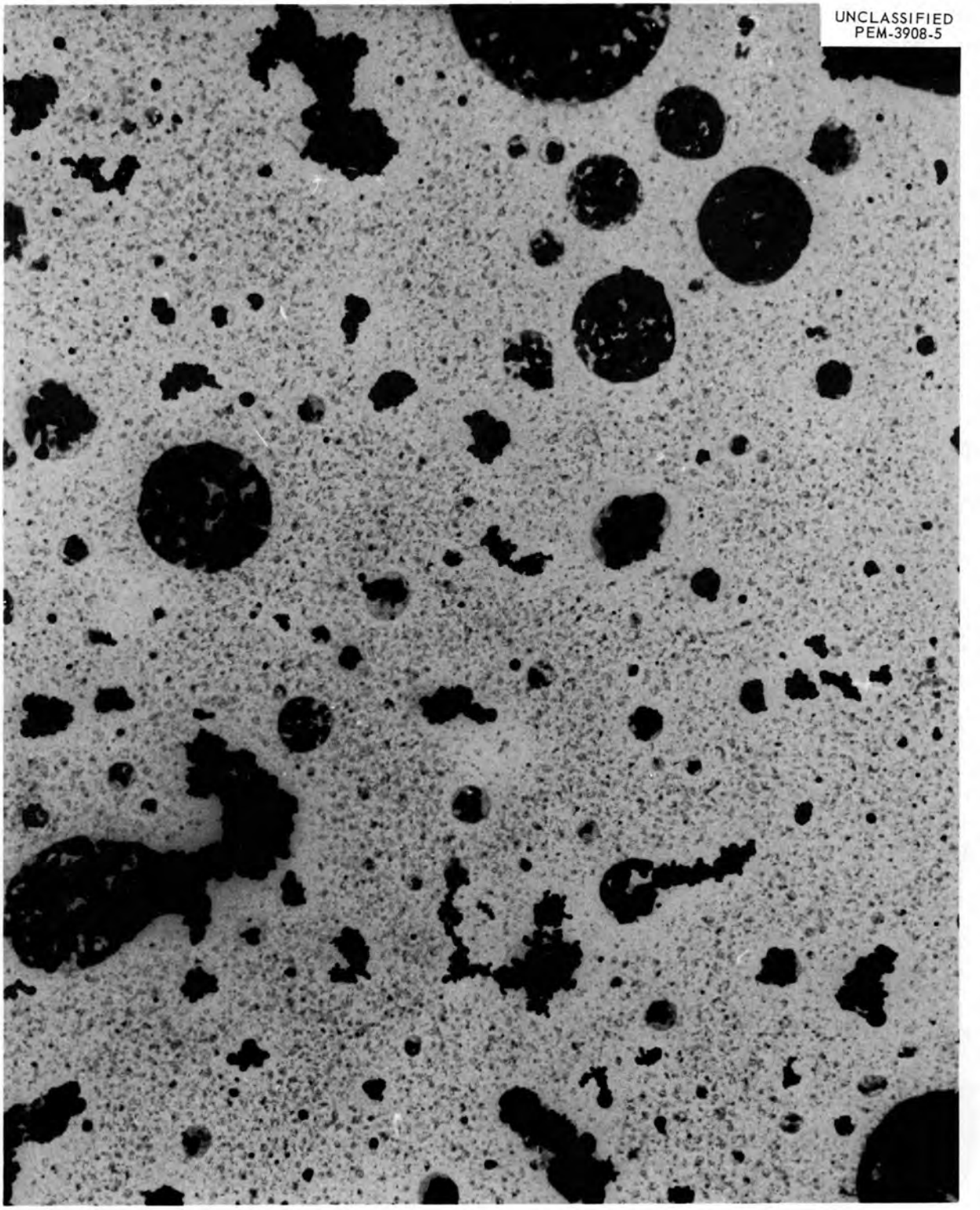

Fig. 1.11. "Rosette" Type Particles Collected on Membrane Filter After Melting Stainless-Steel-Clad UO_2.

Fig. 1.12. Very Small and Very Large Particles from UO_2 Melting Collected by Electrostatic Precipitation.

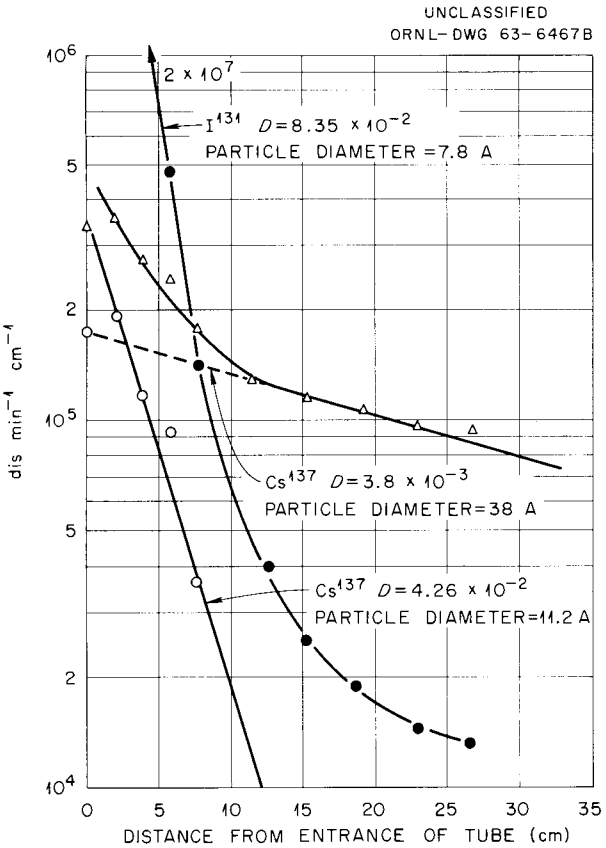

Fig. 1.13. Deposition of Unfiltered Iodine and Cesium from Aluminum-Uranium Alloy Melting in Diffusion Channel (Moist Air).

adaptation[9] of the Gormley and Kennedy equation,[10] were obtained by radiochemical determinations of material deposited at known distances from the entrance end of the tube. It is thus possible to correlate sizes of particles that deposit in diffusion tubes with type of activity. It should be noted that diffusion equations from which particle sizes are calculated assume that the diffusion tube wall acts as a perfect sink; that is, all particles striking the wall remain there. This assumption is probably valid for molecular iodine striking a silver surface, and for particles in the size range investigated.

[9]W. E. Browning, Jr., and R. D. Ackley, *Nuclear Safety Program Semiann. Progr. Rept. Dec. 31, 1962*, ORNL-3401, p. 44.

[10]P. G. Gormley and M. Kennedy, *Proc. Roy. Irish Acad., Sect. A* **52**, 163 (1949).

Diffusion tube data shown in Figs. 1.13 and 1.14 indicate that cesium activity in the first diffusion tube was associated with particles of two sizes, 11 and 38 A, while a large fraction of the iodine exhibited a particle diameter of 7.8 A, indicating that it was molecular iodine. The iodine data also show minor indications of larger particles. Other data, less definitive than those shown in Figs. 1.13 and 1.14 because total activity values were employed rather than radiochemical analyses, indicate the presence of particles of about 100 and 200 A. These have been shown to be mainly associated with Cs^{137} activity. A summary of the different particle sizes observed, their percentage of the total iodine activity, and theoretical retention factors are given in Table 1.6.

Comparison of the ratio of iodine and cesium activity deposited from unfiltered moist air on the wall of the first diffusion tube with the theoretical

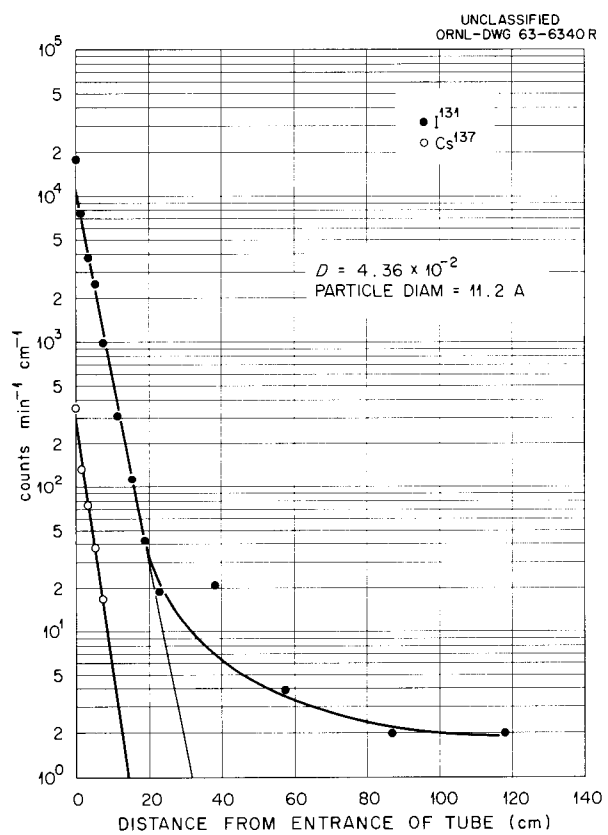

Fig. 1.14. Deposition of Filtered Iodine and Cesium from Aluminum-Uranium Alloy Melting in Diffusion Channel (Moist Air).

Table 1.6. Distribution of Released Radioiodine Between Molecular and Particulate Forms

Distribution of Radioiodine	Diffusion Tube Number	Calculated Diameter of Particle (A)	Distribution of Radioiodine in the Aerosol, Each Size[a] (%)	Percent of Iodine Inventory in Fuel Represented by Each Size
Aluminum-Uranium Alloy (23.6% Burnup), Melted in Steam-Air Atmosphere				
Before filtration	1	7.8 (molecular)	94.6	17.3
		26	5.4	1.0
After filtration	2	11 (molecular)	98.1	14.5
		200[b] (and greater)	1.9	0.3
Trace-Irradiated Stainless-Steel-Clad UO_2, Melted in Air				
Before filtration	1	12 (molecular)	80.2	19.5
		24	14.4	3.5
		108[c] (and greater)	5.4	1.3
After filtration	2[d]	11 (molecular)	75.2	8.7
		18	21.9	2.5
		64[e] (and greater)	2.9	0.5

[a]Calculated from area under deposition rate lines for each particle size.
[b]Theoretical retention in diffusion tube of 300 cm length is 24%.
[c]Theoretical retention in diffusion tube of 300 cm length is 55%.
[d]Preceded by bronze screens to remove molecular iodine.
[e]Theoretical retention in diffusion tube of 300 cm length is 79%.

ratio for cesium iodide showed that very little of this compound could have been deposited from the air sample passing through the tube. An upper limit of 7% of the iodine in the aerosol that could have been present as the compound was set by the amount of iodine found in the exit filter.

Radioiodine Released from Stainless-Steel-Clad UO_2

Iodine was the only type of activity found in the diffusion tubes under the conditions employed in this experiment. Diffusion tube data are presented in Figs. 1.15 and 1.16 and in Table 1.6. One difference between the conditions employed in the UO_2 melting experiment and those used in the previous aluminum-uranium alloy melting experiments should be noted, namely, the use of bronze screens in the former case to remove molecular iodine. In both instances the aerosol passed through roughing and absolute filters before being sampled by the side stream passing through the second diffusion tube. This treatment presumably would remove most of the particles 0.1 μ and larger, but very little of the molecular iodine. A distinct surprise was noted in the UO_2 experiment, where a large part of the iodine activity was stopped on the roughing filter. This anomaly is tentatively ascribed to the effect of trace concentration. The roughing filter, which includes two organic-bonded glass screens and a thick bed of mineral fiber, may have sufficient surface reactivity to pick up a large fraction of iodine activity when present at trace concentration. The air sampled by the second diffusion tube in the UO_2 melting experiment, as mentioned above, had passed through four thicknesses of bronze filter media in addition to the two filters. The bronze filters removed a significant fraction (but apparently not all) of the molecular iodine from the aerosol stream. Comparison of the diffusion tube

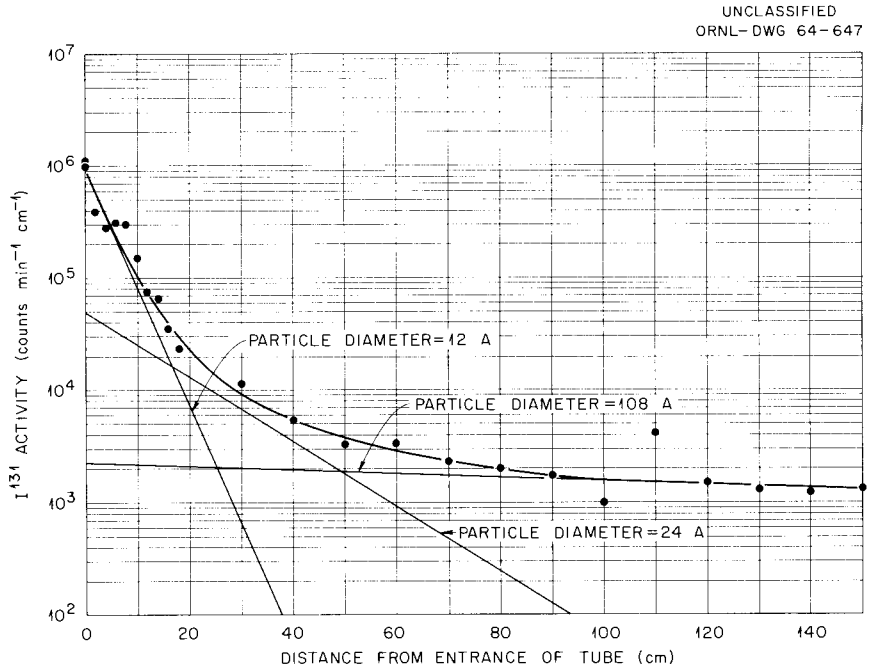

Fig. 1.15. Diffusion-Tube Deposition of Unfiltered Iodine from UO_2 Melting.

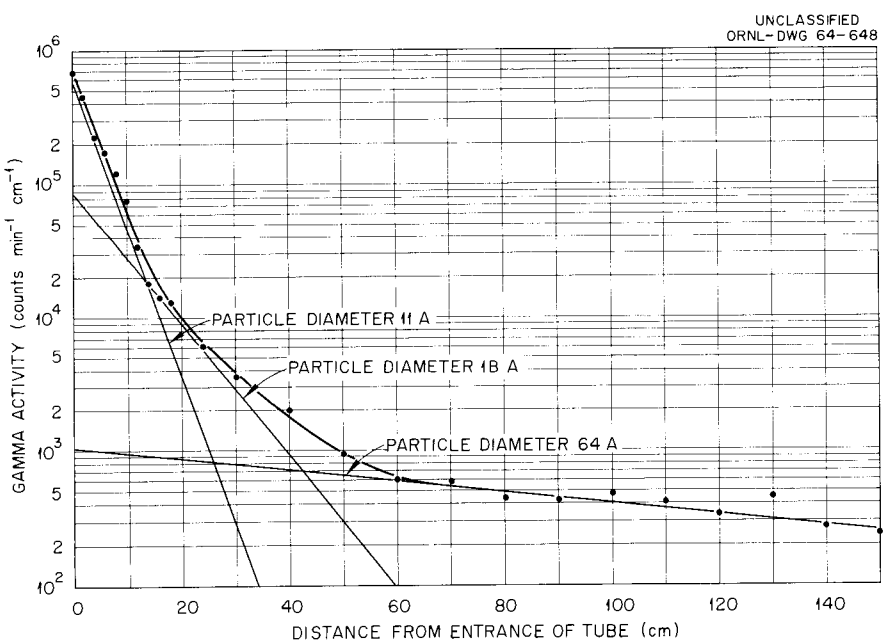

Fig. 1.16. Diffusion-Tube Deposition of Filtered Iodine from UO_2 Melting.

data from the UO_2 melting test, Figs. 1.15 and 1.16, with those obtained in the aluminum-uranium experiments, Figs. 1.13 and 1.14, shows a more complex particle spectrum in the UO_2 experiment.

IODINE REMOVAL FROM OXIDIZING GASES AT HIGH TEMPERATURES

The need for trapping materials for radioiodine that are less susceptible than charcoal to oxidation in air or other oxidizing gases at high temperatures was discussed in the previous progress report.[11] The results of a limited number of tests on the retention of iodine on potassium iodide and platinized alumina were presented. No additional data with potassium iodide beds were obtained since the previous report, but a few tests were conducted with other materials. A comparison of the effectiveness of platinized alumina (−12 +16 mesh) and the same type of alumina without the added platinum for the removal of iodine is presented in Fig. 1.17.

Tests were performed by heating irradiated aluminum-uranium alloy in a flowing air stream at about 750°C, filtering out particulate fission products on quartz wool, and then collecting the fission product iodine in the test bed. An active distribution curve was determined on the bed following the initial deposition of iodine by drawing the bed part and small aperture between two lead bricks separating the tube and a scintillation crystal. The output of the crystal was fed into a single-channel spectrometer set for the 360-kv I^{131} gamma. The area under the curve was compared with that produced by a similar scan performed after passing air through the bed for 30-min periods at controlled temperatures. The data confirm the qualitative statement[11] that platinized alumina retains iodine better than ordinary alumina; but the results indicate that, at temperatures above 400°C, platinized alumina would serve only to delay the passage of radioiodine in addition to acting as a heat sink. Since cheaper materials are readily available that could act as a heat sink, it seems desirable to continue the study of other materials that may be more effective in retaining radioiodine in the presence of oxidizing gases at temperatures above the combustion point of charcoal.

During the course of the tests with platinized and unplatinized alumina mentioned above, it was noted that quartz wool used to hold the alumina beds in place seemed to retain iodine to some extent in flowing hot air. A single test was performed to determine the iodine-retention capacity of this material. Irradiated aluminum-uranium alloy specimens were employed as the source of radioiodine, as in the previous tests, and the iodine was deposited on the quartz wool at room

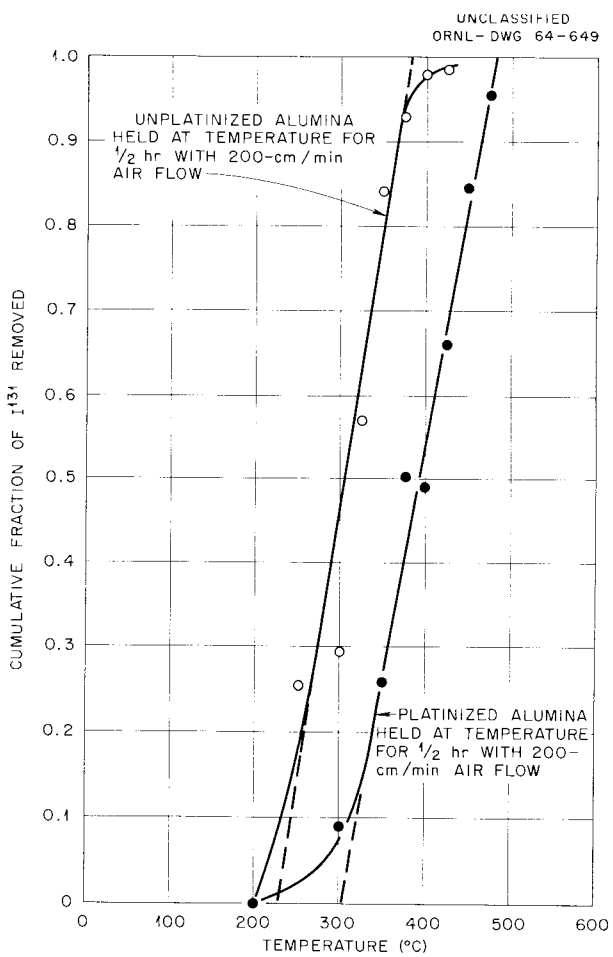

Fig. 1.17. Removal of Iodine from Platinized and Unplatinized Alumina by High-Temperature Air.

[11] C. J. Barton, G. W. Parker, and M. E. Davis, *Nuclear Safety Semiann. Progr. Rept. June 30, 1963*, ORNL-3483, p. 14.

temperature. Heating the contaminated wool for 1 hr at 100°C in air flowing at a velocity of 200 cm/min removed a large, but undetermined, fraction of the retained iodine. Of that which remained after this treatment, 34% was removed by air flowing at the same rate for 1 hr at 200°C, 69% was removed after an additional hour at 300°C, and 97% after the third hour at 400°C. Although these data are not directly comparable to those in Fig. 1.17, it appears that quartz wool does not retain iodine in high-temperature flowing air nearly as well as unplatinized alumina.

---

2. Release of Fission Products on In-Pile Melting of Reactor Fuels Under Transient Reactor Conditions

G. W. Parker R. A. Lorenz C. E. Miller, Jr.

The purpose of the ORNL fission product release experiments in the ANL TREAT facility is to study the release of fission products from the fuel during a reactor accident in which the fuel melts rapidly as the result of a reactor transient. The objectives of this program are to measure and interpret the release of fission products as a function of fuel type, cladding, atmosphere, burnup, and transient characteristics. A major interest in the study is the comparison of fission product release from transient melting with that from slower, in-pile melting experiments that simulate loss-of-coolant accidents.

Two experiments have been performed in the TREAT reactor. Previously unirradiated, stainless-steel-clad uranium dioxide specimens were heated in an argon atmosphere in both experiments. These experiments simulated the type of accident that could occur during the start-up of a new reactor or during a SPERT-type experiment where the only fission products available for release are due to fissions that occur during a very short time. Experiments will be performed with preirradiated fuel during the calendar year of 1964.

EXPERIMENTAL ASSEMBLY

A flow diagram of the experimental assembly is shown in Fig. 2.1. The apparatus was composed of three interconnected parts: a fuel autoclave, a diffusion system that included a flow regulator, and a second autoclave, initially evacuated, to collect filtered gas from the fuel autoclave. The fuel autoclave contained an electric heater to preheat the fuel specimen in an argon atmosphere. The flow regulator allowed gas from the fuel autoclave to flow slowly, after the reactor transient, into the gas-collection autoclave until pressure equilibrium was attained.

A drawing of the fuel autoclave is shown in Fig. 2.2. The stainless-steel-clad UO_2 fuel was supported by a $^7/_8$-in.-long rod on the lower end of the specimen that rested on the bottom of the alumina furnace insulation. The specimen was also supported at the top by spot-welding to the stainless steel basket. The basket was in turn spot-welded to rods screwed into the autoclave top. Spiraled bright-finish tungsten sheet provided reflective thermal insulation for the heater. A Pt–10% Rh heater and a Pt–10% Rh thermocouple were encased in the cast alumina insulator. Two thermocouples were attached to the stainless steel fuel cladding. The 10-mil-diam wires of Pt–10% Rh thermocouples were individually spot-welded to the cladding to provide accurate and rapid temperature response, and a Chromel-Alumel thermocouple was attached to the fuel autoclave exterior. The autoclave was filled at room temperature with argon to a pressure of 25 psia. When the specimen was heated to 800°C, the argon pressure was 40 psia. A pressure cell permitted continuous monitoring of the pressure.

The diffusion system consisted of a 6-ft-long diffusion tube, 0.195 in. in inside diameter, and a flow controller which regulated the flow to 47 cc/min at the temperature and at the pressure range prevailing in these experiments. Valves at the inlet and outlet of the diffusion system isolated the diffusion system from the fuel autoclave and the gas-collection autoclave until after the reactor transient, when they were opened by means of an electrically initiated explosion. The diffusion system was originally filled at room temperature with 40 psia of argon in order to match the fuel autoclave pressure with the specimen heated. This minimized surging of gas between the diffusion system and fuel autoclave when the explosive valves were opened after the reactor transient. The diffusion tube was employed to permit determination of particles in the 30- to 100-A range.

A series of filters at the entrance of the gas-collection autoclave provided a means of sampling particles larger than 0.1 μ. The first two filters were 3.0-μ-pore-size membrane filters; the next two were 0.45-μ membrane filters, and the last one was a glass-fiber filter that should be 98% efficient for particles as small as 0.05 μ.

Two 0.7-in.-long UO_2 pellets were seal-welded in a stainless steel jacket in a helium dry box. Clearance between fuel and cladding was 2 mils on the diameter and 32 mils at the end. Ten-mil-diameter wires of tungsten, rhenium, tantalum, and molybdenum were included in grooves between the two pellets to provide evidence of the maximum temperature reached during the reactor transient. Detailed specimen characteristics are given in Table 2.1.

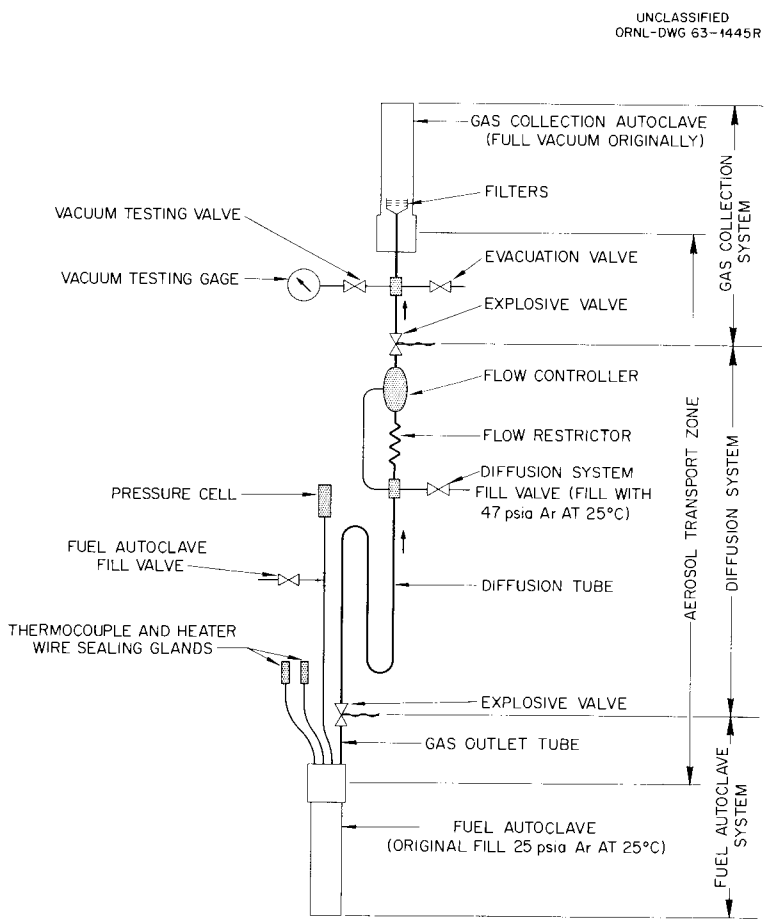

Fig. 2.1. Flow Diagram for Fission Product Release Under Transient Reactor Conditions.

UNCLASSIFIED
ORNL-DWG 64-650

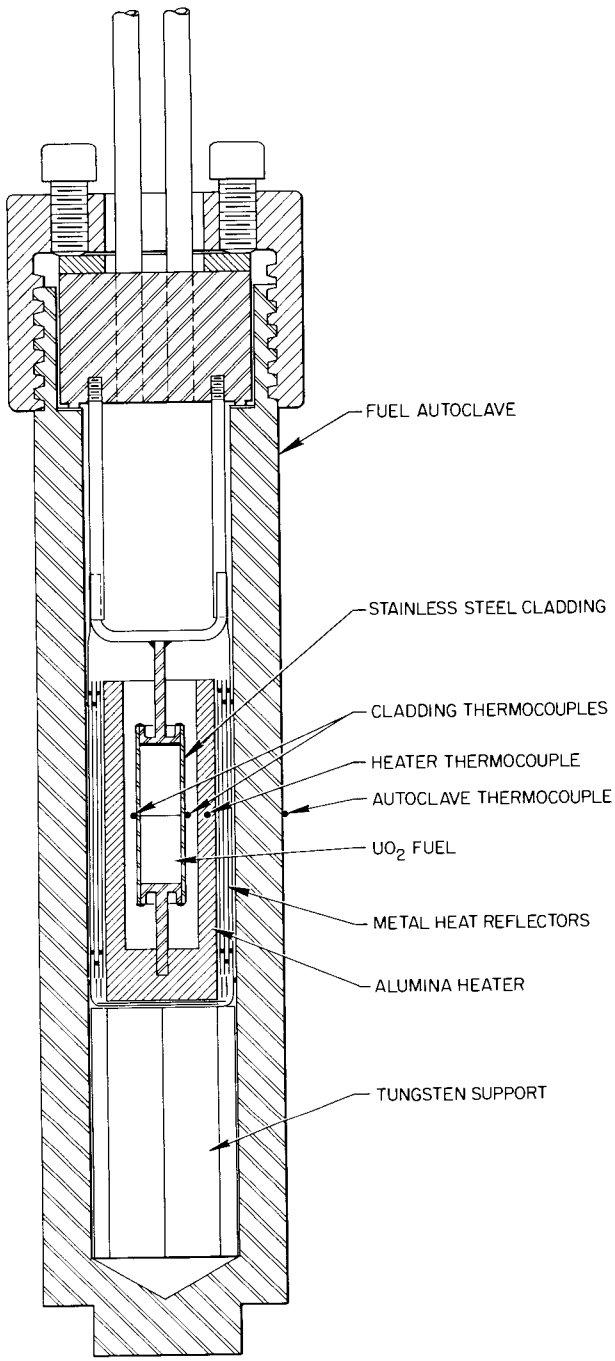

Fig. 2.2. Fuel Autoclave Assembly.

Table 2.1. Fuel Specimen Characteristics

Cladding	
Material	Type 347 stainless steel
Wall thickness	0.035 in.
Inside diameter	0.407 in.
UO_2 Fuel	
Specimen weight	30.4 g (two pellets, 15.2 g each)
Density	10.39 g/cm^3 (94.7% of theoretical)
Diameter	0.405 in.
U	85.3 wt %
U^{235}	10.1% by weight of total U
O/U Ratio	<2.001
N	49 ppm
C	500 ppm
Fe	82 ppm

OPERATING PROCEDURE

Following a hydrostatic pressure test of individual components, the apparatus was assembled and leak-tested with a helium leak tester. The gas-collection autoclave system was evacuated, and the diffusion system and fuel autoclave were filled to 40 and 25 psia, respectively, with argon that was purified by passage through dry-ice-cooled charcoal. A preirradiation test of the loaded experimental assembly was made to test the heater, thermocouples, and pressure cell before it was shipped to the reactor site. Heater and other electrical components were again tested for proper operation after the experimental assemblies were installed in the TREAT reactor.

A preliminary low-power transient of 60 Mw-sec was performed with the first assembly in order to determine the specimen heating rate as a check on the calculated heating rate. The experimentally determined heat input was 0.75 cal per g of UO_2 per Mw-sec, slightly lower than the calculated value of 0.91 cal per g of UO_2 per Mw-sec.

The specimen was preheated electrically to 800°C, in order to simulate realistic reactor conditions and to help reduce fuel fragmentation during the transient. The main reactor transient was performed with the reactor integrated power selected

so that the fuel specimen would be heated to the UO_2 melting point, assuming no heat loss. Twelve seconds after the transient the explosion valves were opened and the argon aerosol from the fuel autoclave flowed through the diffusion system and filters into the gas-collection autoclave until the pressure was equalized throughout the assembly.

The first experimental assembly was removed from the reactor after a period of several hours allowed for cooling and radioactive decay and the apparatus for the second experiment was installed.

A single transient was run in the second experiment using the same procedure as for the main transient of experiment 1. The reactor period was decreased and the integrated power increased as compared to the corresponding reactor parameters in the first experiment. The objective of the changes was to permit melting of a large fraction of the UO_2 specimen and to cause release of a larger fraction of the fission products in the second experiment.

After a one-week delay to permit radioactive decay, both experimental assemblies were shipped to Oak Ridge for disassembly, radiochemical analysis, and other examinations.

A summary of the reactor transient data, radiochemically determined fissions, and calculated specimen fission energy input is given in Table 2.2.

A comparison of the heating of fuel and cladding for both experiments is shown in Fig. 2.3. The time scale was arbitrarily selected to be zero at 7% of the final integrated reactor power, or 23 Mw-sec for both experiments. The stainless steel temperatures were recorded with high-speed equipment. The UO_2 fuel temperature was calculated assuming that no heat was lost from the fuel and that 320 Mw-sec heated the fuel from 800 to 2800°C. This calculation is more accurate for 0.5 sec or less than for longer elapsed times when significant heat loss occurred. The figure shows that the UO_2 fuel reached its maximum temperature in both experiments while the stainless steel cladding remained intact.

Table 2.2. Summary of Reactor Transient Data

	Experiment 1[a]	Experiment 2
Reactor integrated power, Mw-sec	320	328
Reactor period, msec	108	87
Estimated UO_2 temperature range, °C	800 to 2800 ± 150	800 to mp
Stainless steel cladding temperature, °C	800 to mp	800 to mp
Alumina heater temperature, °C	800 to 1050	800 to 1070
Autoclave wall temperature, °C	180 to 240	140 to 200
Argon pressure, psia	39 to 42	40 to 51
Number of fissions (radiochemical analysis)	1.17×10^{15}	1.23×10^{15}
Fissions per μg of U^{235} per w-sec	1.40	1.44
Fission energy input, cal per g of UO_2[b]	250	263
Fission energy input, cal per g of UO_2 per Mw-sec[b]	0.78	0.80

[a]A low-power transient of 60 Mw-sec was run with experiment 1 the day before the main transient. The number of fissions and the heat input value from this preliminary transient are not included in this tabulation.

[b]These values were obtained by using the radiochemically determined number of fissions and assuming 170 Mev per fission absorbed by the fuel specimen.

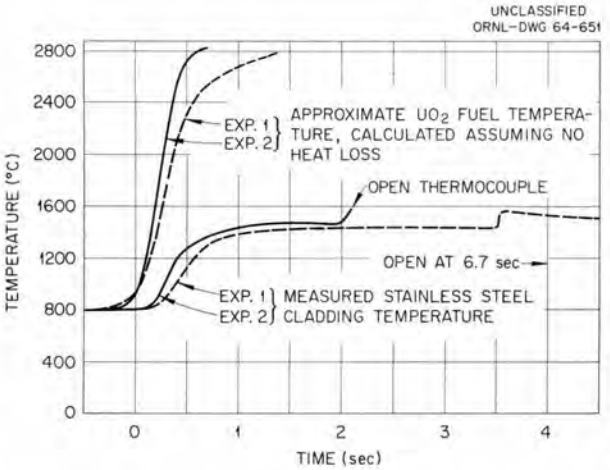

Fig. 2.3. Comparison of Transient Heating Rates.

PHYSICAL EXAMINATION OF COMPONENTS OF THE EXPERIMENT 1 ASSEMBLY

The experimental assembly was opened and examined at Oak Ridge. The heater, metal reflectors, and exposed wires in the fuel autoclave were in good condition. A very light, gray film was observed on the wire insulators and on the autoclave top above the heater. The bottom of the alumina heater was cut off to remove the UO_2 and cladding residue. A light, gray film was present on the inside surface of the heater. The cladding had melted away from the UO_2 and some contacted and adhered to the alumina. Figure 2.4 shows the opened heater and the lower portion of the fuel specimen removed from the heater. The upper two-thirds of the top UO_2 pellet broke off during disassembly and it is shown in Fig. 2.5. General deep surface cracking of the UO_2 is apparent. Internal cracks are seen at the radial break in Fig. 2.5 and where the two pellets were

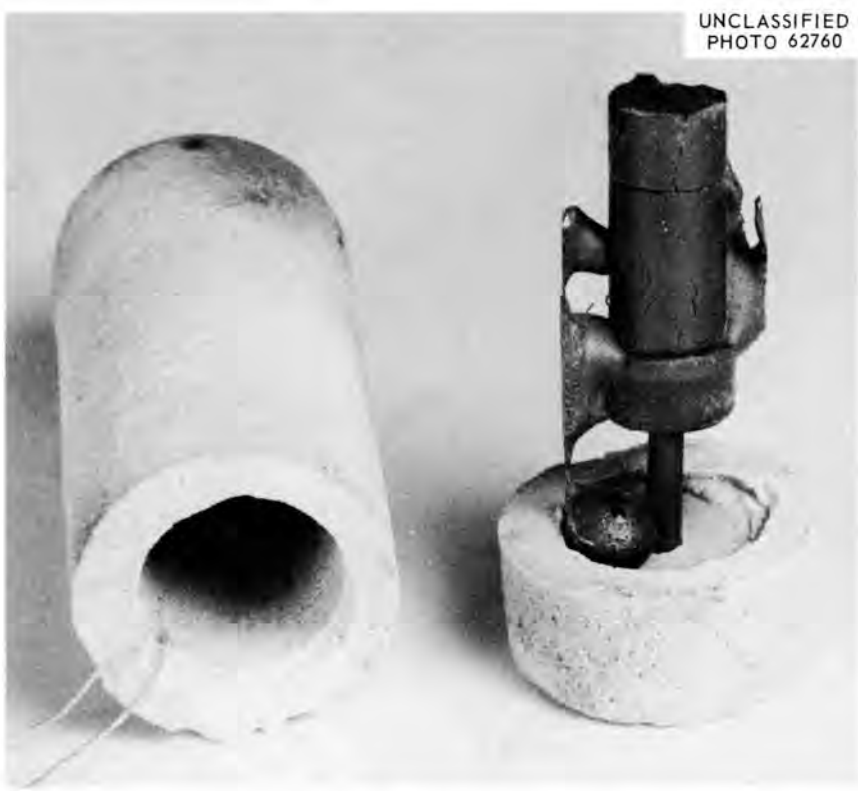

Fig. 2.4. Alumina Heater with UO_2 Fuel and Melted Stainless Steel Cladding from Experiment 1.

Fig. 2.5. Upper Portion of Top UO_2 Fuel Pellet and Unmelted End Cap from Experiment 1.

separated at their original interface. The diameter of the pellets was uniformly 9 mils or 2% larger than the original diameter. The radial break, Fig. 2.5, showed a distinct rim approximately 30 mils wide around the outer circumference apparently caused by a difference in grain structure of the inside portion as compared with the cooler outer rim.

The two pellets adhered to each other but were separated by use of force at their original interface. Some UO_2 from each pellet stuck to the other pellet. Portions of the four wires originally placed in grooves at the pellet interface were visible. More than half of the molybdenum wire (mp, 2620°C) had melted or otherwise disappeared from the center portion of its groove. The tantalum wire (mp, 2996°C) had bowed up into the upper pellet, deepening its original groove near the center. The rhenium wire (mp, 3167°C) was essentially in its original condition. The tungsten wire (mp, 3370°C) was intact but it was somewhat thinner near the center of the pellet than at the outside edges. Impressions of the two wires in each pellet were formed in the face of the other pellet indicating plastic flow of the UO_2.

The filters were removed and examined. A light film of gray material was deposited on the first filter with no visible deposits on other filters.

PHYSICAL EXAMINATION OF COMPONENTS OF THE EXPERIMENT 2 ASSEMBLY

When the experiment 2 fuel autoclave was opened, a gray film of material was observed on parts above the heater. The film was somewhat heavier than in experiment 1. The fuel pellets are shown in Fig. 2.6.

The cladding was melted away, and the pellets were split down on the side at the point where approximately 10% of the UO_2 flowed out from the center. Swelling of the pellets was 18% on the diameter at the center with swelling and bowing visible when they were rotated 90° from the view shown in Fig. 2.6. The UO_2 which flowed out of the pellets had a clinker-like appearance. Although some of this UO_2 broke loose from the pellets during disassembly, there was no evidence of shattering or dispersal of UO_2 fragments. Surface cracking of the UO_2 was not as pronounced as in experiment 1.

The alumina heater, with its base cut off and with the melted stainless steel cladding exposed, is shown in Fig. 2.7. The film inside the heater was considerably heavier and darker than that observed in experiment 1. The stainless steel melted and ran down without adhering to the heater walls. Small pieces of the UO_2 that flowed out of the pellets were visible as inclusions in the puddled stainless steel.

Fig. 2.6. UO_2 Fuel Pellets from Experiment 2.

The two pellets were forcibly separated at their original interface which was identified toward the center of the pellets by a portion of the break which exposed three pieces of wires originally located between the pellets. The pellet interface in the interior was $\frac{1}{8}$ in. lower than the interface at the pellet surface indicating that the fluid UO_2 moved downward in addition to flowing out of the pellet shell. No conclusions were drawn from the appearance of the wires with regard to the maximum temperature reached.

A heavier, darker film of material was deposited on the first filter of experiment 2 as compared with experiment 1. There were no visible deposits on the other filters. Analyses of the particle-size distribution of the particles collected on the first filter in both experiments, determined from electron photomicrographs, are shown in Fig. 2.8.

METALLOGRAPHIC EXAMINATION OF FUEL

Samples of the fuel from experiments 1 and 2 were submitted for metallographic examination. Figures 2.9 to 2.13 show sections taken from samples of unirradiated fuel, experiment 1 fuel, and experiment 2 fuel.

Comparison of Figs. 2.9 and 2.10 shows very little difference and indicates that the fuel in experiment 1 did not melt. A slight increase in porosity is evident in Fig. 2.10 as compared to Fig. 2.9. This can also be seen by comparing the edges of the sample in Fig. 2.10 with the center portion. This increase in porosity is probably associated with the volume increase of the fuel.

Figure 2.11 shows that the center of the fuel in experiment 2 foamed and flowed. The white solid portion is a part of the original stainless steel cladding which collected on the side of the fuel specimen. The UO_2 that flowed out of the center of the fuel pellet can be seen on the opposite side of the stainless steel. The fact that UO_2 flowed from the fuel pellet indicates that the inside of the pellet probably did melt although the cast structure that usually results from the

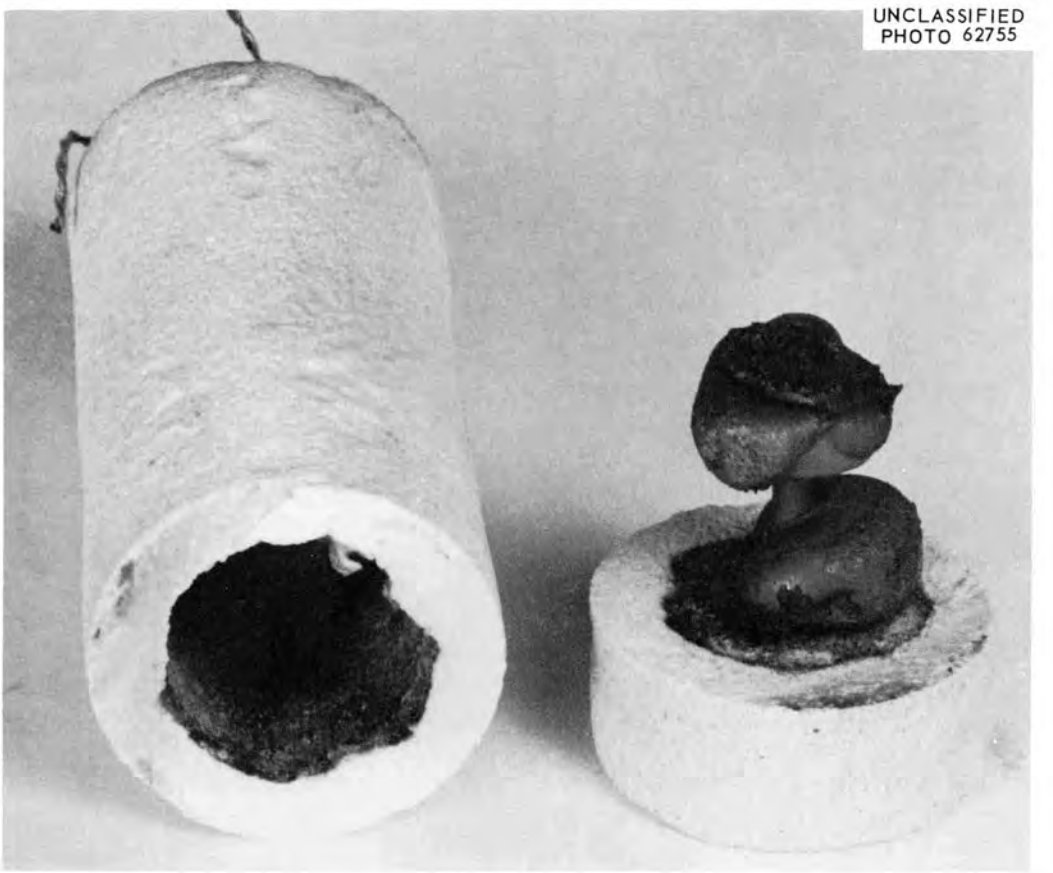

Fig. 2.7. Alumina Heater and Melted Stainless Steel Cladding from Experiment 2.

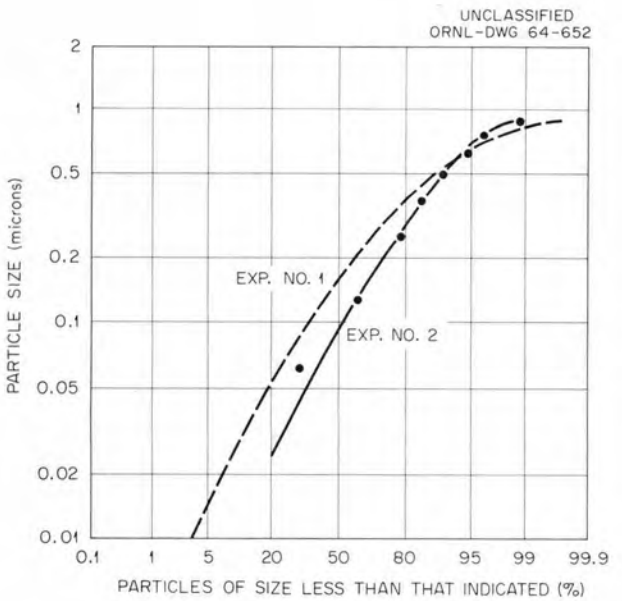

Fig. 2.8. Size of Particles Released from Transient-Heated UO_2.

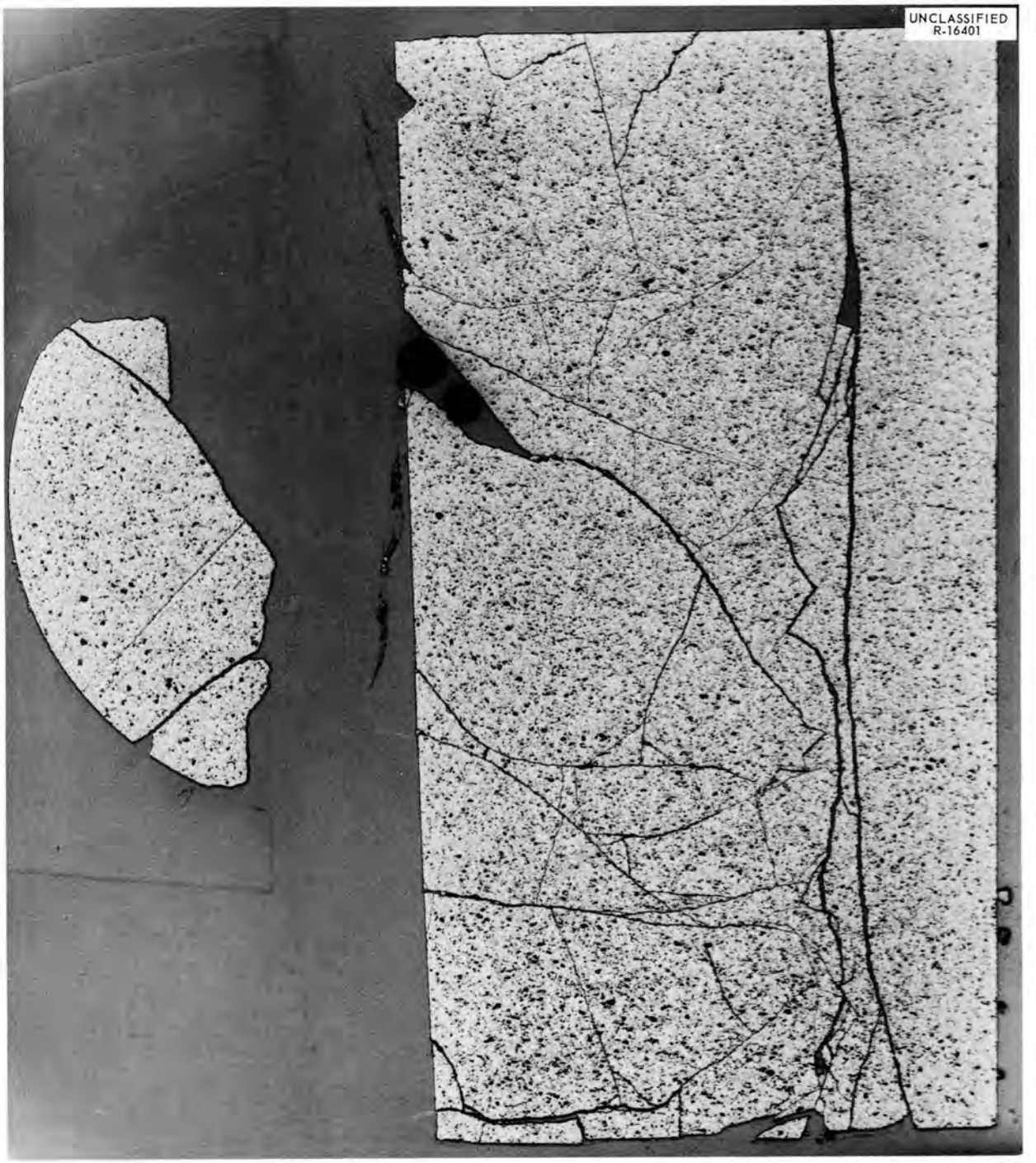

Fig. 2.9. Transverse and Longitudinal View of Unirradiated UO_2 Pellet Used as Control for Experiments 1 and 2.

Fig. 2.10. Transverse and Longitudinal View of Lower UO_2 Pellet from Experiment 1.

Fig. 2.11. Transverse and Longitudinal View of Upper UO_2 Pellet from Experiment 2.

solidification of molten material is not present. This is perhaps due to the very short time in which melting and freezing took place. Photomicrographs of the center portion of experiment 1 fuel and experiment 2 fuel are shown in Figs. 2.12 and 2.13 respectively. The differences in porosity between the two fuels and the lack of cast structure in the experiment 2 fuel can be seen. Physical measurements of the UO_2 shell visible in Fig. 2.11 indicate that approximately 65% of the fuel in experiment 2 "melted."

Metallic inclusions recognized in metallographic sections of both unirradiated and irradiated fuel and evident in Figs. 2.12 and 2.13 as white spots are possibly tungsten. Etching of the metallographic mounts and their exposure to air indicated that the inclusions are not stainless steel nor uranium. Chemical and spectrographic analyses of unirradiated fuel from the same batch as the pellets used in these experiments have shown that tungsten is present in the fuel. The source of this tungsten is not yet known.

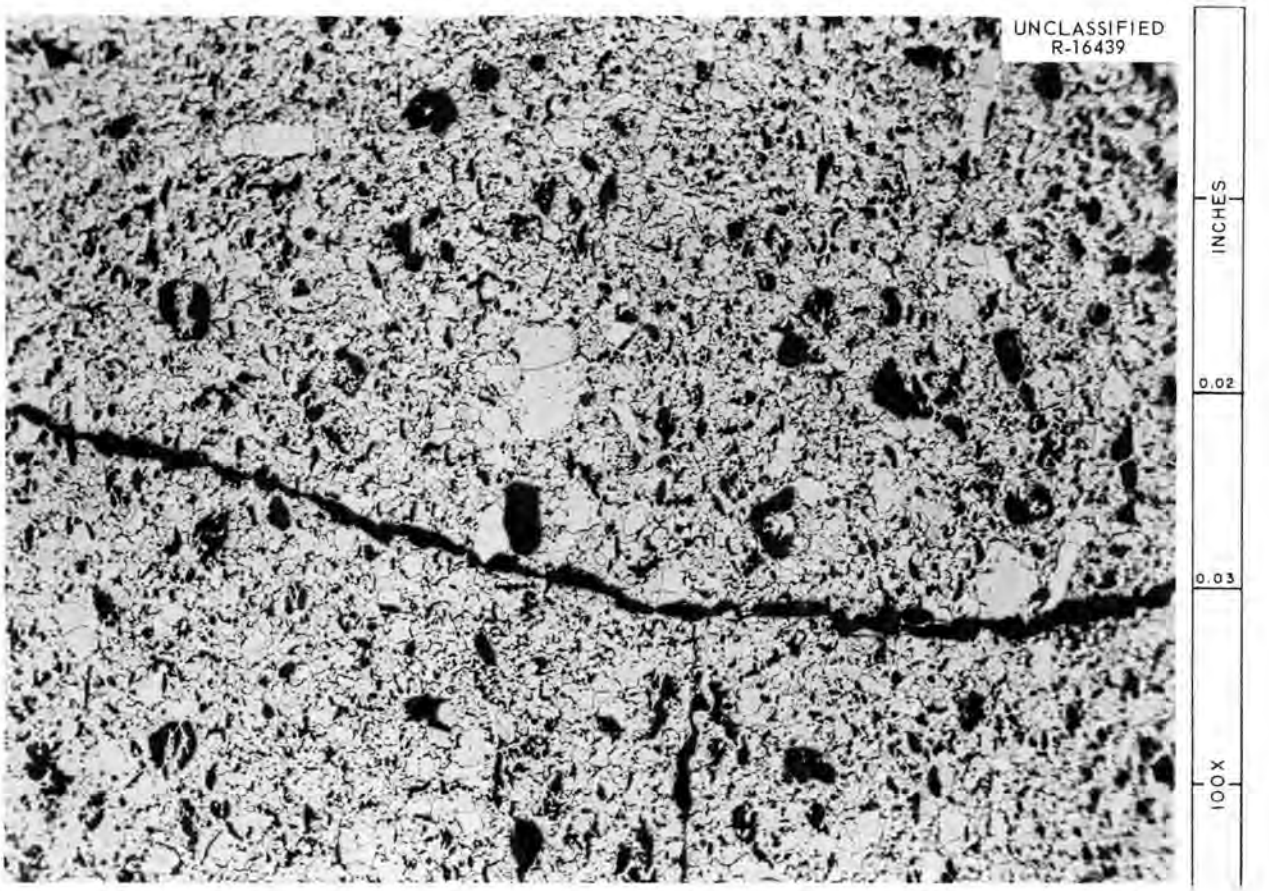

Fig. 2.12. Microstructure of Center of UO_2 Pellet from Experiment 1. Etchant: H_2O, H_2SO_4, H_2O_2.

The grain size was measured near the edge and in the center of the pellets and it was found to be 17 and 16 μ, respectively, for the unirradiated control pellet, 18 and 20 μ for experiment 1, and 19 and 50 μ for experiment 2. Photomicrographs of the center region of experiment 1 fuel showed slightly more porosity and some loss of grain integrity as compared with the unirradiated pellet. Most of the surface cracks in experiment 2 fuel were small and were filled with stainless steel. The surface cracks in experiment 1 fuel were larger and contained no stainless steel or other metal.

In experiment 1, partial sintering occurred between UO_2 pellets toward the center. Partial sintering was evident between pellets at the outer rim in experiment 2.

RADIOCHEMICAL RESULTS

Radiochemical analyses have been obtained for the two experiments. Eight fission products and uranium were determined throughout each experiment so that a complete fission product balance was obtained. Thus, each fission product served as a fission monitor, providing eight independent measurements of the total number of fissions which occurred during each experiment. Table 2.3 shows the total number of fissions determined for each isotope in the two experiments. The ratio of reactor power in experiment 1 to that in experiment 2, determined from the ratio of the weighted average number of fissions, was 1.13 while the ratio determined from the reactor power recorders was 1.16.

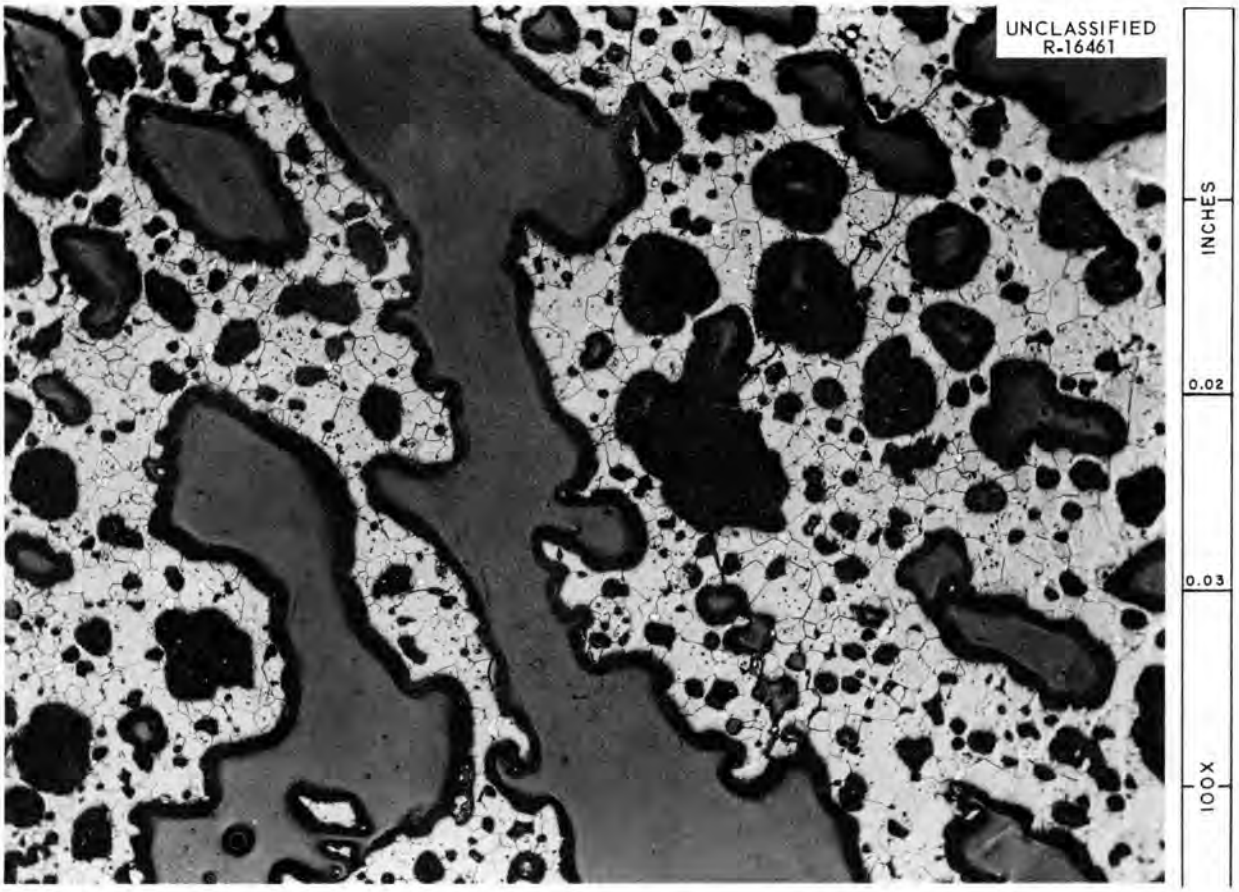

Fig. 2.13. Microstructure of Center of UO_2 Pellet from Experiment 2. Etchant: H_2O, H_2SO_4, H_2O_2.

Table 2.3. Radiochemical Determinations of Number of Fissions Determined by Isotopes

	Experiment 1	Experiment 2
	$\times 10^{15}$	$\times 10^{15}$
Strontium	1.30	1.01
Cesium	1.43	1.24
Barium	1.83	1.57
Iodine	0.69	1.55
Tellurium	1.37	1.44
Cerium	1.35	1.09
Zirconium	1.34	1.37
Ruthenium	1.45	1.31
Weighted average	1.39[a]	1.23

[a]This figure represents the sum of a 60 Mw-sec preliminary transient resulting in 0.22×10^{15} fissions and a 320 Mw-sec transient resulting in 1.17×10^{15} fissions.

Tables 2.4 and 2.5 show the detailed distribution of fission products in the two experiments. The fission products are grouped in these tables roughly according to the characteristics of the principal precursors that were present during the transient heating period and the first few seconds thereafter. The three groups are (1) volatile materials, (2) metals which alloy readily with stainless steel, and (3) nonvolatile materials. Table 2.6 shows the pertinent fission product decay chains for thermal fission of U^{235}. The relation between the isotope measured and its precursors can be seen from this table. The high release values observed for Sr^{89} and Cs^{137} resulted from their noble-gas precursors, which were also responsible for these isotopes being found throughout the experimental systems. Most of the released I^{131} and Te^{129} was found in the stainless steel cladding, probably as a result of alloying between the metal precursors and stainless steel.

Table 2.4. Distribution of Fission Products and Fuel in Experiment 1

Location of Activity	Percentage in Each Location[a]								
	Group 1			Group 2		Group 3			
	Sr^{89} (Br + Kr)	Cs^{137} (I + Xe)	Ba^{140} (Xe + Cs)	I^{131} (Sn + Sb)	Te^{129} (Sn + Sb)	Ce^{144} (Ba + La)	Zr^{95} (Rb + Sr)	Ru^{103} (Tc)	UO_2
UO_2 fuel	77	74	92	54[b]	79	93	99.8	99.9	99.99
Stainless steel cladding	0.072	2.0	0.074	35	14.6	1.83	0.026	0.055	0.00110
Alumina heater	2.3	5.1	4.9	7.2	6.0	5.2	0.172	0.0026	0.0036
Metal heat reflectors	2.0	2.3	0.85	1.12	0.079	0.017[c]	0.00093[c]		0.000126
Fuel autoclave walls	4.4	2.5	1.39	1.80	0.22[c]	0.019[c]	0.0045[c]	0.0052[c]	0.000014
Gas-transport zone[d]	5.4	5.7	0.84	0.108	0.028[c]	0.022	0.0026	0.0046	0.00011[c]
Filters[e]	0.66	0.036[c]	0.077	0.33[c]	0.031[c]	0.0031[c]	0.0017[c]	0.0042	0.000014[c]
Gas-collection autoclave[e]	8.1	8.2	0.047			0.0096		0.024	0.000050[c]

[a]For fission products, the radiochemically analyzed isotope is listed. The principal precursors present at the time of the transient are shown in parentheses. See Fig. 2.1 for identification of gas-transport zone.

[b]Error ±11%. Most of the values not footnoted have a probable error of ±5%.

[c]Error ±100%.

[d]Only approximately 58% of the transient-generated aerosol enters the gas-transport system.

[e]Only approximately 40% of the transient-generated aerosol enters and is sampled by the filter and gas-collection autoclave.

Table 2.5. Distribution of Fission Products and Fuel in Experiment 2

Location of Activity	Percentage in Each Location[a]								
	Group 1			Group 2		Group 3			
	Sr^{89} (Br + Kr)	Cs^{137} (I + Xe)	Ba^{140} (Xe + Cs)	I^{131} (Sn + Sb)	Te^{129} (Sn + Sb)	Ce^{144} (Ba + La)	Zr^{95} (Rb + Sr)	Ru^{103} (Tc)	UO_2
UO_2 fuel	42	47	58	70	79	91.2	98.5	99.4	99.2
Stainless steel cladding	0.60	2.8	1.30	19.8	15.7	0.62	0.61	0.43	0.51
Alumina heater	7.3	6.1	21	8.8	3.9	7.7	0.72	0.112	0.143
Metal heat reflectors	4.7	6.3	4.6	0.50	0.40	0.120	0.073	0.00052[b]	0.041
Fuel autoclave walls	12.7	9.3	11.4	0.85	1.16	0.30	0.120	0.0034[b]	0.059
Gas-transport zone[c]	14.3	13.2	2.7	0.024[b]	0.049[b]	0.144	0.0082	0.052	0.00026
Filters[d]	2.5	1.84	0.58	0.22[b]	0.032	0.0026[b]	0.0020	0.0071[b]	0.000014[b]
Gas-collection autoclave[d]	16.2	13.5	0.070	0.0090[b]	0.022[b]	0.0028[b]	0.00046[b]	0.00112[b]	0.000094[b]

[a]For fission products, the radiochemically analyzed isotope is listed. The principal precursors present at the time of the transient are shown in parentheses. See Fig. 2.1 for identification of gas-transport zone.

[b]Error ±100%.

[c]Only approximately 58% of the transient-generated aerosol enters the gas-transport system.

[d]Only approximately 40% of the transient-generated aerosol enters and is sampled by the filter and gas-collection autoclave.

Table 2.6. Fission Product Decay Chains from Thermal Fission of U^{235}[a]

Z	Element	Mass No. 89			Mass No. 95			Mass No. 103			Mass No. 129			Mass No. 131			Mass No. 137			Mass No. 140			Mass No. 144		
		$t_{1/2}$	I.Y.	T.Y.	$t_{1/2}$	I.Y.	T.Y.	$t_{1/2}$	I.Y.	T.Y.	$t_{1/2}$	I.Y.	T.Y.	$t_{1/2}$	I.Y.	T.Y.	$t_{1/2}$	I.Y.	T.Y.	$t_{1/2}$	I.Y.	T.Y.	$t_{1/2}$	I.Y.	T.Y.
33	As		0.01	0.01																					
34	Se		0.57	0.58																					
35	Br	4.5s	2.0	2.6																					
36	Kr	3.2m	1.8	4.3	Short	0.40	0.40																		
37	Rb	15.0m	0.38	4.7	<2.5s	2.1	2.5																		
38	Sr	50.4d	0	4.7	0.8m	2.8	5.3																		
39	Y				11m	0.94	6.3		0.01	0.01															
40	Zr				65d	0.02	6.3		0.39	0.40															
41	Nb								1.3	1.7															
42	Mo								1.1	2.8															
43	Te							1.2m	0.22	3.0															
44	Ru							40d	0	3.0															
45	Rh																								
46	Pd																								
47	Ag																								
48	Cd																								
49	In											0.11	0.11		0.18	0.18									
50	Sn										1h/6.2m	0.34	0.45	3.4m	0.97	1.2									
51	Sb										4.3h	0.29	0.74	23m	1.3	2.5									
52	Te										33d/67m	0.06	0.80	1.2d/25m	0.46	2.9		0.46	0.46						
53	I													8.05d	0.01	2.9	24s	2.2	2.7		0.29	0.29			
54	Xe																3.9m	2.7	5.4	16s	2.0	2.3	~1s	0.01	0.01
55	Cs																30y	0.81	6.2	66s	3.0	5.3	Short	0.78	0.79
56	Ba																			12.8d	1.1	6.4	Short	2.4	3.2
57	La																			40.2h	0.04	6.4	Short	2.0	5.2
58	Ce																						285d	0.38	5.6
59	Pr																								
60	Nd																								

[a]Decay chains are headed by the mass number of the chain. Decay progresses toward increasing Z. The half-lives ($t_{1/2}$) listed are taken from the Chart of the Nuclides, KAPL, revised December 1962. The calculated instantaneous percent yield (I.Y.) and the total percent yield (T.Y.) for each isotope are taken from USNRDL-TR-633.

Two release values were determined for each experiment. The first is release from the fuel and the second is release from the high-temperature zone. The high-temperature zone includes the fuel, cladding, heater, and reflectors. These release values for experiments 1 and 2 are given in Tables 2.7 and 2.8 respectively. The greater release from the fuel in experiment 2 as compared to experiment 1 was apparently due to the more rapid rate of heating that resulted in less heat loss and a higher maximum temperature in the fuel. The release of most isotopes from the high-temperature zone, except those with rare-gas precursors, was quite low under the conditions of these experiments and the values were approximately proportional to the release from the fuel in both experiments. The release values of the volatile and metal groups observed in experiment 1 are surprisingly high, since, as mentioned before, the fuel apparently did not melt in this experiment. This is interpreted as an indication of very rapid diffusion rates of the precursor isotopes at temperatures near the melting point of UO_2.

CONCLUSIONS

Results of the first two experiments performed in the TREAT reactor to study fission product release from stainless-steel-clad UO_2 fuel specimens heated under transient conditions demonstrated that meaningful fission product release data can be obtained by use of the initial design

Table 2.7. Material Released from Transient-Heated UO_2 in Experiment 1[a]

Release Zone	Release (%)								
	Sr^{89} (Br + Kr)	Cs^{137} (I + Xe)	Ba^{140} (Xe + Cs)	I^{131} (Sn + Sb)	Te^{129} (Sn + Sb)	Ce^{144} (Ba + La)	Zr^{95} (Rb + Sr)	Ru^{103} (Tc)	UO_2
Total release from UO_2 fuel	23	26	8.2	46	21	7.0	0.21	0.095	0.0050
Release from high-temperature zone	18.6	16.4	2.4	2.2	0.27	0.046	0.0088	0.038	0.00018

[a]For fission products, the radiochemically analyzed isotope is listed. The principal precursors present at the time of the transient are shown in parentheses. The high-temperature zone includes the fuel, cladding, heater, and reflectors.

Table 2.8. Material Released from Transient-Heated UO_2 in Experiment 2[a]

Release Zone	Release (%)								
	Sr^{89} (Br + Kr)	Cs^{137} (I + Xe)	Ba^{140} (Xe + Cs)	I^{131} (Sn + Sb)	Te^{129} (Sn + Sb)	Ce^{144} (Ba + La)	Zr^{95} (Rb + Sr)	Ru^{103} (Tc)	UO_2
Total release from UO_2 fuel	58	53	42	31	21	8.8	1.53	0.60	0.75
Release from high-temperature zone	46	38	14.8	1.10	1.26	0.32	0.130	0.064	0.059

[a]For fission products, the radiochemically analyzed isotope is listed. The principal precursors present at the time of the transient are shown in parentheses. The high-temperature zone includes the fuel, cladding, heater, and reflectors.

and operating procedures. The equipment permitted argon gas present in the fuel autoclave during the reactor transient to be transferred at a controlled rate to another container. Fission products deposited from the gas stream at high and at low temperature were separated and identified. Particle-size determinations were made with particles removed from the aerosol by filters and by studying the distribution of activity on the walls of a diffusion tube. Fragmentation of the fuel, which has occurred in experiments in the TREAT reactor on steam-fuel reactions conducted by Argonne National Laboratory experimenters, was not observed in the experiments described here, possibly due to preheating of the fuel. The gross appearance of the fuel specimen resembled that observed when UO_2 pellets were heated by means of centered tungsten resistors. Surface cracking was quite evident in the specimen that did not melt, in experiment 1; and clear evidence of flowing and "foaming" of UO_2 was observed by postirradiation examinations of the fuel specimen from experiment 2.

Fission product release under the conditions of these experiments was shown to be related to the physical characteristics of precursor species present while the fuel was at or near its maximum temperature. Release from the high-temperature zone was found to be less than 2% except for isotopes that had rare-gas precursors.

---

3. Behavior of Fission Products Released During In-Pile Destruction of Reactor Fuels

W. E. Browning, Jr.
C. E. Miller, Jr.
B. F. Roberts
R. P. Shields

In-pile experiments of the type previously described[1] are being continued to study the characteristics and behavior of fission products released during simulated reactor accidents. These experiments use fission products released by melting or vaporizing miniature stainless-steel-clad UO_2 fuel elements in the Oak Ridge Research Reactor (ORR) in a helium atmosphere. Eleven such experiments have been conducted and analyzed. Studies have been made of the effects of gas velocity on fission product release and behavior, of the fine-particle and vapor forms of released fission products, of the particulate material collected by filters, of the distribution of released fission products, and of the fractionation of fission products. These studies are described in detail in the following sections.

A monitor has been made to survey the neutron and gamma fluxes in the in-pile fuel melting facility of the ORR throughout the reactor cycle. This device was made by replacing the fuel in a fuel melting experimental unit with a chamber through which argon gas can be passed. Activation of the argon is measured to determine the neutron flux. The temperatures of the ceramic parts of the unit indicate the intensity of gamma heating. These measurements will assist in the control of the intensity of heating in the in-pile experiments, a factor which has been found to have a strong effect on fission product release. The off-gas system of the in-pile facility has been modified to accommodate the flux monitor and to permit transferring the released gaseous fission products from the liquid-nitrogen-cooled charcoal trap to a reservoir where samples can be taken without removing the charcoal trap from the shielded enclosure.

[1] W. E. Browning, Jr., *et al.*, *Nuclear Safety Program Semiann. Progr. Rept. June 30, 1963*, ORNL-3483, pp. 22–26.

EFFECT OF GAS VELOCITY ON RELEASE AND BEHAVIOR OF FISSION PRODUCTS

Experiments 10 and 11 were performed to study how the helium sweep gas flow rate affects fission product release. The gas velocity evaluted at fuel melting temperature was increased from 60 fpm, used in previous experiments (3 to 9), to 125 fpm in experiment 10, and to 350 fpm in experiment 11. Other conditions remained the same as in previous experiments. The results of radiochemical analysis of the fission product distributions in these experiments are given in Table 3.1 and 3.2 along with the results of previous experiments for comparison. The conclusions regarding the effects of flow rate are:

1. An increased helium flow rate lowered the maximum temperature of the fuel. Based on the extent of melting and on the appearance of the fuel, the maximum temperature of experiment 11 appeared to be between those of experiments 7 and 8 which did not melt completely.

2. Release of fission products from the fuel itself does not appear to be affected by flow (except as flow affects temperature) since the release values for experiment 11 fall between those of experiments 7 and 8.

3. Release of the more volatile isotopes iodine, tellurium, and cesium from the high-temperature zone of the furnace does not appear to be affected by an increased flow rate, but the release of the less volatile isotopes increased fourfold with a sixfold increase in rate.

4. The above effects are apparently insignificant for moderate increases in flow rate since they could hardly be detected in experiment 10.

Analysis of the deposits of fission products in the diffusion tube in experiment 10 showed the fine-particle pattern found in previous experiments; while the deposits in experiment 11 indicated the presence of vapor forms of fission products, as will be discussed in detail in the next section.

These results indicate that the release of fission products from melted fuel is rather insensitive to flow rates; but that the form of the released fission products and their behavior can be affected if the gas velocity, evaluated at the melting temperature of the fuel, is of the order of 300 fpm.

Table 3.1. Material Released from the Fuel in UO_2 Melting Experiments[a]

Experiment	Release (%)								
	I^{131}	Te^{132}	Cs^{137}	Ru^{106}	Sr^{89}	Ba^{140}	Zr^{95}	Ce^{144}	UO_2
2				83	99.8	99.8	87	93	50
3				48	93	96	87	85	43
4	99.6			81	77	94	56	59	44
5	99.4	99.2	98	91	57	55	43	44	34
6	99.0	95	99.3	59	55	52	60	49	47
7	96		96	11	5.2	14	0.91	2.5	0.72
8	99.0	98	98	57	44	70	58	43	36
9	99.7	99.1	99.0	93	71	71	72	70	70
10	97	96	96		69	72	58	59	56
11	98	99.4	96	48	18	26	12	7.6	5.1

[a]Sample length, 1 in.; diameter, 0.210 in.; sample molten 5 min except experiment 2, 10 min; helium velocity evaluated at fuel melting point, 60 fpm, except experiments 10 and 11, 125 and 350 fpm.

Table 3.2. Material Released from High-Temperature Zone[a] of the Furnace in UO_2 Melting Experiments

Experiment	Release (%)								
	I^{131}	Te^{132}	Cs^{137}	Ru^{106}	Sr^{89}	Ba^{140}	Zr^{95}	Ce^{144}	UO_2
2				3.3–5.1	21	17–27	0.12	0.60	4.1
3				0.64	1.2	0.73	0.10	1.8	0.052
4	91			5.9	2.3	0.94	.036–.044	0.30–0.40	0.077
5	88	80	82	5.2	1.4	2.3	0.019	0.32	0.23
6	94	52	82	0.70–1.3	0.91	0.55	0.090	0.068	0.29
7	50	12	74	1.8–2.2	0.87	0.58	0.037	0.32	0.015
8	95	82	88	1.7	1.3	0.82	0.051	0.24	0.020
9	80	90	59	3.8	0.97	1.1	0.12	0.30	0.013
10	89	72	81		2.1	2.8	2.8	1.0	0.29
11	89	69–92	88	0.13–0.17	2.9	8.0	0.57	1.2	1.6

[a]High-temperature zone includes fuel material and thermal insulation; minimum temperature, 1000°C; sample length, 1 in.; diameter, 0.210 in.; sample molten 5 min except experiment 2, 10 min; helium velocity evaluated at fuel melting point, 60 fpm, except experiments 10 and 11, 125 and 350 fpm.

RELEASED FISSION PRODUCTS ASSOCIATED WITH FINE-PARTICLE AND VAPOR FORMS DETERMINED BY DIFFUSION COEFFICIENT MEASUREMENT

Analysis of the distribution of released fission products and uranium deposited from a gas flowing laminarly through a diffusion tube yields information about vapors, gas-borne particles in the range of 10 to 100 A in diameter, and the amounts of released material associated with these forms. The tube connecting the in-pile fuel melting furnace with the filter unit is used for this purpose, and the data are analyzed by the technique developed by Browning and Ackley.[2] The preliminary results[3] have been refined and the results for all the experiments have been obtained.

All the experiments show similar diffusion coefficients with the exception of experiment 11 which had a higher flow rate. For example, the deposition of fission products along the isothermal part of the tube for experiment 6 is shown in Fig. 3.1. The slopes of the lines and thus the diffusion coefficients and particle sizes for the various fission products are quite similar. The intercepts are related to the total amounts of material associated with the corresponding diffusion coefficients; however, corrections must be applied to compensate for the effects of high temperature of the tube near the furnace. The results of such calculations are treated below.

The deposition of fission products for experiment 11 is shown in Fig. 3.2. The relative gas velocity, which was 1.0 for experiment 6, was 5.75 for this experiment. The slopes and thus the diffusion coefficients for this experiment are considerably greater than those for other experiments. Experiment 10 did not show these changes in diffusion coefficients even though the relative gas velocity was 2. The experiment 11 data indicate that the deposited fission products were carried in the vapor form rather than being associated with small particles. Theoretical estimates of the diffusion coefficients of the various elemental fission products and their oxides have been made and are consistent with the observed values within a factor of 2; however, it is not possible to distinguish between the elemental and oxide forms of the fission product vapors.

[2]W. E. Browning, Jr., and R. D. Ackley, *Nuclear Safety Program Semiann. Progr. Rept. June 30, 1962*, ORNL-3319, pp. 44–50.

[3]W. E. Browning, Jr., *et al.*, *Nuclear Safety Program Semiann. Progr. Rept. Dec. 31, 1962*, ORNL-3401, pp. 27–35.

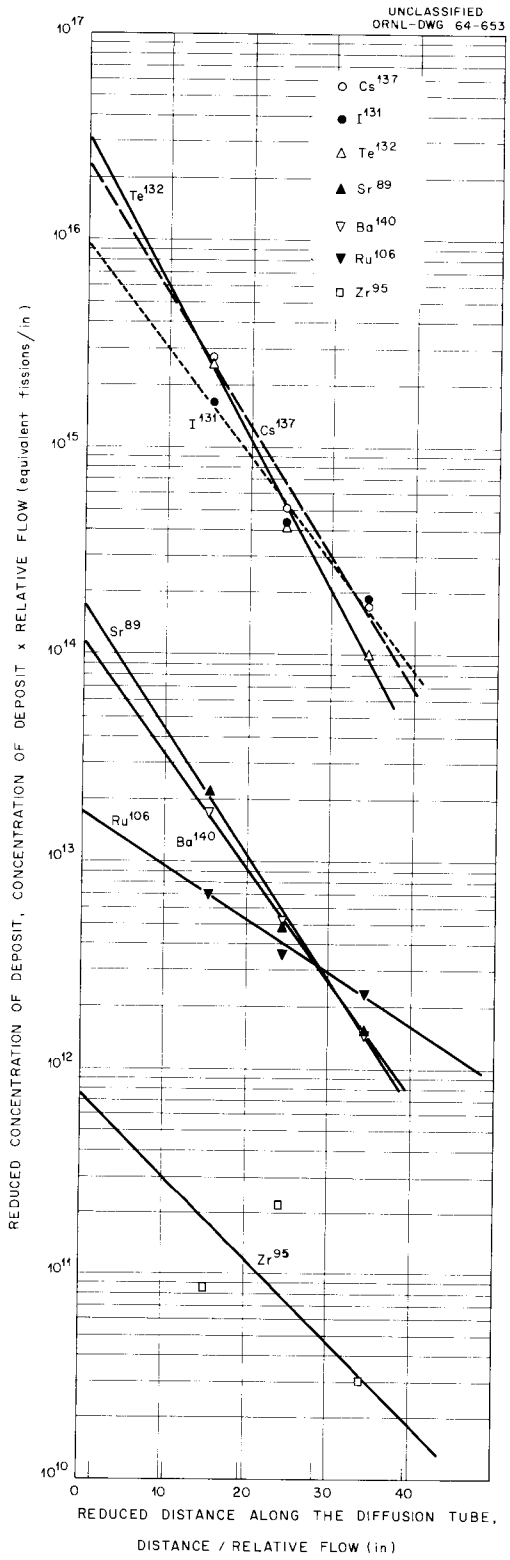

Fig. 3.1. Concentrations of Deposited Materials Along the Diffusion Tube of In-Pile Meltdown Experiment 6. Slopes correspond to fine particle forms of materials.

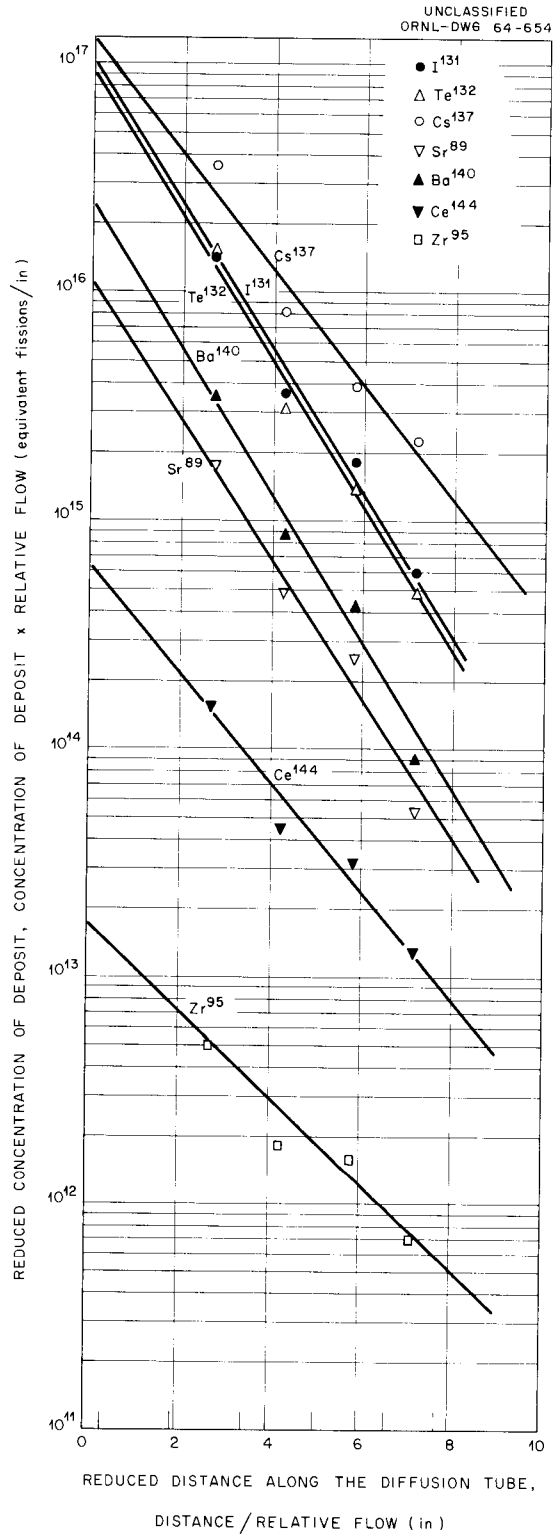

Fig. 3.2. Concentrations of Deposited Materials Along the Diffusion Tube of In-Pile Meltdown Experiment 11. Slopes correspond to vapor forms of materials.

Table 3.3 shows particle sizes calculated for individual fission products and uranium by the diffusion-tube technique for the experiments on the melting of UO_2 (experiments 2 to 11) and also for the experiments on the burning of fuel composed of pyrolytic-carbon-coated uranium carbide in a graphite matrix (experiments G-1 and G-3). Table 3.4 shows the amounts of material associated with the corresponding diffusion coefficients for these experiments. These amounts of material are expressed as percentages of those released from the high-temperature zone of the furnace. In those cases where fission products associated with vapor or with gas-borne particles in the range of 10 to 100 A in diameter could not be detected by this technique, the limits of sensitivity for 25-A particles are given and are indicated by < symbols. Dashes in the tables indicate either that radiochemical data were not obtained or that they contained an inconsistency. In determining averages, dash entries and limits of sensitivity are ignored. The data in these tables indicate that particles having an average diameter of about 25 A were released in experiments 2 to 10 and experiments G-1 and G-3. Considerable amounts of released I^{131}, Te^{132}, and Cs^{137} are always carried by these fine particles. Smaller amounts of released Sr^{89} and Ba^{140} always, of uranium frequently, and of Ru^{106} infrequently are carried by these particles in the UO_2 melting experiments but these substances did not appear to be carried by particles of this size in the uranium carbide–graphite burning experiments. In the case of the UO_2 melting experiments, Zr^{95} and Ce^{144} are very seldom carried by particles of this size, but they are usually carried by these particles in the uranium-carbide–graphite burning experiments. Besides being carried by these small particles, the various fission products and uranium are probably also carried by larger particles which pass through the diffusion tube and are retained on the filters. Although the particle sizes

Table 3.3. Diameter of Small Particles Associated with Fission Products and Uranium Released from the In-Pile Furnace as Calculated from Diffusion Coefficient Measurement

Experiment Number	Diameter (A)									Average Diameter
	I^{131}	Te^{132}	Cs^{137}	Ru^{106}	Sr^{89}	Ba^{140}	Zr^{95}	Ce^{144}	U	
2	20	–	26		23	18				22
3	21	–	22		17	22			32	23
4	24	22	26		25	19		28	28	24
5	21	22	27		19	18			18	21
6	23	18	20	33	21	22	26		30	24
7	20	24			25	45				28
8	24	28	39	38	36	45				35
9	20	19	21		20	22				20
10	16	16	18		18	18			26	18
Average (Expt. 2–10)	21	21	25	35	22	25	26	28	27	24
11	Vapor	Vapor	Vapor	Vapor	Vapor	Vapor	Vapor	Vapor	Vapor	
G-1	25	14	14				27	34		23
G-3	30	14	35				19			24
Average (Expt. G-1 and G-3)	28	14	24				23	34		24

Table 3.4. Fission Products and Uranium Carried by Small Particles or as Vapors Expressed as Percentage[a] of That Released from High-Temperature Zone of the In-Pile Furnace

Experiment	Percentage Released (%)								
	I^{131}	Te^{132}	Cs^{137}	Ru^{106}	Sr^{89}	Ba^{140}	Zr^{95}	Ce^{144}	U
2	–	–	25	<11	22	12	<83	<100	<6.0
3	–	–	16	<10	9.7	4.4	<1.3	<0.24	5.4
4	12	1.6	5.8	<15	4.4	6.0	<4.8	13	0.38
5	56	2.8	29	<29	17	17	<11	<43	19
6	38	68	25	3.1	15	14	1.1	<34	–
7	3.1	6.4	<0.85	<17	1.3	3.5	<30	<27	<19
8	6.1	3.8	6.2	2.4	2.4	1.8	<1.0	<4.8	<0.075
9	37	24	33	<3.1	11	4.2	<1.3	<5.6	<7.2
10	9.0	3.8	8.9	–	2.1	1.4	<0.43	<12	0.68
Average (Expt. 2–10)	23	16	18	4.8	9.5	7.0	1.1	13	6.4
11	46	22	29	20	50	55	1.0	13	13
G-1	13	8.4	14	<2.3	<2.3	<5.3	10	26	<3.4
G-3	58	32	25	<4.7	<5.5	<8.0	8.2	<19	<7.1
Average (Expt. G-1 and G-3)	36	20	20				9.3	26	

[a]The symbols (<) indicate limits of sensitivity for 25-A particles where small particles were not detected. Dashes indicate that radiochemical data were not obtained or that they contained an inconsistency.

as calculated using the data of certain fission products appear to show a consistent deviation from the average, there is insufficient evidence to demonstrate that different fission products are associated with particles of different sizes in the 10- to 100-A diameter range.

The tables also show the fission products which were carried as vapors in experiment 11. Considerable amounts of released I^{131}, Sr^{89}, and Ba^{140} and smaller amounts of Te^{132} and Cs^{137} were carried as vapors. However, only small amounts of Zr^{95}, Ce^{144}, Ru^{106}, and U were carried as vapors. The appearance of vapor forms of these materials at higher gas velocities could be caused by their more rapid transport from the release site and their greater dilution, both of which would reduce the tendency for particle formation.

Diffusion coefficient measurements have given information about the amounts and forms of fission products released in trace level experiments. The association of significant fractions of the released fission products and uranium with fine particles approximately 25 A in diameter could have important effects on the behavior of these materials in reactor accidents.

PARTICULATE MATERIAL COLLECTED BY FILTERS

The sweep gas from the in-pile fuel melting and burning experiments is passed through a series of filters to obtain information about the particulate material which is formed. Figure 3.3 shows the filter assembly which was designed for this purpose. Figure 3.4 shows the three filters

Fig. 3.3. Filter Assembly and Charcoal Trap Used in In-Pile Fuel Destruction Experiments.

from a typical UO_2 melting experiment, No. 10. Both the roughing filter, Fig. 3.4*a*, and the HV-70 filter, Fig. 3.4*b*, collected a visible deposit. The deposit on the 10-mμ membrane filter, Fig. 3.4*c*, was not visible to the naked eye, but the deposit could be detected by its radioactivity and by electron microscopy. The sizes of particles, their states of aggregation, and certain other information about them can be determined by electron microscopy. Most of the filters, especially those initially encountered by the gas stream, have been too radioactive for electron microscopy, but data on a few filters have been obtained.

Electron-photomicrographs of particle collections from two of the filters studied in the UO_2 melting experiments are shown in Figs. 3.5 and 3.6. Figure 3.5 shows the particles of experiment 11 which were collected on an HV-70 filter after they had passed through a coarse glass roughing filter. This material is similar to that shown in Fig. 3.4*b*. A wide range of particle sizes is present since even the large round objects appear to be single particles. The particles are highly agglomerated, and each agglomerate consists of particles having a narrow size range. That is, some agglomerates consist mostly of small particles and some consist mostly of larger particles. This condition suggests that particles of widely differing sizes occurred only at different times or places during the experiment and did not have an opportunity to agglomerate together. For those particles small enough to be partially transparent to elec-

trons, there is a significant variation in the opacity of individual particles of the same size, as evidenced by the variation from gray to black of the smaller spots in Fig. 3.5. Perhaps the more dense particles are UO_2 and the less dense ones are stainless steel.

Figure 3.6 shows the particles of experiment 10 which were collected on a 10-mμ membrane filter after they had passed through a roughing filter and an HV-70 filter. These particles were on the filter shown in Fig. 3.4c. The shapes and transparencies of many of them suggest that they are platelets. Although there is much material on this filter, there are too few isolated particles to yield a reliable particle-size distribution. Techniques are being introduced to use a different method of

UNCLASSIFIED
PHOTO 64103

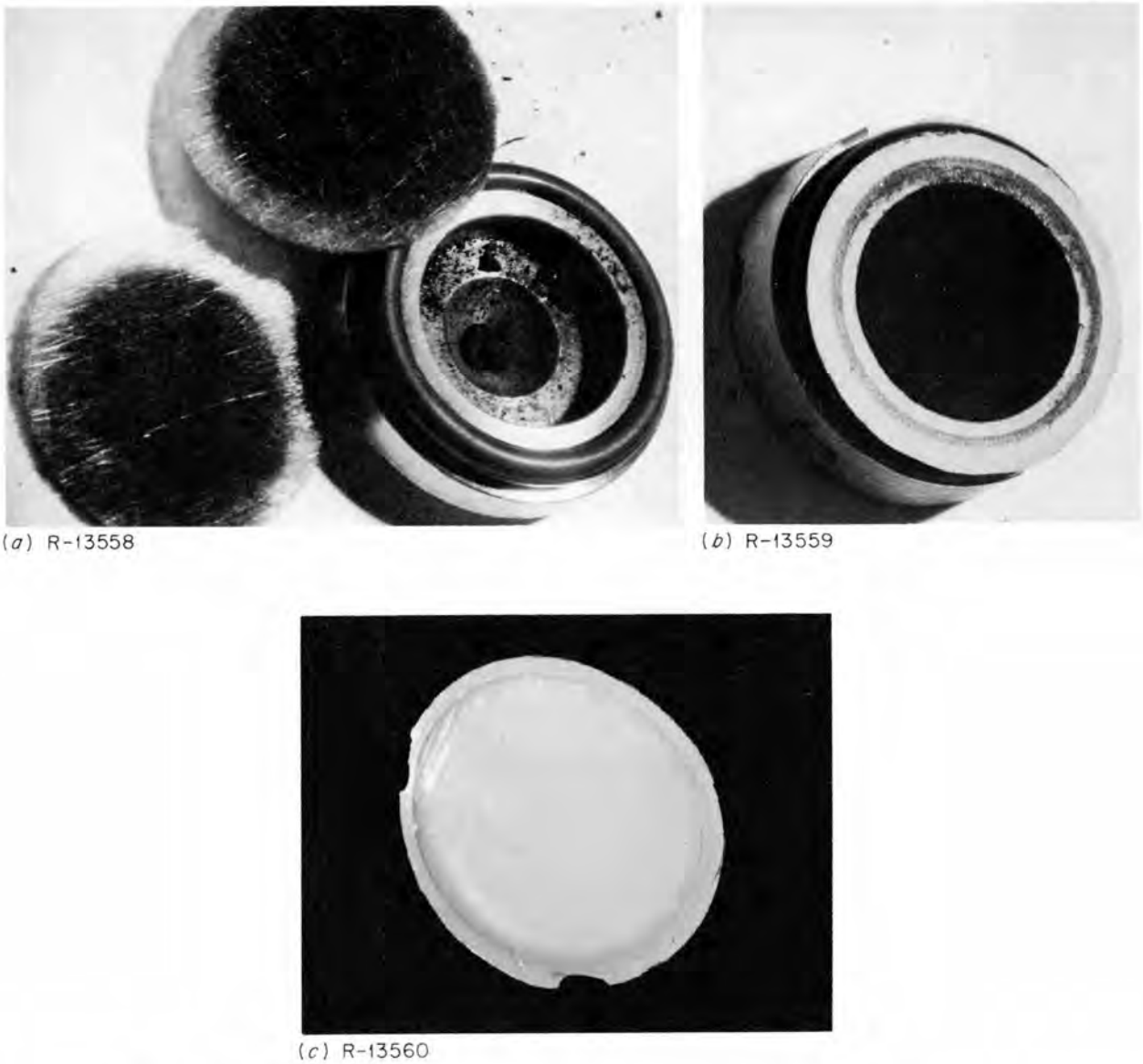

(*a*) R-13558 (*b*) R-13559

(*c*) R-13560

Fig. 3.4. Filters from UO_2 Melting Experiment 10. (*a*) First filter (layers of coarse glass fibers) and entrance cap to the filter housing containing part of the filter deposit. (*b*) Second filter (HV-70). (*c*) Third filter (10-mμ membrane).

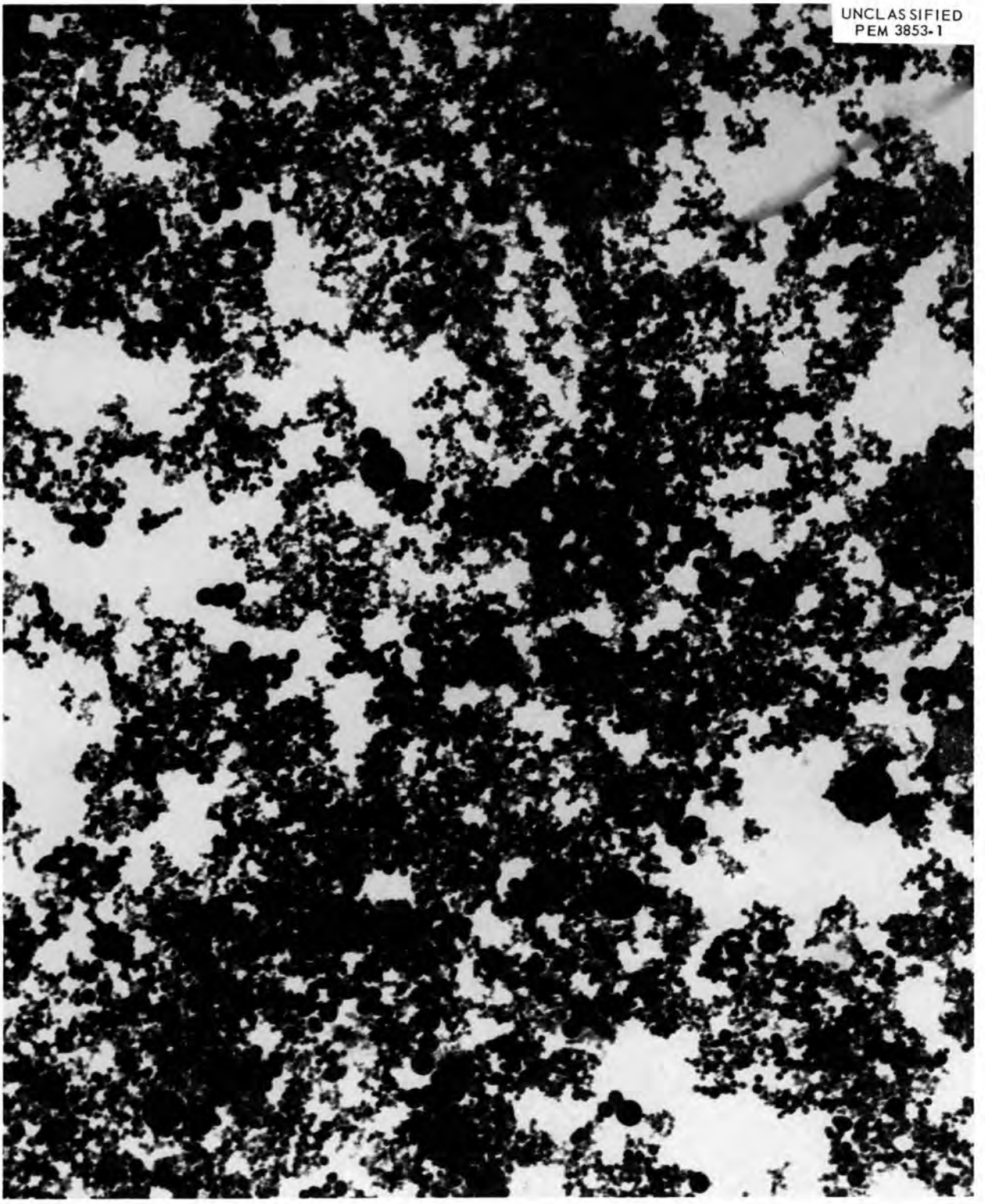

Fig. 3.5. Material Collected on Filter 2 of In-Pile UO_2 Melting Experiment 11. 32,000X.

Fig. 3.6. Material Collected on Filter 3 of In-Pile UO_2 Melting Experiment 10. 32,000X.

sample preparation in hopes of obtaining a more suitable dispersion on the microscope grid.

Figures 3.7 and 3.8 show the size distributions measured by electron microscopy of particles collected on various filters. The particles found on the filters of experiment G-1 are considerably larger than those found on the filters of the UO_2 melting experiments. There are insufficient data to indicate whether this is a general characteristic of the uranium carbide–graphite burning experiments; however, since the data were obtained on a broken filter, the distribution of particles on the filter from experiment G-3 is not necessarily evidence to the contrary. The results of these measurements are summarized in Table 3.5. It must be emphasized that these data refer not to the material originally carried by the gas, but to that which penetrated one or more filters and which was collected by a subsequent filter. The type of filter preceding the filter on which particles were collected is shown in the table because the number and size of particles caught on a filter are greatly influenced by the preceding filter. The last column of the table gives the median diameter of the particles found on the filter if isolated particles were found in sufficient number to represent the distribution reliably. If an insufficient number of isolated particles were found, the indicated size range is given.

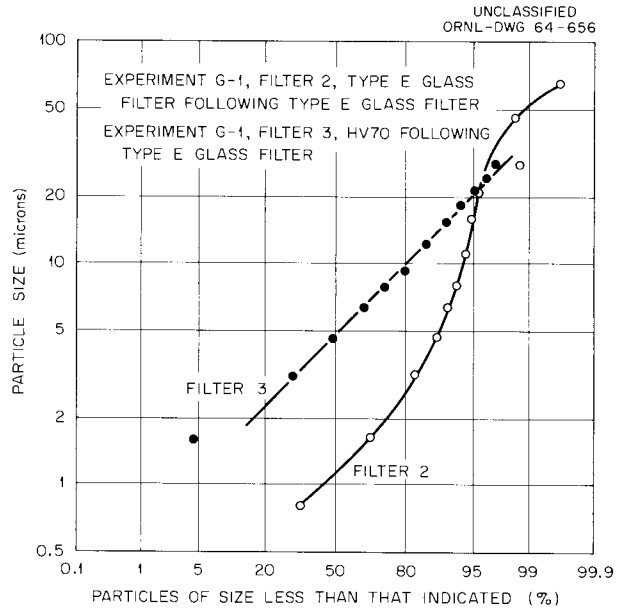

Fig. 3.8. Size Distribution of Particles Retained on Filters of Fueled Graphite Burning Experiment.

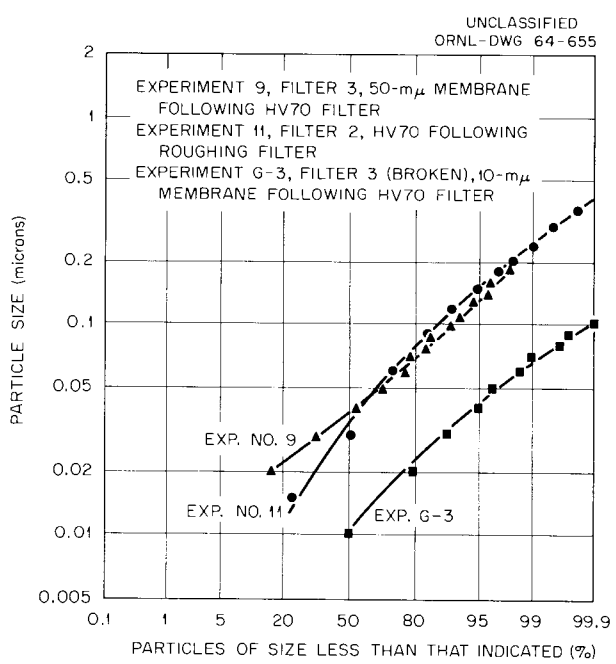

Fig. 3.7. Size Distribution of Particles Retained on Filters of In-Pile Fuel Destruction Experiments.

These data indicate that particles ranging in size from 0.015 to over 1 μ occur downstream from the initial filter in the UO_2 melting experiments. Median particle diameters ranged from 0.01 to 5 μ in the corresponding filters in the uranium carbide–graphite burning experiments. In the UO_2 experiments agglomerates of like-sized particles and particles of various densities were observed. In some cases particles were spheres and in others they appear to be platelets.

DISTRIBUTION OF RELEASED FISSION PRODUCTS THROUGH OFF-GAS SYSTEM

In each of the in-pile fuel destruction experiments, the distribution of the released fission products and uranium between the various parts of the furnace, the diffusion tube, the filter assembly, and the charcoal trap are determined by radiochemical and chemical analysis. These data for all the in-pile experiments are being processed and evaluated for presentation in a condensed form in a forthcoming progress report. The data in their original form are much too voluminous for inclusion

Table 3.5. Sizes of Particles on Filters Studied by Electron Microscopy

Experiment Number[a]	Filter Number	Type of Filter	Filter Preceded by a Filter of Type:	Particle Diameter
9	3	50-mμ membrane	HV-70	Median particle diameter, 0.04 μ; geometric standard deviation (GSD), 2.2
10	3	10-mμ membrane	HV-70	Highly agglomerated particles, diameter range of 0.015 to 1.2 μ
11	2	HV-70	Coarse glass fiber	Median particle diameter, 0.03 μ; GSD, 2.8
11	3	0.8-μ membrane	HV-70	Highly agglomerated particles, diameter range of 0.015 to 0.64 μ
G-1	2	Type E glass	Type E glass	Median particle diameter, 1.2 μ; GSD, 3.4
G-1	3	HV-70	Type E glass	Median particle diameter, 5 μ; GSD, 2.6
G-3	3	10-mμ membrane (broken)	HV-70	Median particle diameter, 0.01 μ; GSD, 2.7

[a]"G" prefix indicates experiments with uranium carbide–graphite fuel. Others were with UO_2.

here. However, in Tables 3.6 and 3.7 some of the information is shown for experiment 9, which is typical of many of the in-pile UO_2 melting experiments. Sixty to ninety percent of the three more-volatile fission products (iodine, tellurium, and cesium) escaped from the high-temperature zone of the furnace and were distributed more or less evenly between the cold stainless steel enclosure of the furnace, the diffusion tube, and the roughing filter. The HV-70 filter collected about 3% of the inventory of iodine and cesium. Approximately 3% of the iodine and 4% of the cesium were found downstream of the HV-70 filter. Contamination interfered with the measurement of tellurium in experiment 9, but less than ½% of the tellurium penetrated the HV-70 filter in other experiments. Four percent of the ruthenium escaped from the hot zone and half of that was stopped by the HV-70 filter. Most of the remainder was found on the membrane filter or its support. The other fission products (strontium, barium, zirconium, and cerium) and uranium were released from the hot zone in amounts of 1% or less. Not more than 0.25% of the inventory of these materials was found downstream from the HV-70 filter. The filters exhibited a rather low percentage of effectiveness against the

Table 3.6. Material Found in Specified Regions of the Off-Gas System of In-Pile UO_2 Melting Experiment 9

Region	Percentage of Total Inventory								
	I^{131}	Te^{132}	Cs^{137}	Ru^{106}	Sr^{89}	Ba^{140}	Zr^{95}	Ce^{144}	U
Furnace primary (cold wall)	24	67	15	0.05–0.25	0.42	0.79	0.075	0.17	0.0071
Diffusion tube	13	8.6	12	0.06–0.08	0.057	0.02	0.0013	0.011	0.0007
First filter (coarse glass fiber)	30	*a*	22	0.053	0.20	0.13	0.0024	0.020	0.0014
Second filter (HV-70)	3.2	*a*	3.6	1.9	0.027	0.015	0.0061	0.018	0.00014
Third filter (50-mμ membrane)	0.49	*a*	0.11	0.63	0.0048	0.0022	0.0085	0.0090	0.00043
Charcoal	0.39	*a*	2.2	0.0–0.01	0.23	0.1	0.00087	0.0030	0.0

[a]Sample contaminated.

Table 3.7. Material Downstream from Specified Regions of In-Pile UO_2 Melting Experiment 9[a]

Region	Percentage of Total Inventory								
	I^{131}	Te^{132}	Cs^{137}	Ru^{106}	Sr^{89}	Ba^{140}	Zr^{95}	Ce^{144}	U
Furnace primary (cold wall)	56	>23	44	3.7	0.56	0.31	0.048	0.13	0.0057
Diffusion tube	43	>14	32	3.6	0.50	0.29	0.047	0.12	0.0050
First filter (coarse glass filter)	11	>13	9.0	3.2	0.28	0.15	0.019	0.057	0.0035
Second filter (HV-70)	2.8	*b*	4.2	1.3	0.25	0.13	0.013	0.035	0.0033
Third filter (50-mμ membrane)	1.4	*b*	4.1	0.64	0.25	0.12	0.0042	0.025	0.0028
Charcoal	0.063	*b*	0.29	0.022	0.0029	0.00008	0.00027	0.0030	0.00040

[a]Since only the more significant parts are tabulated, care must be exercised if numbers from Tables 3.6 and 3.7 are used together.

[b]Sample contaminated.

materials which arrived at their faces, but the materials which penetrated were very small fractions of the total inventory.

FISSION PRODUCT FRACTIONATION

In fission product release experiments, fission products appear in varying proportions in various locations, and sample compositions are in general different from those predicted for normal fission yields. This fractionation occurs because differences in the physical and chemical characteristics of individual fission products result in differences in their behavior in release, transport, or deposition processes.

Fractionation of fission products is expected to occur similarly in reactor accidents. Thus, certain

fission products will be retained disproportionately and the total hazard will be much less than would result from the release of unfractionated fission products. One of the central purposes of reactor safety experiments is to generate information about the processes of release, transport, and deposition of fission products so that realistic hazard assessments can be made.

A quantitative theoretical analysis of the observed variation in fission product proportions can be used to test the validity of various proposed mechanisms of fractionation. Knowledge of these mechanisms will make available a new tool for the prediction of the hazards of fission product release associated with reactor accidents and will help to recognize conditions which are important in their effects on fission product release, transport, and deposition so that those conditions might be explored as variables in laboratory experiments.

A study has been made in which the fractionation predicted by several different models was compared with experimental results. Basically, there are two models, cocondensation and vapor transpiration. In the first model, fission products in the gas phase are fractionated by cocondensation of the fission products with some other material in the gas phase, for example, stainless steel. In the second model, fractionation is brought about by evaporation of the fission products from the fuel and by their removal by a carrier-gas stream. In either model each sample collected represents the composition of the fractionated gas phase at some particular instant during the experiment. The vapor transpiration model gives the most satisfactory agreement with the data from the in-pile fission product release experiments.

Vapor Transpiration Model

The vapor transpiration model deals with the fractional vaporization of fission products from the heated fuel at various temperatures. The carrier gas removes the vaporized materials to regions of lower temperature where they are rapidly cooled without further change in composition. These materials are then deposited at locations which depend upon their forms and indirectly upon the temperatures at which they were vaporized. These three details of the model are assumed arbitrarily and their justification depends upon the success of the model in predicting the fractionation of fission products.

The following additional assumptions are made in the development of this model:

1. The concentrations of the vapors of fission products and other materials in the gas passing over the fuel are proportional to the concentrations corresponding to solubility equilibrium between gaseous and condensed phases.
2. The modified Henry's law constants for this equilibrium are independent of temperature.
3. The fuel residue changes negligibly in composition.

The first assumption is based on the expectations that equilibrium would be achieved rapidly at very high temperatures and that the extent of dilution by unequilibrated carrier gas would be the same for various temperatures. The second assumption has been found to be reasonably accurate in other systems. The third assumption is valid in the present experiments for the fission products considered thus far; however, under some conditions it could become a limitation which requires modification of the model.

The evaporation step is described by Henry's law since the fission products can be considered to be dilute solutes in UO_2 solvent. The partial pressure, in atmospheres, of any one fission product vapor in the gas at equilibrium with the UO_2 is

$$P_{eq} = xk \ , \tag{1}$$

where x is the mole fraction of fission product in the UO_2 and k is Henry's law constant, in atmospheres. The partial pressure after mixing with unequilibrated carrier gas is

$$P = rP_{eq} = rxk \ , \tag{2}$$

where r is the ratio of volumes before and after mixing. The Henry's law constant may be expressed as a function of the vapor pressure of the pure fission product, and Eq. (2) becomes:

$$P = rxk'P^0 \ , \tag{3}$$

where P^0 is the vapor pressure of pure fission product, a function of temperature, in atmospheres, and k' is the modified Henry's law constant, assumed independent of temperature, dimensionless.

As the fission product vapor is carried to regions of lower temperature, it is quenched so that for each dV of volume quenched, an amount of sample containing dn_s moles of fission product is collected and so from the gas law

$$dn_s = \frac{P\,dV}{RT_{std}}\,, \tag{4}$$

where

dn_s = increment of sample, moles;

dV = increment of gas volume, cm^3;

R = gas constant, cm^3 atm $mole^{-1}$ deg^{-1};

T_{std} = temperature at which gas volume is measured, °K.

The volume of gas flowing past the fuel is a function of time and is given by

$$V = ft\,, \tag{5}$$

where

V = total gas volume, cm^3;

f = gas flow rate, cm^3/sec, a constant;

t = time, sec.

Taking the differential of Eq. (5) and substituting it and Eq. (3) into Eq. (4) gives

$$dn_s = \frac{rfk'xP^0\,dt}{RT_{std}}\,. \tag{6}$$

Calculations of the amount of fission product vaporized at various temperatures requires a relation between time and temperature. In experiments or reactor accidents of short duration, the temperature history during heating can be approximated crudely but adequately by a straight-line relation of the form

$$T = a + bt\,, \tag{7}$$

and by a similar expression during cooling. The exact form of Eq. (7) is not very important for the present purpose as long as the proper range of temperatures is covered. Other temperature-time functions have been examined, and since ratios of fission products are used, the choice seems to have no effect on the final outcome of the theoretical treatment. Substituting the differential of Eq. (7) into Eq. (6) gives

$$dn_s = \frac{rfk'xP^0\,dT}{bRT_{std}}\,. \tag{8}$$

The total number of moles released from the fuel into the gas during the temperature excursion is given by

$$n_g = \int dn_s = \frac{2rfk'x}{bRT_{std}} \int_{T_i}^{T_m} P^0\,dT\,, \tag{9}$$

where

T_i = initial temperature, °K,

T_m = maximum temperature, °K.

The limits to the integral will be omitted below for typographical simplicity. Here the factor 2 arises to account for both the periods of ascending and descending temperature.

Values for the modified Henry's law coefficient, k', are not readily available for solutions of vapors of the various fission products in UO_2; however, data from fission product release experiments can be used to evaluate n_g and the value of k' can be determined by rearranging Eq. (9):

$$k' = \frac{bRT_{std}n_g}{2rfx}\left(\frac{1}{\int P^0\,dT}\right). \tag{10}$$

Substituting Eq. (10) into Eq. (8), canceling terms, and expressing the result as fraction of the total number of moles of fission product give

$$\frac{dn_s}{n_t} = \frac{n_g P^0\,dT}{2n_t \int P^0\,dT}\,, \tag{11}$$

where n_t is the total number of moles of fission product inventory in the experiment.

Experimental testing of Eq. (11) would require data on the temperature and the temperature interval associated with each sample. Since fuel temperatures in the in-pile experiments cannot be measured directly, and the beginnings and ends of periods associated with individual samples are entirely obscure, it is convenient to eliminate these quantities by combining the expressions for different fission products. Thus elimination of

the temperature interval, dT, yields

$$\frac{dn_{2s}/n_{2t}}{dn_{1s}/n_{1t}} = \frac{(n_{2g}/n_{2t})\,P_2^0}{(n_{1g}/n_{1t})\,P_1^0}\;\frac{\int P_1^0\,dT}{\int P_2^0\,dT}, \qquad (12)$$

where subscripts 1, 2, etc., indicate various fission products.

The vapor pressure of a pure fission product, P^0, is a function of temperature and may be expressed in the Clausius-Clapeyron form:

$$P^0 = Be^{-\Delta H/RT}, \qquad (13)$$

where

ΔH = heat of vaporization of fission product, cal/mole,

R = gas constant, cal deg^{-1} mole^{-1},

B = coefficient in vapor pressure expression, atm.

Substituting Eq. (13) for each fission product into Eq. (12) and taking the natural logarithm of both sides give

$$\ln\frac{dn_{2s}/n_{2t}}{dn_{1s}/n_{1t}} = \frac{\Delta H_1 - \Delta H_2}{RT} + \ln B_2 - \ln B_1 + \ln\frac{n_{2g}/n_{2t}}{n_{1g}/n_{1t}} + \ln\frac{\int P_1^0\,dT}{\int P_2^0\,dT}. \qquad (14)$$

Equation (14) is also true for other combinations of fission products:

$$\ln\frac{dn_{3s}/n_{3t}}{dn_{1s}/n_{1t}} = \frac{\Delta H_1 - \Delta H_3}{RT} + \ln B_3 - \ln B_1 + \ln\frac{n_{3g}/n_{3t}}{n_{1g}/n_{1t}} + \ln\frac{\int P_1^0\,dT}{\int P_3^0\,dT}. \qquad (14a)$$

Elimination of T between Eqs. (14) and (14a) yields

$$\ln\frac{dn_{2s}/n_{2t}}{dn_{1s}/n_{1t}} = \left(\frac{\Delta H_1 - \Delta H_2}{\Delta H_1 - \Delta H_3}\right)\ln\left(\frac{dn_{3s}/n_{3t}}{dn_{1s}/n_{1t}}\right) - \left(\frac{\Delta H_1 - \Delta H_2}{\Delta H_1 - \Delta H_3}\right)\left(\ln B_3 - \ln B_1 + \ln\frac{\int P_1^0\,dT}{\int P_3^0\,dT}\right) + \ln B_2 - \ln B_1 + \ln\frac{\int P_1^0\,dT}{\int P_2^0\,dT} - \left(\frac{\Delta H_1 - \Delta H_2}{\Delta H_1 - \Delta H_3}\right)\ln\frac{n_{3g}/n_{3t}}{n_{1g}/n_{1t}} + \ln\frac{n_{2g}/n_{2t}}{n_{1g}/n_{1t}}. \qquad (15)$$

Equation (15) predicts that plotting $\ln\,[(dn_{2s}/n_{2t})/(dn_{1s}/n_{1t})]$ vs $\ln\,[(dn_{3s}/n_{3t})/(dn_{1s}/n_{1t})]$ will produce a straight line having a slope given by

$$a = \frac{\Delta H_1 - \Delta H_2}{\Delta H_1 - \Delta H_3}, \qquad (16)$$

and an intercept given by

$$b = \ln B_2 - \ln B_1 + a(\ln B_3 - \ln B_1) + \ln\frac{\int P_1^0\,dT}{\int P_2^0\,dT} - a\ln\frac{\int P_1^0\,dT}{\int P_3^0\,dT} + \ln\frac{n_{2g}/n_{2t}}{n_{1g}/n_{1t}} - a\ln\frac{n_{3g}/n_{3t}}{n_{1g}/n_{1t}}. \qquad (17)$$

The slope, a, depends only upon the heats of vaporization, which are determined by the chemical species of the fission products evaporating from the fuel. The intercept, b, depends upon this and also upon the ratio of the fractions in the gas phase of the total amounts of fission products during the experiment. The integrals in Eq. (17) have upper and lower limits, T_m and T_i, respectively, as defined earlier. These integrals can be evaluated by integrating by parts and by using a numerical approximation, described by Hastings *et al.*,[4] for the exponential integrals, Ei (x), which result. The terms arising from the lower

[4]Cecil Hastings, Jr., J. T. Hayward, and J. P. Wong, Jr., *Approximations for Digital Computers*, Rand Corporation Report R-264, p. 188 (November 1954).

limits are negligible if the temperature range is not small. Thus,

$$P^0\,dT = B\int e^{-\Delta H/RT}\,dT$$

$$\simeq P^0(T_m)\left[1 - \frac{a_0 + a_1(\Delta H/RT_m) + (\Delta H/RT_m)^2}{b_0 + b_1(\Delta H/RT_m) + (\Delta H/RT_m)^2}\right], \tag{18}$$

where $a_0 = 0.251$, $a_1 = 2.33$, $b_0 = 1.68$, and $b_1 = 3.33$. This expression does not involve the temperatures of formation of individual samples but does depend upon the maximum temperature, T_m. The ratios of the integrals are quite insensitive to T_m, and Eq. (17) can be evaluated numerically using only an estimated value for T_m. Thus information from the literature on vapor pressures of fission product materials and experimental data on the amounts vaporized can be used in Eq. (15) to predict the proportions of the fission products in various samples.

Comparison of Theoretical with Experimental Fractionation

The validity of the vapor transpiration model can be tested by comparing the fission product compositions of experimental samples with those predicted by the theory. Figures 3.9 and 3.10 are examples of fractionation plots for strontium, barium, and zirconium in experiments 5 and 10 respectively. The points are actual experimental data while the lines drawn through the points are the theoretical lines predicted by Eq. (15). In Fig. 3.9 the line represents the release of these fission products as oxides from the fuel, while in Fig. 3.10 it represents their release as metals. The theoretical lines were drawn without adjustment of empirical parameters. The choice of whether to use the line for oxides or for metals was dictated by the slope of the data. That this decision is unambiguous can be seen by noting the difference between the slopes in Figs. 3.9 and 3.10. Once this is made the slope of the theoretical line is fixed. Its intercept is determined by the chemical forms of the fission products as well as by the ratio of the number of moles of fission products released to the gas phase. The latter is obtained by summing all the values of samples downstream from the fuel. The agreement between the experimental data and the theoretical lines indicates that Eq. (15) describes adequately the fractionation of strontium, barium, and zirconium in the experiments in which UO_2 is melted in-pile.

Results of Fractionation Analysis

The success of the vapor transpiration model in predicting the fractionation of fission products during in-pile melting of UO_2 validates the assumptions of the model and identifies the mechanism of fractionation. The chemical forms of the fission products during vaporization are identified also in the same operation. In most of the experiments with stainless-steel-clad UO_2, the strontium, barium, and zirconium were vaporized in the metallic form; however, in experiment 5 they were in the oxide form. This type of investigation is being continued, specifically applied to

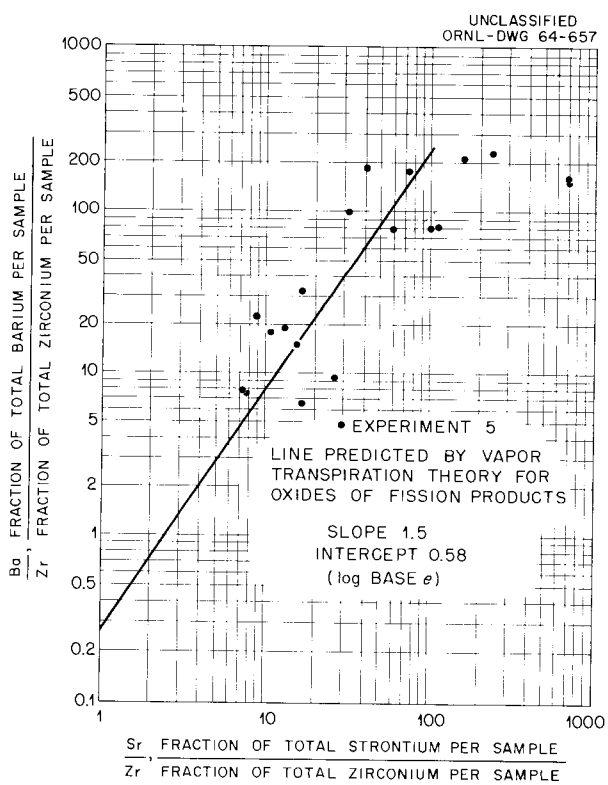

Fig. 3.9. Fractionation of Three Fission Products as Oxides During In-Pile Melting of UO_2.

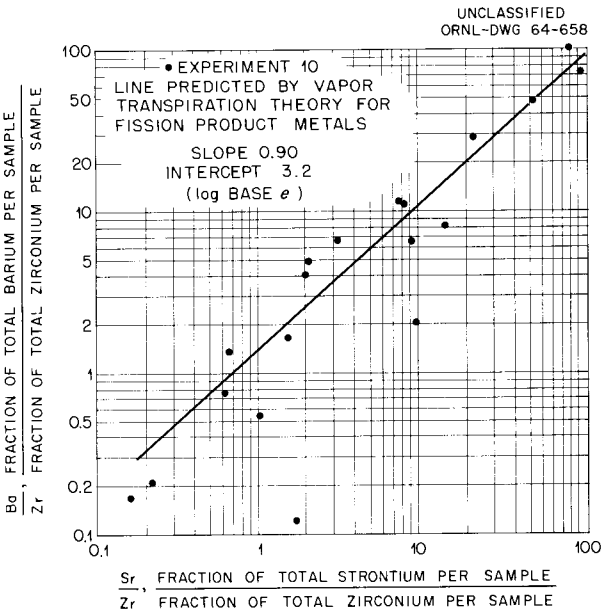

Fig. 3.10. Fractionation of Three Fission Products as Metals During In-Pile Melting of UO_2.

the other fission products for which data are available: iodine, tellurium, cesium, ruthenium, and cerium.

The temperatures can be calculated at which the material in individual samples vaporized if the maximum temperature is known. Otherwise a relative temperature scale can be constructed whose absolute values depend upon the maximum temperature. Thus all the samples can be ranked according to their vaporization temperatures. Ratios of modified Henry's law coefficients, k', for pairs of fission products can be obtained from the data, but not their absolute values. Efforts are being continued to determine T_m and k' values from the data. Such information would make possible theoretical prediction of the amounts of various fission products which would be released given only the temperature history of the fuel, the gas flow rate past it, and the chemical forms of the fission products.

Data on vaporization of fission products and other materials, and related to this theory have been reported in the literature. Freiling[5] has examined empirically the fractionation in fallout from weapons tests. McKenzie[6] has studied the fractional vaporization of uranium-plutonium alloys. In the Cox chart method[7] of treating vapor pressure data, a straight-line plot similar to those in Figs. 3.9 and 3.10 is obtained for which the slope depends only upon the heats of vaporization. The present theory differs from that upon which the Cox plot is based in that mixtures of materials are treated. Preliminary investigations of other applications of this fractionation theory to some of the data in the literature have revealed that fallout data from nuclear weapons tests, fission product release from out-of-pile fuel melting experiments, and from several different types of reactor loop experiments provide information on chemical species similar to that presented for these in-pile experiments.

Further fractionation studies will be made upon data on fission product release from fuels melted with various gas velocities, atmospheric compositions, fission product concentrations, and fuel types to determine if there are correlations with chemical species of released fission products. This would provide a better knowledge of fission product release chemistry and make it possible to predict the hazards of various kinds of fission product release accidents.

---

[5]E. C. Freiling, *Science* **133**, 1991–8 (1961).

[6]D. E. McKenzie, *Can. J. Chem.* **34**, 515–22 (1956).

[7]D. A. Hougen and K. M. Watson, *Chemical Process Principles*, pp. 65–68, Wiley, 1943.

4. Characterization and Control of Accident-Released Fission Products

INVESTIGATION OF THE OCCURRENCE AND BEHAVIOR OF DIFFERENT FORMS OF RADIOIODINE

W. E. Browning, Jr. R. D. Ackley
R. E. Adams

As has been discussed in the previous report of this series, compounds of iodine are observed to occur in air, along with the elemental form, when air and what is presumed to be I_2 vapor are mixed.[1] Since the behavior of these compounds could greatly affect the fate of iodine in reactor accidents and the operating efficiency of iodine removal systems, considerable emphasis is being placed here and elsewhere on the determination of the origin, identity, and behavior of these compounds. A method had been developed earlier for the characterization of gas-borne radioactive vapors and particulates, with the initial principal interest having been in particulates.[2] The method involved measuring the distribution of radioactivity in a channel after gas carrying radioactive materials had flowed through the channel under viscous conditions. Mathematical analysis of the distribution profiles resulting from diffusional deposition yielded diffusion coefficients which are related to molecular properties or particle size. Consequently, when the importance and universality of the iodine compound problem became apparent, use of the diffusional deposition technique was directed toward aiding in the solution of this problem. The initial work of this type has been reported in some detail[1] and will be summarized here. Experimentally, air containing iodine, principally as I_2, was passed through a composite diffusion tube with first silver and then rubber inner surfaces. The silver surface quantitatively removed I_2 and the rubber surface apparently quantitatively removed an iodine compound to yield an indicated diffusion coefficient for it, in air at 1 atm and 25°C, of about 0.05 cm^2/sec, a value suggesting a molecular weight well in excess of that for molecular iodine. Mass spectrometry of the iodine source remaining after the experiment revealed masses of 284 and 338 (amu), both masses being compatible, approximately, with a diffusion coefficient of 0.05 cm^2/sec. The elemental iodine source was prepared by the palladium iodide method which is described in a following section.

Investigation of Iodine Compound Formation at Relatively High Concentrations

More recently, further studies have been conducted using iodine sources produced by the palladium iodide method. Also, iodine produced by what will be referred to as the dichromate method has been utilized in conjunction with both air and helium as the associated gases and at relatively high and very low concentrations in these gases. The work at higher concentrations with iodine prepared by the dichromate method will first be described.

Experiments at Higher Concentrations with Iodine Produced by the Dichromate Method. – The initial objective here was to be able to prepare pure radioiodine and, subsequently, to allow such material to contact other gases and various surfaces, and then to determine if volatile radioactive compounds were produced. The method of iodine preparation investigated was similar to that described by British workers[3,4] and involved the evolution of iodine from melted potassium dichromate containing NaI^{131} and KI^{127}. The experimental procedure was such that the resulting iodine concentrations were in the 10 to 100 mg/m^3 range. The purity was determined by means of the behavior of the iodine in diffusion tubes. With helium as a carrier gas, a purity of

[1] W. E. Browning, Jr., and R. D. Ackley, *Nuclear Safety Program Semiann. Progr. Rept. June 30, 1963*, ORNL-3483, pp. 26–28.

[2] W. E. Browning, Jr., and R. D. Ackley, *Nuclear Safety Program Semiann. Progr. Rept. June 30, 1962*, ORNL-3319, pp. 44–50.

[3] A. C. Chamberlain *et al.*, *Discussions Faraday Soc.* 30, 162–69 (1960).

[4] W. J. Megaw and F. G. May, *Reactor Sci. Technol.* 16, 427–36 (1962).

99.6% was achieved; but with air, the purity was only 98.8% and the principal impurity had a diffusion coefficient in air of about 0.05 $cm.^2$/sec, as had been obtained earlier. Since these observations indicated that the air source was at least partially responsible for the appearance of compounds, attention was directed toward it. The air used in the test yielding 98.8% was plant air passed through an activated carbon trap. A typical relative humidity for plant air expanded to 1 atm is 2%. Since the activated carbon itself might have desorbed gases which subsequently reacted with iodine, as only traces would be required, it was replaced in the next experiment with a trap filled with Linde molecular sieves type 5A. A small portion of the evolved radioactivity did not reach the diffusion tube but deposited, probably due to a gas-phase reaction, as a yellow solid at a point where the air stream carrying the radioactivity was diluted by the main air stream. Preliminary indications are that the deposit was an iodine-oxygen compound. The diffusion tube train had, in addition to silver-plated and rubber tubing, a following section of tube lined with activated carbon dust, which was applied after coating the inside of the tube with an adhesive. Results for this diffusion tube are shown in Fig. 4.1. Virtually all the I^{131} radioactivity which evolved from the dichromate melt and which entered the diffusion tube train was retained in the train, and of this iodine, 99.3% was indicated to be elemental. Most of the remaining 0.7% deposited on the rubber tubing and exhibited a diffusion coefficient in air of about 0.035 cm^2/sec, not greatly different from previous results for rubber tubing. About 0.1% penetrated the silver-plated and the rubber tubing and deposited in the tube lined with activated carbon to yield a diffusion coefficient of 0.10 cm^2/sec, which corresponds to HI or a slightly larger molecule.

The preceding results showed that elemental iodine with a purity in excess of 99% could be prepared without great difficulty for use in further iodine compound investigation where relatively high iodine concentrations are desired. Iodine so prepared will be expected to find use also when studies of the behavior of I^{131}-labeled aerosols are resumed.

Experiments at Higher Concentrations with Iodine Produced by the Palladium Iodide Method. – Experiments in an associated study utilized iodine sources produced by what may be termed the palladium iodide method. Iodine (I^{131} + I^{127} carrier), contained as NaI in a basic sodium sulfite solution, is precipitated as palladium iodide by the addition of an acidified solution of palladium chloride. This precipitate is recovered, washed, dried, and decomposed, under vacuum, at an elevated temperature. The liberated I_2 is then collected in a removable glass U-tube cooled by liquid nitrogen. This iodine is removed from the U-tube as a vapor and introduced into the experiment at hand.

It was observed that, when gas is passed through the iodine source while it is thermostated to a temperature of –70°C, there is a rapid initial transport of I^{131} activity from the source followed by a slower, reasonably constant rate of transport. This and other observations indicate that these iodine sources contain, but not necessarily at all times, two or more components. The initial, rapid release of I^{131} activity from these iodine sources is suggestive of an iodine compound more volatile than elemental iodine, and the gradual release of I^{131} activity following the initial release may be characteristic of either elemental iodine or a compound slightly more volatile than elemental iodine.

The analytical technique of mass spectrometry was applied to these iodine sources. A freshly

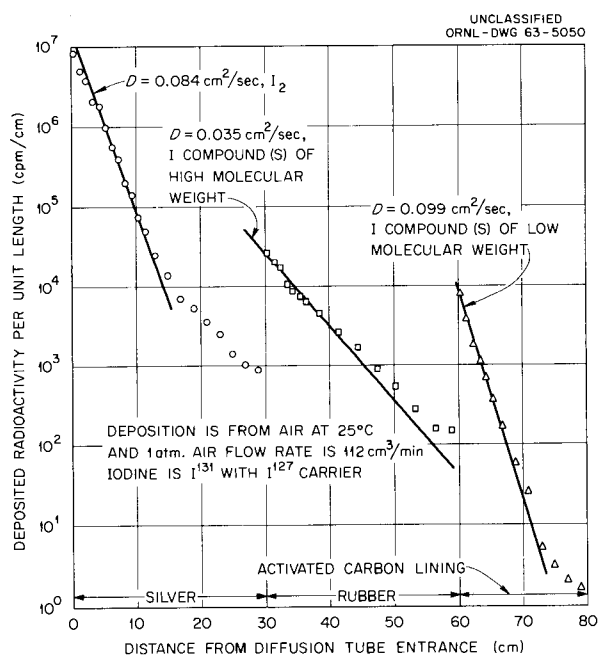

Fig. 4.1. Diffusional Deposition of Elemental Iodine and Iodine Compounds.

prepared iodine source which had not been allowed to reach a temperature greater than that of solid CO_2 was found to contain masses corresponding to those of HI, ICl, and I_2. Diffusion channel analysis was also used to investigate the two fractions of iodine activity. These measurements showed that the more volatile fraction deposited on a charcoal-lined diffusion tube with a diffusion coefficient of approximately 0.10 cm^2/sec, but not on silver or rubber surfaces. This information is displayed in Fig. 4.2. The less volatile fraction deposited primarily on silver with a diffusion coefficient of 0.08 cm^2/sec characteristic of molecular iodine; and small amounts of other iodine compounds deposited on the rubber and charcoal surfaces in a fashion characteristic of the behavior shown in Fig. 4.1.

Investigation of Iodine Compound Formation at Very Low Concentrations

A few diffusion-tube experiments were performed wherein the iodine was, again, prepared by evolution from melted potassium dichromate but no KI^{127} carrier was employed. The resulting iodine concentrations, in air or in helium. were consequently very low, being considerably less than 10^{-3} mg/m^3. At these lower concentrations, the proportion of iodine present as compounds, as measured by radioactivity and diffusion-tube deposition, was considerably increased, for example, to 30%, in comparison to the roughly 1% indicated above for the higher iodine concentrations. Even when pure helium was the associated gas, extensive compound formation was indicated; this may result from reaction of I_2 with unknown components in the melt, with surfaces of the apparatus, or with gaseous impurities carried by the helium after passage over surfaces. Diffusion coefficients for deposition of compounds when plant air was the carrier gas indicated that the compounds might have been, in part at least, the same as observed earlier. An example of the data obtained when plant air was employed is shown in Fig. 4.3; here, the distributions on silver and rubber both apparently reflect some degree of nonquantitative deposition of one or more compounds. The material which previously had been observed to deposit on rubber with an indicated diffusion coefficient of 0.05 cm^2/sec may have been present in this experiment, but, if so, its presence was masked by these effects.

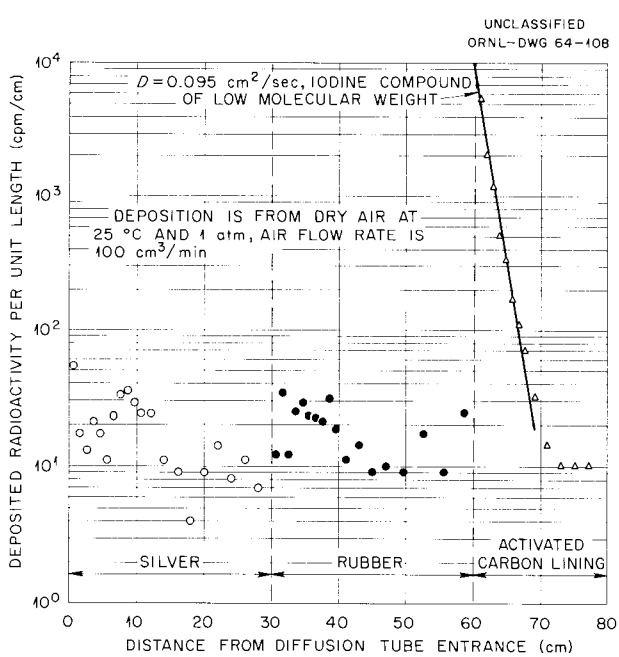

Fig. 4.2. Diffusional Deposition of a Volatile Iodine Compound of Low Molecular Weight.

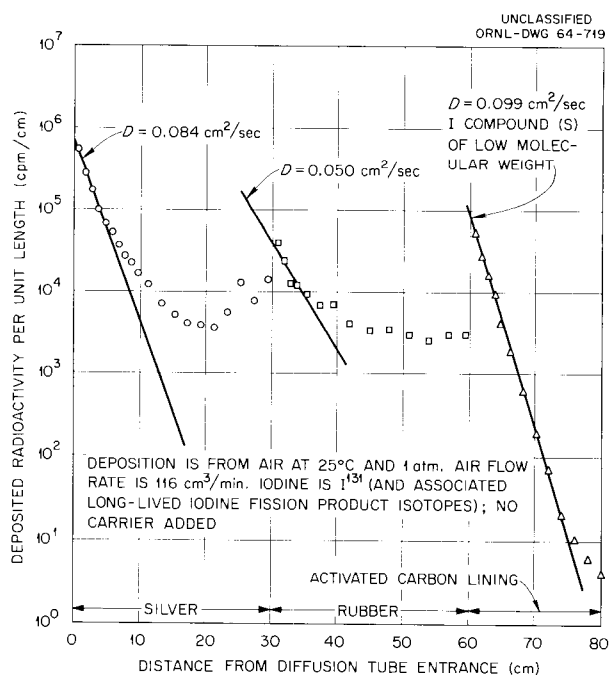

Fig. 4.3. Diffusional Deposition of Iodine and Iodine Compounds at Very Low Concentrations.

While a variety of information pertaining to the nature and identity of the compounds of iodine which occur in conjunction with the elemental form has been obtained, additional information that is more specific and more detailed will ultimately be required and could currently be utilized. Continuation of work on the iodine compound identification problem is therefore planned.

Removal of Iodine and Volatile Iodine Components from Air Systems by Activated Charcoal

Since activated charcoal adsorbers are often used in engineered safeguards, their effectiveness against the various forms of iodine must be known to evaluate the reliability of such systems for containing reactor accidents.

In some earlier experiments, where the iodine sources were prepared by the palladium iodide method, the two iodine fractions, which have now been observed in such sources, were not distinguished; and when moisture was added to the air sweep gas, the iodine adsorption efficiency of charcoal was sometimes decreased significantly and the distribution of I^{131} in the components downstream of the charcoal unit became abnormal compared to the distribution when the air sweep was dry. In the "dry" experiments, the relative humidity was approximately 1 to 3%, while in the "moist" experiments, the relative humidity evaluated at room temperature was increased to approximately 60% by passing the incoming air sweep over water. In later experiments where the two iodine fractions were distinguished, it was noted that moisture affected the behavior of the volatile fraction to a much larger extent than it did the less volatile fraction.

Initial results of the study of this behavior are presented in Table 4.1, and the test apparatus is illustrated schematically in Fig. 4.4. The behavior of iodine in tests 1 and 2 is representative of that in a charcoal system when no effort is made to separate the two fractions of the iodine source. Test 3 illustrates the efficiencies that are obtained when the iodine source is divided into

Table 4.1. Efficiency of Charcoal in Removing Iodine and Volatile Iodine Compounds from Air

Test	Iodine Fraction[a]	Charcoal	Temperature (°C)	Humidity[b] (%)	Efficiency (%)
1	*A* + *B*	BPL	23	~60	90–95
2	*A* + *B*	BPL	23	1–3	>99.9
3	*A*	BPL	23	1–3	>98.0
	B	BPL	23	1–3	>99.9
A-1	*A*	BPL	23	~60	50.3
	B	BPL	23	~60	97.9
4	*A*	BPL	100	1–3	98.5
	B	BPL	100	1–3	>99.9
5	*A*	BPL	100	~60	99.1
	B	BPL	100	~60	>99.9
6	*A*	Whetlerite[c]	24	~60	90.5
	B	Whetlerite	24	~60	>99.8
7	*A*	Whetlerite	100	~60	>99.9
	B	Whetlerite	100	~60	>99.9

[a]When the iodine source is at −70°C, *A* is the volatile fraction (low-molecular-weight iodine compounds) and *B* is the less volatile fraction (primarily elemental iodine).

[b]Humidity of entering air evaluated at room temperature.

[c]BPL charcoal impregnated with salts of silver, copper, and chromium.

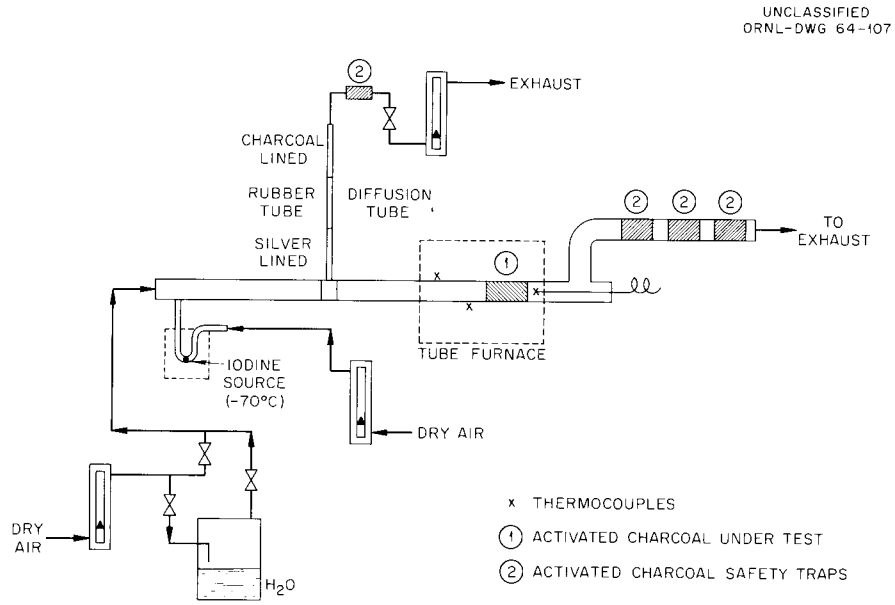

Fig. 4.4. Schematic of Laboratory Apparatus to Study Retention of Iodine Compounds by Activated Charcoal.

two fractions, the first being that part which is vaporized in less than 10 min at –70°C, and the second being that which is vaporized after 10 min. The volatile fraction, *A* in Table 4.1, exhibits the diffusion pattern shown in Fig. 4.2 and appears to be a low-molecular-weight compound of iodine. The less volatile fraction, *B*, has approximately the vapor pressure and diffusion coefficient of elemental I_2 and probably consists primarily of that species. Tests 4 to 7 indicate, to a small degree, the variation of efficiency with the parameters of humidity, temperature, and type of charcoal. Elevated temperature and the presence of metallic impregnants in the Whetlerite charcoal together seem to enhance the adsorption or retention of the volatile iodine fraction by charcoal. These nonelemental compounds (volatile fraction) are by no means the major fraction of the iodine vapor source; thus, it is probable that only moderate efficiencies for removal of these forms of iodine may be required to yield adequate overall iodine efficiencies. The investigation of the behavior of these volatile iodine forms in charcoal systems is being continued.

MEASUREMENT OF THE CHARACTERISTICS OF RADIOACTIVE AEROSOLS BY USE OF FIBROUS FILTERS

W. E. Browning, Jr. M. D. Silverman

Prediction of the behavior of fission products released in a reactor accident, or the effectiveness with which they can be removed from gas streams, requires a knowledge of the amounts of various fission products associated with the different sizes of particles which may be released during a reactor accident. A method for characterizing radioactive aerosols has been developed, which interprets the distribution of radioactive particles in a series of uniform fiber filters in terms of the three main mechanisms of filtration, that is, diffusion, interception, and inertial impaction. The data for this analysis are obtained by previously reported experimental techniques.[5] The radioactive aerosol

[5]W. E. Browning, Jr., and M. D. Silverman, *Nuclear Safety Program Semiann. Progr. Rept. Dec. 31, 1962*, ORNL-3401, pp. 50–55.

is transported through a series of uniform Dacron filters; and the particle distribution vs depth in the filter bed, composed of discrete layers of fibers, is determined by radioassay.

Data from the initial series of experiments, using a radioactive test aerosol containing Zn^{65} particles in the diameter range 20 to 300 A and conducted at linear velocities from 0.4 to 88 fpm, have been analyzed in terms of the three mechanisms of filtration. Analysis of the data in the diffusion region has been reported.[6–8]

The data obtained in the initial series of experiments, at the higher flow rates of 10 to 88 fpm (interceptional and impaction regions), have been analyzed in terms of theories of fiber filtration as evolved by Davies,[9] Chen,[10] and Torgeson.[11] All these theories are derived on the basis of the collection efficiency of a single isolated fiber. However, all filters are composed of many fibers; most have a variable porosity. The effect of neighboring fiber interference on the collection efficiency of individual fibers has been investigated to some extent,[10,12,13] but there is disagreement on how to correct for varying porosity. Chen[10] found that fiber efficiencies in mats were always greater than those calculated for isolated fibers, and he developed a linear expression to correct for α, the volume fraction of fibers in filter mats. Wong and co-workers[12] tried to correct for this term by interpreting pressure drop measurements. The initial series of experiments in the present work were conducted with filter mats having an α of 0.28, well above the region treated theoretically by the above investigators. Extrapolation of the theories by correcting for the high α values according to Davies[9] has yielded fiber efficiencies not in agreement with those obtained experimentally, making it difficult to estimate particle sizes accurately in the higher flow range. A second series of experiments, in which the volume fraction α has been lowered to less than 0.1, has been completed, and analysis of the data is in progress. It is believed that these data can be treated according to a theory of filtration to characterize particle sizes more accurately in this flow region.

---

[6] W. E. Browning, Jr., and R. D. Ackley, *Nuclear Safety Program Semiann. Progr. Rept. June 30, 1963*, ORNL-3483, pp. 29–31.

[7] W. E. Browning, Jr., R. D. Ackley, and M. D. Silverman, *Characterization of Gas-Borne Fission Products*, paper presented at the Eighth AEC Air Cleaning Conference, Oak Ridge National Laboratory, October 1963.

[8] M. D. Silverman and W. E. Browning, Jr., "Fibrous Filters as Particle-Size Analyzers," to be published in *Science*.

[9] C. N. Davies, *Proc. Inst. Mech. Engrs. (London)* **B1**, 185 (1952).

[10] C. Y. Chen, *Chem. Rev.* **55**, 595 (1955).

[11] W. L. Torgeson, *Upper Atmosphere Monitoring Program*, TID-16988, Appendix B (June 1961).

[12] J. B. Wong, W. E. Ranz, and H. F. Johnstone, *J. Appl. Phys.* **27**, 161 (1956).

[13] H. L. Sadoff and J. W. Almlof, *Ind. Eng. Chem.* **48**, 2199 (1956).

5. Measurement and Prediction of Behavior of Released Fission Products in Reactor Systems

INNOCUOUS SIMULATION OF AEROSOLS PRODUCED BY REACTOR ACCIDENTS

W. E. Browning, Jr. R. E. Adams

A program has been started to develop ways of simulating the radioactive materials which would be released during a reactor accident, making use of test materials which are not hazardous themselves. Such innocuous "simulants" will be of great value for investigating the transport by gases of materials in reactor installations. Tests could be carried out in the installation after construction and possibly during operation to determine the behavior of released fission products in the various stages of containment and in gas cleaning equipment. "Simulants" must be found for the various forms of fission products, including molecular dispersions of the appropriate elements and their compounds, and particles of sizes which are produced in reactor accidents.

Since radioiodine is generally considered to be the most significant of the volatile fission products from a hazards standpoint, the behavior of radioiodine is being given first consideration. Natural iodine, in the elemental form, is being applied as a "simulant" for radioactive iodine in the in-place testing of iodine adsorbers on the Nuclear Ship "Savannah." Natural iodine is introduced into the gas system as a vapor and the amount of iodine sampled at various points is determined by neutron activation analysis. In the laboratory, sources of supposedly pure iodine crystals have been shown by diffusion tube measurements and mass spectrometer analysis to contain small amounts of one or more compounds of iodine. In addition to I_2, the compounds CH_3I, HI, and ICl and others of higher molecular weight have been observed. It is important that these and other compounds be fully identified and their behavior characterized so that proper simulation under test conditions can be accomplished. As more understanding of iodine behavior is obtained, the application of nonradioactive iodine vapor and compounds for accident simulation will become more acceptable. More sensitive and faster methods of analysis for natural iodine, other than neutron activation, are being investigated. The search for methods of simulating other fission products will be continued.

DECONTAMINATION FACTORS FOR PARTICLE DEPOSITION IN LEAKS AS APPLIED TO LEAK TESTING OF CONTAINMENT VESSELS

W. E. Browning, Jr. R. D. Ackley

In the event of a major nuclear reactor accident, a significant fraction of the radioactivity released from the reactor core would probably be in the form of airborne radioactive particulates. When such an aerosol escapes through leaks in the containment vessel wall, particles would tend to be removed from the leaking air by diffusional deposition to the inner surfaces of the leaks. Equations and figures indicating the theoretical extent of this attenuation process were presented in the preceding report[1] of this series for the case of viscous flow through two idealized types of leaks, cylindrical and thin rectangular. Since then, this process has been studied in greater detail, particularly with regard to application of the results in determining criteria for testing of containment vessels using conventional leak testers. This further study was made because a potentially large cleanup factor for particulates might be built into the containment system provided the leak-testing procedures are sufficiently stringent. The leaks under consideration have characteristic dimensions in the range 5 to 200 μ, where this dimension is the diameter in the cylindrical case, or is the smallest cross-sectional dimension in the thin rectangular case. Particle diameters considered are 2 μ and less. The results presented earlier showed that the calculated decontamination factor was a very strong function of particle size and of leak size, increasing as either decreases.

[1] W. E. Browning, Jr., and R. D. Ackley, *Nuclear Safety Program Semiann. Progr. Rept. June 30, 1963*, ORNL-3483, pp. 39–42.

Air Flow Rates Through Leaks

The leak models are right circular cylinders and the space between parallel planes. The Poiseuille equation for viscous flow through cylindrical channels and its analogy for parallel planes may be found, for example, in Kennard.[2] The equations were used for calculating air flow rates as given in the following expressions:

$$\text{cylindrical:}\quad \phi = \frac{\pi d^4 \Delta p}{128 \eta L}, \tag{1}$$

$$\text{thin rectangular:}\quad \phi = \frac{b^3 w \Delta p}{12 \eta L}, \tag{2}$$

where

ϕ = the volumetric flow rate as defined below, cm^3/sec,

d = leak diameter, cm,

b = smallest dimension of rectangular leak (distance between parallel planes), cm,

w = width of rectangular leak, cm, and $w >> b$,

Δp = pressure drop through leak, $dynes/cm^2$,

η = coefficient of viscosity, poises,

L = length of leak or wall thickness of containment vessel, cm.

The volumetric flow rate, ϕ, is evaluated at that cross section in the leak where the pressure is equal to $(p_1 + p_2)/2$, where p_1 is the pressure inside the vessel and p_2 is the pressure outside.

Equations (1) and (2) are illustrated in Figs. 5.1 and 5.2 for the following conditions: air at 25°C, a Δp of 7 psig, and an L of 1 in., and, for Eq. (2), a leak width w of 1 cm. In the figures, d and b are in microns. Also, it may be noted that the leak rates are variously expressed including percent per day per leak for an arbitrary containment volume of about 3×10^6 ft^3. Flow rates for other combinations of Δp and L could obviously be obtained from Figs. 5.1 and 5.2 with the aid of the relations of Eqs. (1) and (2) provided viscous flow prevails, regarding which the next part will be concerned.

[2]E. H. Kennard, *Kinetic Theory of Gases*, p. 294, McGraw-Hill, New York, 1938.

Maximum and Minimum Leak Dimensions for Viscous Flow. – To obtain information as to the range of applicability of Eqs. (1) and (2), the Reynolds number, **R**, for each of the two cases was expressed as a function of, among other quantities, leak dimension. This gives:

$$\text{cylindrical:}\quad \mathbf{R} = \frac{\rho d^3 \Delta p}{32 \eta^2 L}, \tag{3}$$

$$\text{thin rectangular:}\quad \mathbf{R} = \frac{\rho b^3 \Delta p}{6 \eta^2 L}, \tag{4}$$

where ρ is gas density, the other quantities having been defined already. These equations are illustrated in Fig. 5.3 for the aforementioned conditions and, arbitrarily, for $(p_1 + p_2)/2$ equal to 1 atm to provide a basis for ρ. Figures 5.1 and 5.2 are thus applicable for characteristic leak dimensions up to 210 and 120 μ respectively. Use of Fig. 5.3 together with Eqs. (3) and (4) affords a means of testing for the upper limits of viscous leak dimensions for various combinations of ρ, Δp, and L, bearing in mind that the upper limit of the Reynolds number for viscous flow is about 2000.

As d or b becomes smaller, and/or as pressure becomes lower, the effect referred to as slip becomes relatively more important, resulting in Eqs. (1) and (2) predicting flows which are biased low. However, it was calculated that at a pressure of 1 atm and for 5-μ leaks, the error due to this effect would not be much greater than 10%. Therefore, for d or $b \geqq 5\ \mu$ and for the pressures of interest herein, Eqs. (1) and (2) should be adequate with regard to slip.

Decontamination Factors for Particle Deposition. – Since this particular phase of the study was reported earlier,[1] only a few additional comments will be made here.

The particle decontamination factor equations, which were previously presented,[1] implicitly contained the expressions for ϕ as given by Eqs. (1) and (2). The ϕ values so obtained are only approximations, as employed in the decontamination factor equations, but their use, rather than the values which are more rigorous, from the standpoint of residence time in the leak channel, greatly simplifies the mathematical treatment. Also, the error introduced, which increases as the pressure

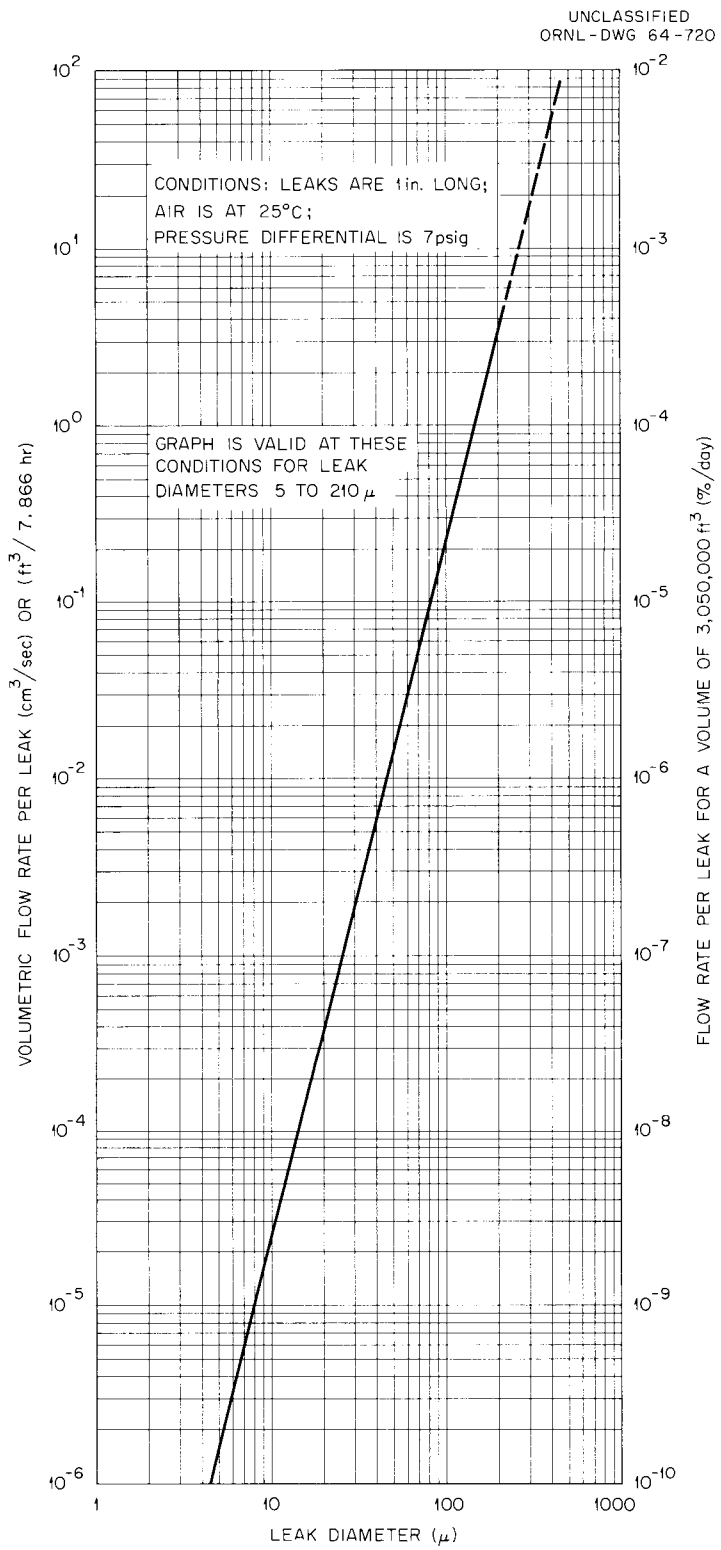

Fig. 5.1. Calculated Air Flow Rates in Cylindrical Leaks for a Given Set of Conditions.

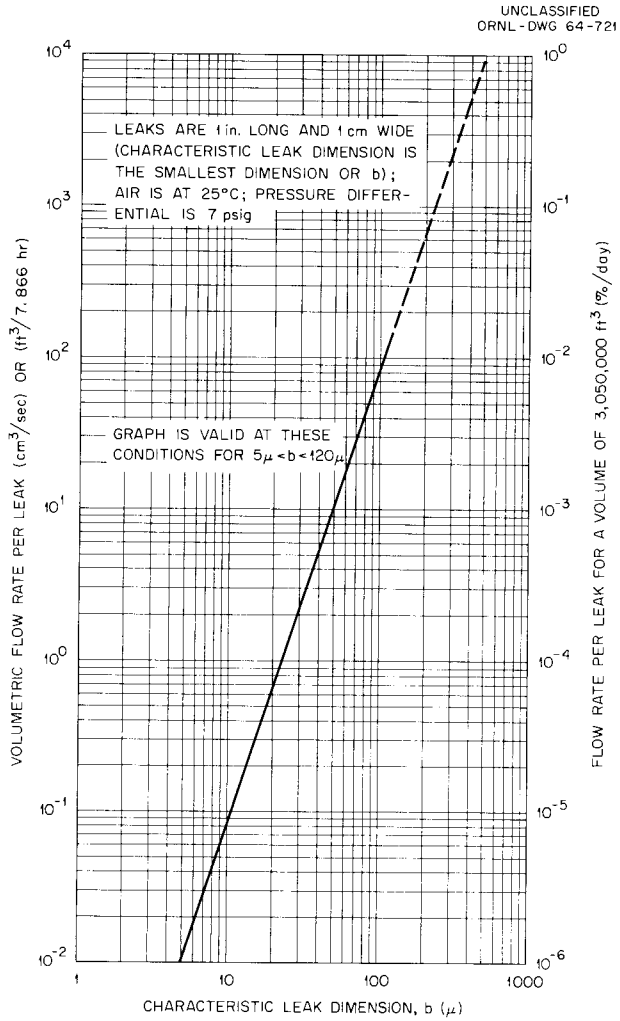

Fig. 5.2. Calculated Air Flow Rates in Thin Rectangular Leaks for a Given Set of Conditions.

ratio, p_1/p_2, increases, is generally not of practical importance, the error in ϕ being only 22% at a pressure ratio of 10 : 1. Furthermore, the bias is such that the approximation is pessimistic since it results in decontamination factors which are too low.

These calculations involve the assumption that the leak wall is a perfect sink for the particles. Information on this point appears rather meager but one gets the impression from the literature that this is not a matter of concern with particles less than 1 μ in diameter. Because, however, of the possible importance to reactor safety that the sticking probabilities of particles be close to 1, consideration should be given to obtaining experimental test of this assumption.

In this same connection, the volume of radioparticulates depositing in a leak might conceivably constitute an appreciable fraction of the leak volume. Also, the exponential nature of the deposition profile might result in most of the particles depositing at the leak entrance and plugging it. Whether this would be beneficial or whether the

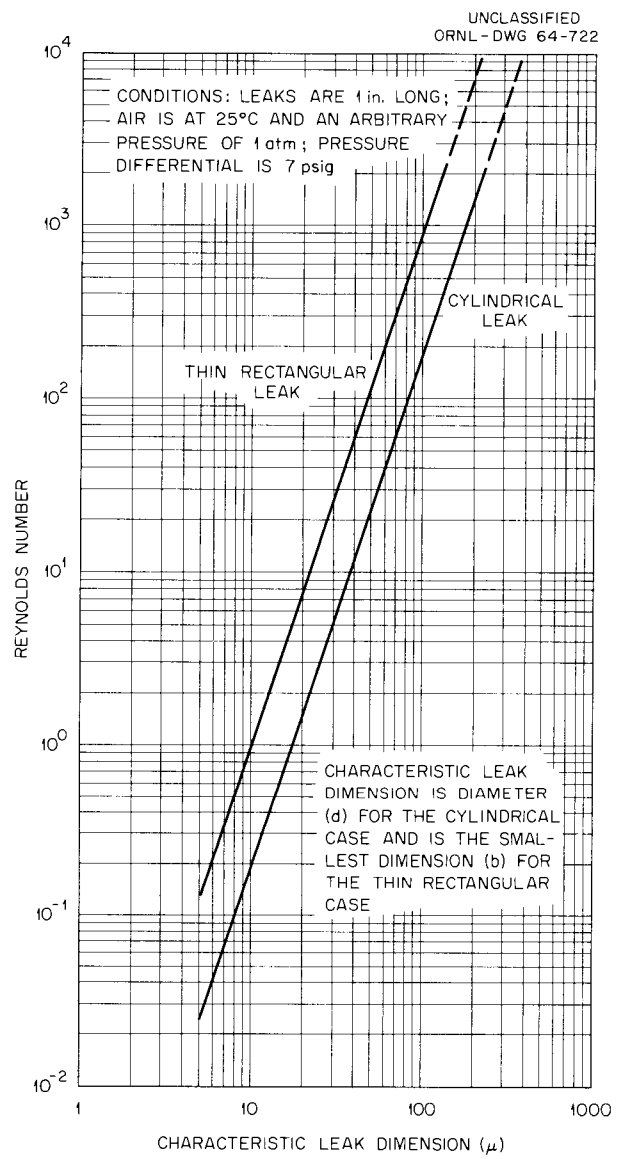

Fig. 5.3. Calculated Reynolds Number vs Leak Dimension for Cylindrical and Thin Rectangular Leaks and for a Given Set of Conditions.

particles might be expelled as a plug is not known. This aspect, too, may require experimental investigation.

Deposition of Atomic and Molecular Species. – Since the diffusion coefficients of atoms and molecules are generally much larger than those of particles, decontamination factors calculated on the basis of the leak walls being a perfect sink would be much greater for fission products in the form of atoms and molecules than for fission products in the form of particles, for the same size of leak. However, high decontamination factors for molecular radioiodine would probably be realized only under rather exceptional circumstances which would not normally prevail during a reactor accident. One consideration is that the quantity of iodine (including the stable and long-lived isotopes), even if it is all elemental, would probably be far more than enough to saturate the exposed leak surfaces; another is that part of the iodine would be in the form of compounds not readily adsorbable. These aspects of radioiodine behavior suggest that consideration be given to lining the inside surface of the containment vessel with an adsorbent porous material, perhaps in the form of tiles, having the designed purpose of removing elemental iodine and, if possible, all iodine compounds. A suitably constructed containment vessel liner should be effective against the more volatile forms of the other fission products. That there would be extensive deposition in containment vessel leaks of certain of the fission products occurring in the form of atoms, clusters of atoms, or molecules, after some type of reaction, appears likely.

Particle Decontamination Factors and Leak Testing of Containment Vessels

The rather idealized results already presented suggest their possible application in determining specifications for testing containment vessels using conventional leak testers. To provide some idea of the possible value, as measured by the calculated decontamination factor, of eliminating all leaks corresponding to a given leak detector sensitivity, Fig. 5.4 is presented. Since, for a given flow rate, the cylindrical geometry gives more pessimistic decontamination factors than the thin rectangular geometry, the former was employed in calculating these results. Also, it is assumed

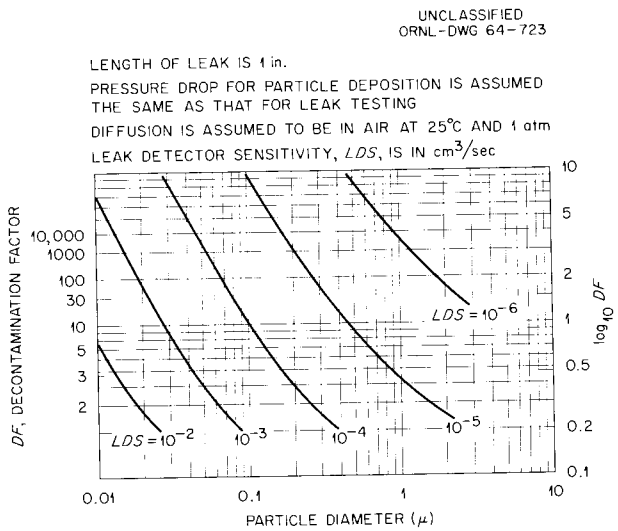

Fig. 5.4. Calculated Decontamination Factors for Cylindrical Leaks Corresponding to Various Leak Detector Sensitivities.

that the containment vessel wall is 1 in. thick, that the pressure drop and gas properties during leak testing are equal to the pressure drop and gas properties when particles are being carried through the leak, that the leak flow rate is measured at the arithmetic average of the inner and outer pressures, and that laminar flow prevails. The equation used to obtain Fig. 5.4 was

$$\log_{10} \mathrm{DF} = 0.0867 + 4.989\, DL/\phi\,, \qquad (5)$$

where

DF = decontamination factor or the ratio of the number of particles entering the channel to the number penetrating,

D = particle diffusion coefficient in air, cm^2/sec,

and L and ϕ are as already defined.

Equation (5) was obtained from the Gormley and Kennedy expression for deposition in cylindrical channels[3] by dropping the secondary exponentials and then writing their equation in terms of the decontamination factor. (Use of only the first term in the exponential series results in only a 3% error for a DF of 1.6, and a lesser error for any

[3] P. G. Gormley and M. Kennedy, *Proc. Roy. Irish Acad., Sect. A* **52**, 163–9 (1949).

higher DF.) Diffusion coefficients for particles in air were presented earlier.[1]

Referring to Fig. 5.4, it appears that the elimination, if practical, of all leaks equal to or larger than those represented by a sensitivity of 10^{-6} cm^3/sec would be a highly worthwhile objective. Halogen-sensitive leak detectors and a helium mass spectrometer with ideal sensitivities of 1×10^{-9} cm^3/sec and 1×10^{-10} cm^3/sec, respectively, have been described, indicating the possible feasibility in practice of achieving the aforementioned sensitivity of 10^{-6} cm^3/sec for the testing of containment vessels. Additionally, work directed toward improving existing leak-testing methods and toward developing new ones should be considered; and containment vessel design should evidently provide for good accessibility for leak testing, particularly in the case of suspect areas such as welds. So far as possible, all leaks detected should be repaired; otherwise, the leak rates should be determined quantitatively and recorded for possible use in hazard evaluation. These measures would be very costly, but the hazard reduction which might be achieved would possibly more than offset the extra cost.

Interpretation and Application of Containment-Vessel Leak-Testing Data

Since the pressure drop during leak testing may be less than for assumed accident conditions, the observed leak rates could be adjusted upward accordingly by multiplying by the appropriate Δp ratio. It is possible that this adjustment will result in the flow rate, ϕ, being in the turbulent regime. Such a circumstance would mean that the use of Eq. (5) or Fig. 4.8 might be pessimistic since the opportunity for particles to collide with the wall for a given residence time would be enhanced to a degree commensurate with the degree of turbulence. On the other hand, the adjusted flow rate ϕ would perhaps be so high that the calculated decontamination factor would not be much greater than 1.

For nonuniform leaks, the flow could be viscous in some sections and turbulent in others. Considering the effect of turbulence on particle deposition and considering that diameter does not appear in Eq. (5), which is for cylindrical leaks, it appears that Eq. (5) could still be applied, provided the leak wall is a perfect sink, realizing that the calculated decontamination factor is pessimistic. The diameter is not involved because when the flow is viscous, its effect on diffusing time and its effect on diffusing distance offset each other. Consequently, when the leak geometry is assumed cylindrical, which is a pessimistic assumption, the leak flow rate and not the leak diameter is needed to calculate a decontamination factor; that is, the actual or calculated value of the leak diameter need not be specified.

If, in leak testing a certain area, the measured leak rate should correspond to more than one leak, a calculated decontamination factor based on the presumption of one leak would again be pessimistic. This is because the flow rate for an individual leak would be less than the observed total flow rate, and the calculated decontamination factor increases exponentially as the flow rate decreases. Obviously, leaks so small as to be beyond the limit of detection would have decontamination factors which are higher than those corresponding to the limit of detection.

This theoretical analysis of the decontamination of aerosols by passage through containment vessel leaks indicates that it may be possible to prove the safety of such vessels by quantitative measurement of leak rates at all points on the surface of the vessel. From the standpoint of particle decontamination, a containment vessel could have a relatively large overall leak rate and still be acceptable provided no one leak or small group of leaks exhibited a flow rate in excess of a certain computed value. However, to utilize this aspect, it would be necessary to prove that the overall leak rate was adequately explained by the combined total of the smaller leaks.

Part II

Containment Engineering

Reactor Division

S. E. Beall, Division Director
W. B. Cottrell, Coordinator

6. Nuclear Safety Pilot Plant

L. F. Parsly
T. H. Row
P. P. Holz
L. F. Franzen

The purpose and design of the Nuclear Safety Pilot Plant were described in a previous semiannual report.[1] Work during the past six months has included completion of design, most of the procurement, installation of equipment and piping, and development testing of the furnace. A hazards report for the facility has been issued,[2] and approval for operation of the NSPP has been granted by the Laboratory Director's Review Committee. Considerable attention has been given to experimental planning, with emphasis on the experiments to be made during the first six months of plant operation.

STATUS OF DESIGN AND CONSTRUCTION

Design of the plant is complete, and construction is in the final stages. All major equipment and piping has been installed, electrical conduit work is complete, and the panel board has been assembled and installed in the control room. The remaining work principally comprises the mounting of instruments, installing wiring in the conduit, and running instrument air tubing inside the working cell. Figures 6.1–6.3 show the installation in the test cell.

FURNACE DEVELOPMENT

Fabrication of the furnace was completed, and a report covering its design and development has been issued.[3] A few experimental runs were made at a temporary out-of-cell installation which included tests to determine the proper method of supporting the dummy fuel element in the melt boat. The initial concept had been to use a thoria liner. Prototype liners were prepared by the ceramic group of the Y-12 Development Division and were tested. These shattered so badly in the temperature gradient that this concept was abandoned, and a tantalum liner separated from the water-cooled boat body by tantalum spacers is now used. Some difficulty is being experienced with melting of the liners, but this can be overcome by replacing the tantalum with tungsten. In addition to the boat liner development, work was done on the flow guide (a shield attached to the furnace lid to channel the gases and vapors evolved from the

[1] M. H. Fontana and C. G. Lawson, *Nuclear Safety Program Semiann. Progr. Rept. June 30, 1962*, ORNL-3319, pp. 51–62.

[2] L. F. Parsly, Jr., *Nuclear Safety Pilot Plant Hazards Summary Report*, ORNL-TM-683 (Oct. 4, 1963).

[3] P. P. Holz and C. M. Smith, Jr., *Plasma Torch Design and Development for Nuclear Safety Pilot Plant Operation*, ORNL-TM-687 (Dec. 20, 1963).

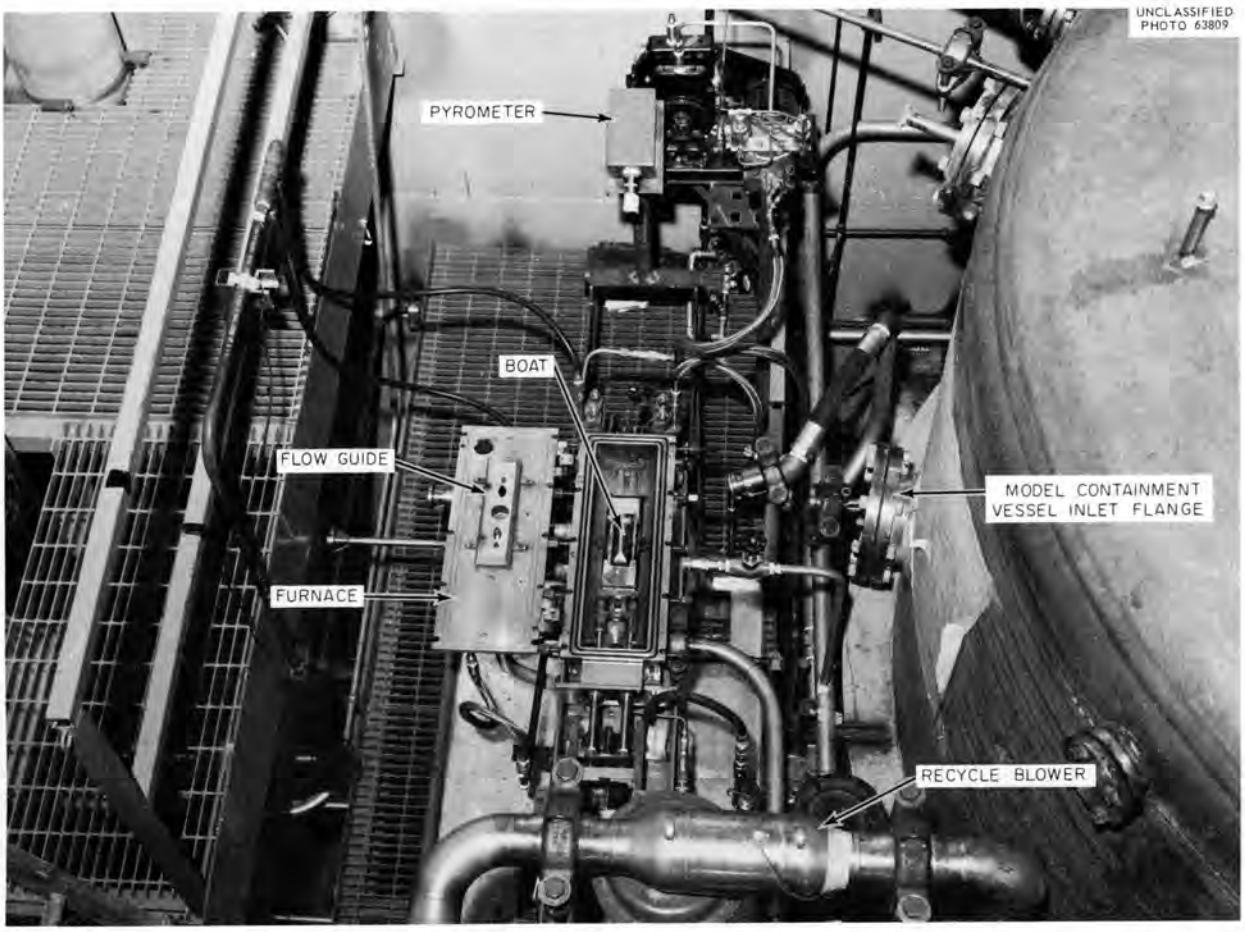

Fig. 6.1. View of Furnace Area from East Side of Cell.

melt to the outlet lines), and a satisfactory flow guide design was achieved. While ZrO_2 was used for most of the runs, three runs were made with UO_2 pellets clad with Zircaloy-2. In all of these runs, significant deposition of dust on the furnace surfaces was observed. Only the plasma gas (approximately 80 scfh of helium) was used. Sweep gas was not tried in the mockup tests. This series of tests had to be terminated to make the furnace, power supply, and controller available for installation in the cell.

A second series of runs was made in the cell with temporary piping connections. These included a demonstration for the Eighth Air Cleaning Conference in which closed-circuit television was used to enable relatively large groups to observe the melting operation, a series of runs using instrumented pellets to obtain temperature distribution in a dummy fuel element, runs to check out the two-color optical pyrometer which will be used to measure the melt temperature, and tests of furnace operation at elevated pressure. A series of three runs was made to obtain motion pictures of the decladding and melting processes.

TEMPERATURE DISTRIBUTION TESTS

The initial experiments of the NSPP will be with EGCR-type UO_2 pellets, their central voids being packed with a mixture of UO_2 powder and crystalline iodine. Since iodine has a low boiling point (181°C) with respect to UO_2 (~2700°C), some concern has been expressed over the fact that the iodine might be prematurely released before significant UO_2 melting occurs. It was therefore necessary to demonstrate the feasibility of the packed-pellet concept.

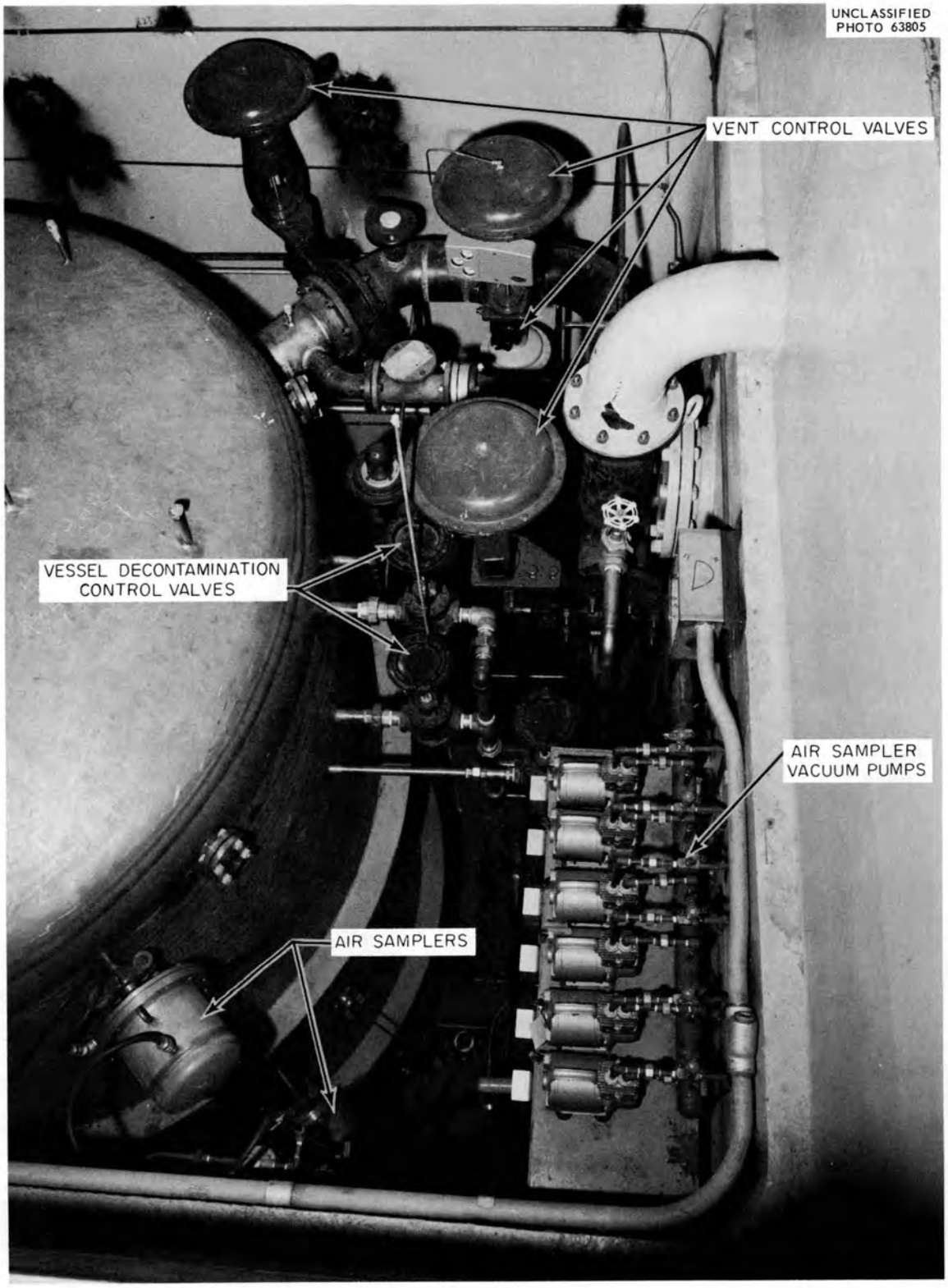

Fig. 6.2. Equipment in North End of Cell.

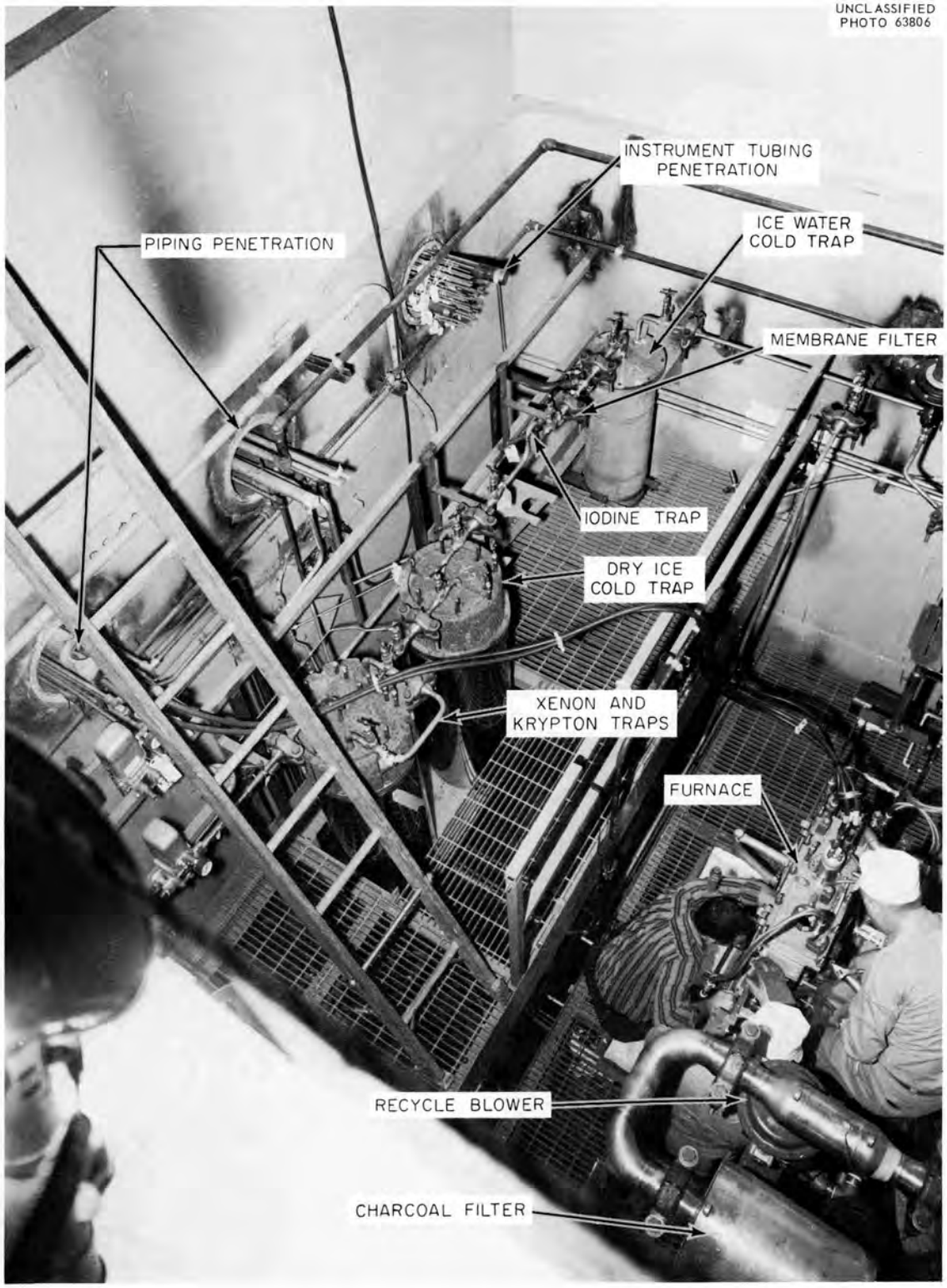

Fig. 6.3. View of South End of Cell.

Several experimental runs were performed with instrumented zirconia pellets to establish the approximate temperature distribution along a specimen during meltdown with the plasma torch. Zirconia was substituted for UO_2 as in the previous development of furnace and torch because of the absence of contamination problems and similar thermal properties.

The results of the experiments indicate that the temperature distribution inside the specimen as a function of time and distance from the plasma flame is favorable to the packed-pellet concept. A solid UO_2 pellet should be placed in front of the packed pellets that contain iodine. More than half of the solid pellet will be melted before the central region of the following pellet reaches temperatures at which the vapor pressure of the iodine becomes significant. This will ensure that a UO_2-iodine mixture will enter the model containment vessel as desired.

PYROMETER TESTS

The Therm-O-Scope two-color pyrometer was set up and was used to measure the temperature of melting ZrO_2. The instrument performed satisfactorily except during some runs at elevated pressure, where vaporization of copper from the anode produced a strong emission in one of the two-color bands. A gradual reduction in the indicated temperature during sustained heating of the ZrO_2 melt was accounted for by reference to the $Zr\text{-}O_2$ phase diagram, which showed that in the oxygen-deficient atmosphere in the furnace, ZrO_2 should lose oxygen until a eutectic melting at 1900°C is formed.

ELEVATED-PRESSURE TESTS

The torch was operated in the furnace under pressures up to 40 psig on two occasions. Above approximately 8 psig, instability of the plasma flame was observed, and at the higher pressure significant amounts of copper were vaporized from the anode and deposited in the furnace. The degree of vaporization observed is great enough to make it desirable not to run fuel meltdowns at the higher pressures unless vaporization can be prevented. A spare torch is being modified to permit variable electrode spacing in an effort to solve the stability problem.

The torch operated a total of 10 hr and 48 min in the test program, of which about 3 hr was at elevated pressures. The torch was still functioning in a satisfactory manner at the end of the tests, although the anode orifice was considerably enlarged as a result of vaporization during the pressure runs. A new anode and cathode have been installed.

TOOLS AND VIEWING

Preliminary testing of deposition-coupon handling procedures and tool shakedown trials was completed. The fallout sample tool will reach any of the designated containment-vessel locations. The tool mechanism operates satisfactorily. Two of the special 500-w caged rod-lights provide ample illumination for remote viewing with either an omniscope or a driftmeter. Definite operation procedures are being delayed until the sample holder design is frozen. The addition of a built-in rotating steel shield plug to provide rapid access to the containment-vessel flange and a shielded indexed tool access for sampling is also being considered.

No problems were encountered with furnace omniscope viewing. Televising a melt via the omniscope barrel to a camera atop the cell was shown to be possible, though minor problems were encountered in retaining precise alignment of furnace viewport and camera on repeated setups. The difficulties should, however, be minimized when the tool setups are operated and indexed through the sleeved top-block openings.

EXPERIMENTAL PROGRAM

The experimental program is now visualized to comprise the following:

Several shakedown runs with stable iodine as a simulated fission product are intended primarily for evaluation of operating and sampling techniques, although it is also hoped that useful data on iodine transport and deposition will be obtained. It is planned to determine iodine by neutron activation analysis.

Assuming that the above technique proves successful, additional stable iodine runs are planned to investigate the effect of plasma-torch operating variables on the nature of the aerosol produced and on the efficiency of transfer from the furnace to the model containment vessel.

A tentative program comprising 14 runs has been laid out. Members of the statistical group of the Laboratory have been requested to review this plan and to make recommendations on improving the experimental design.

Subsequently, it is planned to utilize I^{131}-labeled I^{127} and carrier-free I^{131} to extend the range of iodine concentration investigated below the minimum available from the I^{127} experiments. It should prove feasible in this way to cover a range of iodine concentrations from 10 $\mu g/m^3$ to 100 mg/m^3, that is, up to about the maximum possible if all the iodine in a large power reactor core were released into its containment vessel.

After completion of the iodine experiments, a series of runs is planned with specially irradiated fuel elements, irradiated and cooled to provide 1 to 10 curies of mixed fission products.

7. Reactor Containment Handbook

H. B. Piper

The *Reactor Containment Handbook* is being prepared by ORNL for the AEC, Division of Reactor Development. The purpose of the handbook is to provide detailed information that will be useful in the design, construction, testing, and operation of reactor containment systems. As discussed in the previous report,[1] 8 of the 12 chapters are being prepared by or under the direct supervision of the ORNL staff, while 4 of the chapters are under subcontract to the Bechtel Corporation. The contents of the handbook and the status of each chapter are listed below.

Work on the handbook was begun early in 1962 and has been actively pursued since that time. In late 1962 and early 1963, visits were made with 16 containment designers, constructors, and operators in an effort to gain information and insight concerning the specific problems that were faced and to observe the philosophy held toward containment. Work has continued through 1963, and by January 1964, drafts of all chapters will be completed. After drafts are edited, published as CF memos, and reviewed by ORNL staff members and selected external reviewers, rewriting will be done to incorporate corrections and pertinent comments, and all 12 chapters will then be prepared for publication before the end of the fiscal year. It is expected that the handbook will be published during the summer of 1964. It will be bound in such a way that periodic updating and revision can be accomplished.

Reactor Containment Handbook

		First Draft Completion	Final Draft Completion
I.	Introduction	est. 1-64	est. 4-64
II.	Codes and Criteria	4-63	12-63
III.	Radioactivity – Generation and Transport	est. 2-64[a]	est. 5-64
IV.	Energy Sources	4-63	est. 2-64
V.	Analytical Techniques	est. 4-63[a]	est. 6-64
VI.	Credible Accidents	est. 2-63	est. 5-64
VII.	Containment Proof Testing (Bechtel)	4-63	est. 1-64
VIII.	Specific Containment Systems	est. 3-63[a]	est. 5-64
IX.	Design Details (Bechtel)	4-63	est. 1-64
X.	Containment Accessories (Bechtel)	4-63	est. 2-64
XI.	Economics (Bechtel)	4-63	est. 2-64
XII.	Containment Research	est. 2-63	est. 5-64

[a]The late publication date for these chapters is caused by delay in art work and printing.

[1]T. H. Row, *Nuclear Safety Program Semiann. Progr. Rept. June 30, 1963*, ORNL-3483, pp. 51–52.

Part III

Nuclear Safety Information Center

Reactor Division

S. E. Beall, Division Director
W. B. Cottrell, Coordinator

8. Nuclear Safety Information Center

J. R. Buchanan W. B. Cottrell

The newly established Nuclear Safety Information Center serves the nuclear community by collecting, evaluating, storing, and disseminating nuclear safety information generated throughout the world. Approved by the Commission in March of 1963, the Center became operational about July 1, 1963. Since then over 750 documents have been extracted into the Center's information storage files.

The initial organization and scope of the Center was described in the previous issue of this progress report.[1] Since then the staff has been augmented by two additions, an information specialist whose primary function is to screen all available sources of nuclear safety and route the pertinent documents to the professional staff member responsible for the appropriate area of interest, and a stenographer.

INSTALLATIONS VISITED AND MEETINGS ATTENDED

The meetings and installations listed below have either been attended or visited (as the case may be) by Nuclear Safety Information Center staff representatives since the last report.

American Nuclear Society annual meeting, Salt Lake City, Utah, June 17–19, 1963

Symposium on the Biology of Radioiodine, Hanford, Washington, July 17–19, 1963

Informal conference with personnel of the Radiation Protection Operations Division of General Electric, Hanford, Washington, July 19, 1963

Informal conference with personnel of the Health and Safety Division of AEC's Idaho Operations Office, July 20, 1963

AEC Air Cleaning Conference, Oak Ridge, Tennessee, October 22–25, 1963

"Information Storage and Retrieval," short course at UCLA, October 28–November 8, 1963

Informal conference with personnel of the Health Physics Division of E. I. du Pont de Nemours and Company, Inc., Savannah River, November 5, 1963

American Nuclear Society (winter meeting held jointly with Atomic Industrial Forum and Atomic Fair), New York, November 18–21, 1963

"Training Course on Coordinate Indexing and Abstracting" at BMI, Columbus, Ohio, November 18–22, 1963

Informal conference with personnel from the SPERT Program, NRTS, December 10–11, 1963

[1] W. B. Cottrell and J. R. Buchanan, *Nuclear Safety Program Semiann. Progr. Rept. June 30, 1963*, ORNL-3483, pp. 53–55.

CENTER STUDIES

The special study assignments with which the Center is now concerned were discussed in the previous progress report.[1] The current status of these assignments is outlined below:

Nuclear Safety Contract File

The first issue of the active file of nuclear safety contracts was published in November 1963.[2] Primary purposes of the file are to serve the AEC as an active management tool and the Center as a guide for its specialists. Consequently the distribution is being initially limited to AEC managers and NSIC specialists.

Behavior of Iodine in Reactor Containment Systems

This and the next study replace the radioiodine handbook effort. A comprehensive survey of radioactive release, transport, and removal within containment structures is being made, and an initial draft of the study will be issued early in 1964.

Evaluation of Iodine Effluent Monitoring and Area Monitoring Programs at Savannah River, Hanford, Idaho Falls, and Oak Ridge

The survey is essentially complete, and a report will be issued in the early part of 1964.

Reactivity Effects of Fuel Element Bowing

A report will be prepared and issued early in 1964. Due to a shift in interest this topic has replaced the study previously contemplated on the "Effect of Fuel Element Cladding Thickness in Water Reactors."

Effectiveness of Safety Injection Systems for Emergency Reactivity Control

A report will be prepared and issued in 1964.

[2] J. R. Buchanan, *Nuclear Safety Contract File, ORNL-NSIC-2 Nuclear Safety Special Report,* Nov. 15, 1963.

Kinetics of Large Reactor Cores

A report will be prepared and issued in 1964.

Review of Safety Analysis Procedures and Methods

A report will be prepared and issued in 1964.

Safety of Fast Gas-Cooled Reactors

The study is under way and a report will be issued early in 1964.

Other Assignments

In addition to performing special studies such as these, the AEC will occasionally request that the Center undertake critical reviews of experimental program proposals made to the Commission by independent groups. One such proposal relative to reactor safety system reliability analysis has been reviewed by the Center. The results of this review were made known to the Commission in November.

OTHER INFORMATION ACTIVITIES

Since its inception the Center has received and answered 25 specific requests for nuclear safety information. The requests have come from private companies, government groups, and private individuals. In addition, it has received and filled 45 requests to be added to the distribution of reports prepared by NSIC. Plans are also under way for the preparation of an annotated bibliography of nuclear safety information which would be issued periodically.

A brochure has been prepared that describes the Center's organizational structure, technical scope, and functions. Copies of the brochure were distributed at the November meetings of the American Nuclear Society in New York City and the American Public Health Association in Kansas City. Brochures have also been disseminated on an individual basis to answer requests for additional information on the Center's capabilities.

ORNL-3547
UC-80 – Reactor Technology
TID-4500 (26th ed.)

INTERNAL DISTRIBUTION

1. Biology Library
2-4. Central Research Library
5. Reactor Division Library
6-7. ORNL – Y-12 Technical Library
Document Reference Section
8-42. Laboratory Records Department
43. Laboratory Records, ORNL R.C.
44. Laboratory Shift Supervisor
45. R. D. Ackley
46. R. E. Adams
47. R. G. Affel
48. T. A. Arehart
49. E. D. Arnold
50. S. I. Auerbach
51. J. A. Auxier
52. C. J. Barton
53. S. E. Beall
54. S. R. Bernard
55. D. S. Billington
56. F. T. Binford
57. E. P. Blizard
58. C. J. Borkowski
59. G. E. Boyd
60. J. C. Bresee
61. R. B. Briggs
62. W. E. Browning
63-67. F. R. Bruce
68. J. R. Buchanan
69. T. J. Burnett
70. A. D. Callihan
71. W. B. Cottrell
72. K. E. Cowser
73. J. A. Cox
74. G. E. Creek
75. G. A. Cristy
76. F. L. Culler
77. M. E. Davis
78. Wallace de Laguna
79. J. S. Eldridge
80. L. C. Emerson
81. W. K. Ergen
82. R. B. Evans
83. M. F. Fair
84. B. R. Fish
85. J. L. Fowler
86. A. P. Fraas
87. J. H Frye
88. J. H. Gillette
89. W. R. Grimes
90. E. E. Gross
91. C. E. Guthrie
92. Fred Haywood
93. R. L. Heestand
94. K. M. Henry
95. P. P. Holtz
96. T. W. Hungerford
97. G. S. Hurst
98. E. B. Johnson
99. W. H. Jordan
100. G. W. Keilholtz
101. M. T. Kelley
102. F. Kertesz
103. O. H. Klepper
104. J. O. Kolb
105. D. M. Lang
106. C. E. Larson
107. C. G. Lawson
108. R. A. Lorenz
109. H. G. MacPherson
110. F. C. Maienschein
111. W. D. Manly
112. W. J. Martin
113. H. C. McCurdy
114. A. B. Meservey
115. A. J. Miller
116. C. E. Miller
117. E. C. Miller
118. W. H. Montgomery
119. J. G. Morgan
120. K. Z. Morgan
121. M. T. Morgan
122. F. H. Neill
123. M. L. Nelson
124. J. P. Nichols
125. G. W. Parker
126. R. B. Parker
127. L. F. Parsly
128. H. B. Piper

129. P. H. Pitkanen
130. S. A. Reynolds
131. J. M. Robbins
132. B. F. Roberts
133. T. H. Row
134. G. W. Royster
135. A. F. Rupp
136. J. L. Scott
137. H. E. Seagren
138. R. P. Shields
139. E. G. Silver
140. M. D. Silverman
141. O. Sisman
142. M. J. Skinner
143. W. S. Snyder
144. W. M. Stanley
145. W. G. Stockdale
146. E. G. Struxness
147. J. A. Swartout
148. A. J. Taylor
149. E. H. Taylor
150. D. F. Toner
151. P. R. Vanstrum
152. F. C. VonderLage
153. C. S. Walker
154. G. M. Watson
155. A. M. Weinberg
156. M. E. Whatley
157. G. C. Williams
158. J. W. Youngblood
159. Gale Young

EXTERNAL DISTRIBUTION

160. R. W. McNamee, Union Carbide Corporation, New York
161. F. A. Gifford, USAEC Weather Bureau Office, Oak Ridge Operations Office
162. H. N. Culber, TVA-EGCR Site
163. Morton I. Goldman, Nuclear Utility Services, Inc., 1025 Connecticut Ave., N.W., Washington 6, D.C.
164. Howard Kraig, Westinghouse Electric Corporation, Astronuclear Laboratory, Post Office Box 10864, Pittsburgh 36, Pennsylvania
165. E. R. Irish, HAPO, GE-Richland
166. C. E. Thomas, Atomic Energy Division, Babcock & Wilcox Company, Lynchburg
167. H. W. Behrman, U.S. Atomic Energy Commission, Oak Ridge Operations Office
168. D. F. Cope, U.S. Atomic Energy Commission, Oak Ridge Operations Office
169. F. C. Huffman, U.S. Atomic Energy Commission, Oak Ridge Operations Office
170. Wayne Smalley, U.S. Atomic Energy Commission, Oak Ridge Operations Office
171. Research and Development Division, U.S. Atomic Energy Commission, Oak Ridge Operations Office
172. David B. Hall, Los Alamos Scientific Laboratory, Post Office Box 1663, Los Alamos, New Mexico
173. C. R. Williams, Liberty Mutual Insurance Company, 175 Berkeley Street, Boston 17, Massachusetts
174. John C. Geyer, Department of Sanitary Engineering and Water Resources, Johns Hopkins University, Baltimore 18, Maryland
175. John P. Howe, Cornell University, Ithaca, New York
176. Herbert J. C. Kouts, Brookhaven National Laboratory, Upton, L.I., N.Y.
177. H. W. Newson, Department of Physics, Duke University, Durham, N.C.
178. K. R. Osborn, Manager, Industrial Development, General Chemical Division, Allied Chemical & Dye Corporation, 40 Rector Street, New York 6, N.Y.
179. D. A. Rogers, 11 Lingerwood Place, Morristown, N.J.
180. Leslie Silverman, School of Public Health, Harvard University, 55 Shattuck Street, Boston 15, Massachusetts
181. R. C. Stratton, Apt. 5-J, 98 Garden Street, Hartford 5, Connecticut
182. Theos J. Thompson, Department of Nuclear Engineering, Massachusetts Institute of Technology, Cambridge 38, Massachusetts

183. Dick Duffey, Professor of Nuclear Engineering, Department of Chemical Engineering, University of Maryland, College Park, Maryland
184-186. Advisory Committee on Reactor Safeguards, Atomic Energy Commission, Washington 25, D.C., Attn: R. F. Fraley
187. George P. Dix. U.S. Atomic Energy Commission, Division of Reactor Development, Space Nuclear Propulsion Office, Washington 25, D.C.
188. Merson Booth, U.S. Atomic Energy Commission, Division of Reactor Development, Analysis and Evaluation Branch, Washington 25, D.C.
189. Howard G. Hembree, U.S. Atomic Energy Commission, Division of Reactor Development, Engineering and Testing Branch, Washington 25, D.C.
190. Walter G. Belter, U.S. Atomic Energy Commission, Division of Reactor Development, Environmental and Sanitary Engineering Branch, Washington 25, D.C.
191-193. J. A. Lieberman, Assistant Director for Nuclear Safety, Division of Reactor Development, U.S. Atomic Energy Commission, Washington 25, D.C.
194. P. A. Morris, Assistant Director for Reactors, Division of Compliance, U.S. Atomic Energy Commission, Washington 25, D.C.
195. C. K. Beck, Deputy Director of Regulation, U.S. Atomic Energy Commission, Washington 25, D.C.
196-197. Argonne National Laboratory, 9700 S. Cass Avenue, Argonne, Illinois, Attn: R. C. Vogel
198. Atomic Energy Commission, Army Reactors, Division of Reactor Development, Washington 25, D.C.
199. Atomic Energy Commission, Civilian Reactors, Division of Reactor Development, Washington 25, D.C., Attn: A. Giambusso
200. Atomic Energy Commission, Division of Compliance, Region IV, Post Office Box 15266, Denver 15, Colorado, Attn: John W. Flora
201-207. Atomic Energy Commission, Division of Licensing and Regulation, Washington 25, D.C., Attn: Edson G. Case, J. J. DiNunno
208. Atomic Energy Commission, Maritime Reactors Branch, Division of Reactor Development, Washington 25, D.C.
209-210. Atomic Energy Commission, Naval Reactors Branch, Division of Reactor Development, Washington 25, D.C., Attn: T. Rockwell, R. S. Brodsky
211-215. Atomic Energy Commission, Research and Development Branch, Division of Reactor Development, Washington 25, D.C., Attn: S. A. Szawlewicz
216-217. Atomics International, Post Office Box 309, Canoga Park, California, Attn: A. A. Jarrett
218. Brookhaven National Laboratory, Upton, Long Island, New York, Attn: A. W. Castleman
219. Canoga Park Area Office, Post Office Box 591, Canoga Park, California, Attn: C. W. Richards
220. Chicago Operations Office, Atomic Energy Commission, 9800 S. Cass Avenue, Argonne, Illinois, Attn: D. M. Gardiner
221-222. IIT Research Institute, 10 W. 35th Street, Chicago 16, Illinois, Attn: T. A. Zaker, M. A. Salmon
223-224. Idaho Operations Office, Atomic Energy Commission, Post Office Box 2108, Idaho Falls, Idaho, Attn: George Wehmann, D. Williams
225. National Bureau of Standards, Washington 25, D.C., Attn: C. Muelhause
226. Naval Ordance Laboratory, White Oak, Silver Spring, Maryland, Attn: Walter R. Wise, Jr.
227-234. Phillips Petroleum Company, Post Office Box 1259, Idaho Falls, Idaho, Attn: Glenn O. Bright, Warren E. Neyer, Frank Schroeder, T. R. Wilson
235. San Francisco Operations Office, Atomic Energy Commission, 2111 Bancroft Way, Berkeley 4, California, Attn: Lt. Col. John B. Radcliffe
236-237. Space Technology Laboratories, Inc., One Space Park, Redondo Beach, California, Attn: D. B. Langmuir, S. M. Zivi
238. United Nuclear Corporation, Development Division, 5 New Street, White Plains, N.Y., Attn: C. Graves
239-240. University of California, Institute of Engineering Research, Berkeley 4, California, Attn: Prof. H. A. Johnson, Dr. V. E. Schrock

241. University of Minnesota, Department of Chemical Engineering, Minneapolis, Minnesota, Attn: Prof. H. Isbin
242. USAEC Liaison Office, Post Office Box 985, Toronto 18, Ontario, Canada, Attn: Glen B. Boyer
243. USAEC, Division of Compliance, Washington 25, D.C.
244. G. F. Stone, TVA-EGCR Site
245. Division of Technical Information, AEC, Washington, Attn: R. E. Bowman
246. Division of Reactor Development, USAEC, Washington, Attn: I. E. Jackson

247-858. Given distribution as shown in TID-4500 (26th ed.) under Reactor Technology category (75 copies – OTS)